1982

The effect of processing conditions on the solid-state deformation and consequent properties of high density polyethylene.

Marc Michael Daniels
University of Massachusetts Amherst

THE EFFECT OF PROCESSING CONDITIONS ON THE SOLID-STATE DEFORMATION AND CONSEQUENT PROPERTIES OF HIGH DENSITY POLYETHYLENE

A Thesis Presented

By

MARC MICHAEL DANIELS

Submitted to the Graduate School of the
University of Massachusetts in partial fulfillment
of the requirements for the degree of

MASTER OF SCIENCE

February 1982

Polymer Science and Engineering

THE EFFECT OF PROCESSING CONDITIONS ON THE SOLID-STATE DEFORMATION AND CONSEQUENT PROPERTIES OF HIGH DENSITY POLYETHYLENE

A Thesis Presented

By

MARC MICHAEL DANIELS

Approved as to style and content by:

Roger S. Porter

Dr. Roger S. Porter,
Chairperson of Committee

William J. MacKnight

Dr. William J. MacKnight, Head
Department of Polymer Science
and Engineering

DEDICATION

To my parents.

ACKNOWLEDGEMENT

I would like to express my appreciation to my advisor, Dr. Roger S. Porter for his guidance through the course of this thesis and to Dr. Edwin L. Thomas for his encouragement. I am indebted to my colleagues in the Department of Polymer Science and Engineering, particularly those in Dr. Porter's group, for their friendship, advice, and philosophy. I am grateful to the following people for specific contributions to this thesis: Wade Adams for WAXS and SAXS work on extrudates, Li Hui Wang for TMA work on extrudates, Martin Wai for WAXS analysis of billets, John Giraud of Balloffet Die Corp., Guttenberg, N.J. for construction of dies designed to achieve higher draw ratios, and Peter Morassi of Tog Mold Tool and Die Co., Pittsfield, Mass. for use of the Cordex machine used to trace the profile of a necked billet.

Finally, I would like to thank my parents for their support and encouragement.

ABSTRACT

THE EFFECT OF PROCESSING CONDITIONS ON THE
SOLID-STATE DEFORMATION AND CONSEQUENT
PROPERTIES OF HIGH DENSITY POLYETHYLENE

February 1982

Marc M. Daniels, B.A. Case Western Reserve University, 1976
M.S. University of Massachusetts, Amherst, 1982

Directed by: Dr. Roger S. Porter

This thesis examines the uniaxial drawing process of solid-state extrusion for high density polyethylene. To provide a foundation for the experimental work, a model for solid-state deformation of polyethylene is presented. The literature on drawing and extrusion is reviewed and results are interpreted in terms of the model. Experimental work is divided into three sections: (1) the effect of extrusion conditions on extrudate properties, (2) the effect of extrusion temperature, draw ratio, and die angle on λ, the ratio of pushing to pulling pressures which produce equivalent extrusion rates during pultrusion, and (3) methods to increase draw ratio and tensile modulus.

High density polyethylene (DuPont Alathon 7050, M_W = 59,000, M_N = 19,900) was extruded, using an Instron capillary rheometer (Model A70), at 120^{o}C through a conical die with an entrance angle of 20^{o}. Extrudates of draw ratio 29.1 were produced under three conditions, extrusion at 213 and 182 MPa and pultrusion at 182 MPa pushing pressure plus 4.0 MPa pulling pressure. A range of extrusion rates, 4.31 to

0.54 cm/min., were produced by variation in billet lubrication prior to extrusion. Extrudate tensile modulus, molecular draw ratio, and temperature at the onset of melting increased slightly at decreased extrusion rate. Density, crystallinity, peak melting temperature, and fusion curve width were independent of extrusion rate. It was concluded that a slower extrusion produces a slightly more efficient deformation. Only tensile modulus among these properties was affected by extrusion conditions. Average tensile modulus of the 213 MPa extruded and the pultruded samples were approximately equal and ~10% greater than that of the 182 MPa extruded samples. There was no measurable correlation between molecular draw ratio or thermal properties and radial position within the extrudate.

A trend of increasing λ with increasing die angle and decreasing extrusion temperature was observed. λ increased with increasing draw ratio above draw ratio 29.1 and decreased with decreasing draw ratio below 29.1. Generally, the effectiveness of a pulling pressure relative to that of a pushing pressure increases as extrusion conditions become more difficult. Deformation profiles show that pultrusion has little effect on deformational flow. Lubrication has a significant effect, greatly increasing elongational flow.

Attempts to obtain yet higher draw ratios were made by coextrusion, splitting the billet into four sections prior to extrusion, and modification of die geometry to eliminate sharp corners and provide a constant strain rate. Each method was partially successful. Further work is needed to optimize and combine these techniques.

TABLE OF CONTENTS

LIST OF TABLES

LIST OF FIGURES

C H A P T E R I

DEFORMATION MECHANISM OF POLYETHYLENE BY DRAWING

Introduction

The theoretically high tensile modulus and tenacity of a fully extended polyethylene chain is a result of the high moduli on stretching the carbon-carbon bond and its valence bond opening.[1] Achievement of high modulus on the macroscopic level is dependent on elongation and orientation of individual chains and the development of morphologies that allow transfer of stress between chains. Several methods have been developed to approach this model. Among them are hot[2,3] and cold drawing,[4-7] die drawing,[8,9] crystallization from the melt under the combined effects of orientation and pressure,[10,11] crystallization from stirred polymer solutions,[12-14] and by solid-state extrusion.[15-20] The modulus obtained is a function of the method and conditions for each. Temperature, pressure, polymer molecular weight, deformation rate, die geometry, lubrication, and initial morphology all can affect the deformation process, thus determining the final morphology and resultant properties.

This thesis is concerned with the process of solid-state extrusion through conical dies. To establish a foundation for this study, the generally accepted model for solid-state deformation of polyethylene and the effects of processing conditions on sample properties are reviewed. In the Experimental Section, the effects of extrusion pressure, lubrication, adding a pulling force to the emerging extrudate (pultrusion), and extrusion rate on the deformation process are characterized on

extrudates by tensile tests, shrinkage and density measurements, and thermal analysis. The effects of draw ratio, extrusion temperature, and die angle on pultrusion are determined. This information is coupled with previous reports to propose mechanisms for the deformation process and to develop techniques that may achieve moduli higher than that previously obtained by solid-state extrusion.

Morphology of Polyethylene

High density polyethylene typically consists of a carbon-carbon single bond backbone with fewer than 1 short side chain, 2 to 4 carbon atoms in length, per 200 main chain carbon atoms.[21] This uniform structure promotes formation of a highly crystalline morphology, ~90%, predominantly with an orthorhombic unit cell. Crystallization from the melt produces spherulites comprised of folded chain lamellae radiating from a nucleus. Uncrystallized chains exist as amorphous regions between lamellae and at spherulitic boundaries. Such morphologies can be characterized in terms of spherulite number, size, and interconnection, lamellar thickness, and degree of crystallinity. These variables may be partially controlled by choice of crystallization temperature, pressure, and time. Generally, longer crystallization times at lower undercooling, i.e., nearer the melting point, produces a higher per cent crystallinity. In this way, fewer, but larger spherulites with fewer tie molecules between spherulites are formed. Lamellar thickness increases with increasing crystallization temperature and pressure and extended chain crystals can be formed from the melt at pressures above 2000 atm.[22]

The solid-state deformation mechanism which produces high elongation and moduli has been generally characterized. However, the extent of

deformation is limited by the ability of the initial morphology to follow this mechanism to the desired extremes of draw. Therefore, to achieve high moduli, knowledge of the morphological effects of crystallization conditions must be utilized to develop morphologies well suited for deformation.

Deformation Mechanism of Polyethylene by Drawing

The generally accepted model for the deformation of polyethylene by conventional drawing has been developed by Peterlin.[23] Variations in initial morphology, draw rate, and temperature affect the deformation process and limit the ultimate draw ratio obtainable before fracture. These factors will be examined individually. The basic deformation mechanism, with minor changes to be discussed later, is also valid for deformation by solid-state extrusion.

Morphology of Polyethylene Produced by Drawing

Isotropic and spherulitic polyethylene is transformed into a highly oriented fibrous structure by tensile drawing. The fibrils consist of packed bundles of microfibrils which in turn consist of alternating layers of folded chains and amorphous regions. The fold period (crystal length) is dependent on the drawing temperature and independent, within limits, of the initial lamellar fold period. The microfibril has a diameter of ~100 Å and is several μm in length whereas the fibril has a diameter of ~1 μm and a length of ~10 μm.[23] Single and clusters of tie molecules provide interfibrillar, intermicrofibrillar, and, most importantly, intramicrofibrillar connections.

Deformation - Stage 1

The drawing transformation from spherulite to fibril can be divided into three basic structural deformations that correspond to preyield spherulitic deformation, yielding and neck propagation, and to postneck deformation of the fibrillar structure. (A representation of the deformation process is shown in Fig. 1.[24]) The first stage, preyielding deformation, is attributed to elastic deformation in the amorphous phase and viscous deformation in the crystalline phase. It is a combination of several distinct mechanisms which result in an elongated, but intact, spherulite.

Bowden and Young[25] reviewed the deformation mechanisms observed in crystalline polymers. As drawing begins, spherulite deformation occurs near simultaneously with sample stretching in the amorphous phase.[26] Deformation proceeds by interlamellar slip, interlamellar separation, and stack rotation.[25] Interlamellar slip and separation are caused by shear deformation and stretching, respectively, of the amorphous phase between lamellae. Both are elastic. Stack rotation is rotation of lamellae joined by tie molecules. The stack is surrounded by amorphous chains of sufficient mobility to accommodate the stack rotation.

Crystalline deformation begins at about 1% strain[23] and proceeds mainly through intralamellar chain slip with minor contributions from crystal twinning and phase transformation. Intralamellar chain slip occurs along a slip plane containing a chain axis when the critical resolved shear stress is reached. Slip can occur parallel or perpendicular to the chain axis, depending on the direction of the applied shear stress. Its effect is to rotate and orient the chain axis into the draw direction. Crystal twinning, a rotation of the crystal lattice[19]

FIG. 1. REPRESENTATION OF DEFORMATION MECHANISM OF POLYETHYLENE

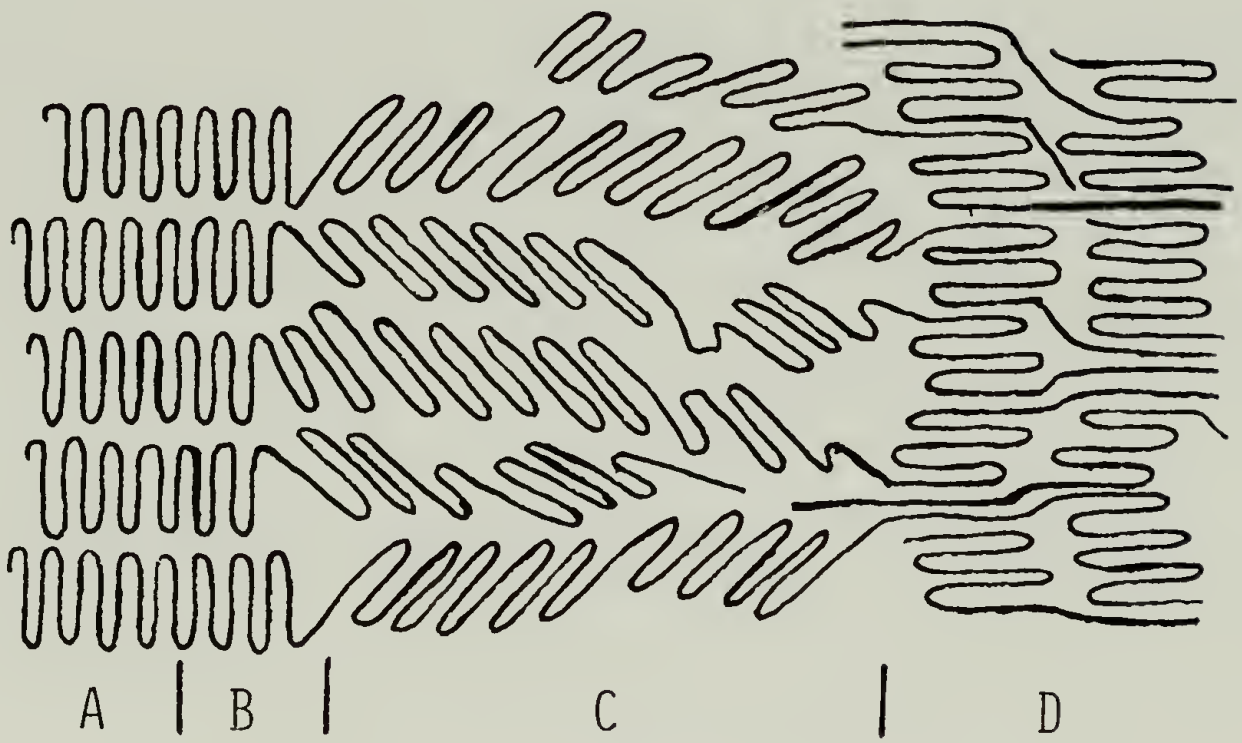

A: UNDEFORMED CRYSTALS

B: STAGE 1 - PHASE TRANSFORMATION, TWINNING

C: STAGE 2 - TILT, SLIP, CRACKS FORMED, CHAINS PULLED OUT OF CRYSTALS, FIBRILS FORMED

D: STAGE 3 - INTERFIBRILLAR SLIP

involving only short range molecular motion, arises when long range motion is inhibited. It occurs along the (110) diagonal when the draw direction is between the (110) diagonal and the a-axis and turns the c-axis perpendicular to the draw direction.[27] [(hkl) refers to Miller indices] Phase transformation from an orthorhombic to a monoclinic unit cell is a third mode of crystalline deformation. It is a response to shear forces when the draw direction is between the b-axis and the (110) diagonal. However, the monoclinic form is unstable and reverts back to the orthorhombic form when stress is removed or the sample is heated above 105°C.[27]

Each mechanism has an activation energy which must be surmounted for the deformation to occur. Therefore, initiation of a particular deformation is dependent on the applied strain and test temperature which control the amount of energy introduced into the system.[28,29] Short range motions in the amorphous phase, hypothesized as crankshaft or kink motions,[30] are associated with the γ-transition and have an activation energy of 11-15 kcal/mole.[31] Longer range motions in the amorphous phase are severely restricted by the strong coupling between crystalline and amorphous phases.[32] This accounts for the weak β-transition observed in polyethylene. The α-transition can be divided into two relaxations of the crystalline phase involving interlamellar and intercrystalline motion with activation energies of approximately 25 and 45 kcal/mole respectively.[29] The expected prevalence of motions within crystals, as more energy is introduced, has been experimentally confirmed.[25]

The sum of the several mechanisms in the first deformation stage is preparation of the spherulite for necking through alignment of the chain, c-axis, in the draw direction. Since large displacement motions of amorphous components is limited, higher strains must be obtained through

lamellar deformation that may occur predominantly by c-axis chain slip.[26] Twinning orients the b-axis with the draw direction and the c and a-axes perpendicular to it. Simultaneously, rotation around the a-axis occurs, orienting the c-axis in the draw direction and turning the b-axis away from it. Small amounts of chain slip occur, also orienting the c-axis in the draw direction. At this point, ~60% strain,[23] large scale chain slip begins as the spherulite enters into the second stage of deformation.

Deformation - Stage 2

The second stage of deformation begins with neck formation and ends when the sample has been completely transformed into a fibrous morphology. This corresponds with the yield point and plateau region of the stress-strain curve.

The orientation of individual lamellae within the spherulite to the applied stress determines the mechanism and timing of their deformation.[33] Lamellae oriented at 45^{o} to the draw direction experience the greatest amount of shear stress in the draw direction. Consequently they are the first to deform by large scale chain slip.[23] Deformation begins at the boundary layers between adjacent crystal blocks which contain crystal defects. Small blocks of unfolded chains are sheared from the lamellae and incorporated, with amorphous regions between them, longitudinally into a microfibril. Visually, deformation appears as a crack in the spherulite bridged by the microfibrils. The cracks grow in the draw direction as the spherulite is elongated and the microfibrils grow by pulling out more blocks from the lamellae. Gradually, the microfibrils originating from the same crack coalesce into a fibril.

As deformation proceeds, lamellae between 45° and the spherulite equator are positioned into a 45° orientation and transformed into microfibrils. Lamellae oriented perpendicular to the draw direction at the spherulitic equator experience a shear stress due to variation in deformation from the center to the perimeter of the spherulite.[34] These lamellae are broken into blocks which are offset from each other by the shear field. These blocks combine with blocks of adjacent lamellae similarly arranged to form skewed microfibrils. Lamellae oriented parallel to the draw direction undergo greater chain slip and tilt before breaking into blocks and forming microfibrils.

A lamellar stack is comprised of five-to-ten parallel lamellae connected by tie molecules.[34] All the lamellae in the stack experience the same stress field and deform into individual microfibrils possessing the same draw ratio. These microfibrils then coalesce into a fibril. Stacks in different locations in the spherulite experience different stress fields and deform to different draw ratios. Thus adjacent fibrils may have different draw ratios which lowers their adhesion and promotes fibrillar slip.

Folds at the ends of the blocks are extended forming intramicrofibrillar tie molecules traversing several crystalline block and amorphous regions. As the draw ratio is increased, yet more tie molecules form and eventually they then limit deformation. Tie molecules joining lamellae in stacks in the initial morphology are maintained to form intermicrofibrillar tie molecules. However, their concentration is lower than that of intramicrofibrillar tie molecules. Interfibrillar tie molecules also are formed from tie molecules connecting adjacent stacks in the initial morphology. The blocks anchoring the molecules restrict their motion

and maintain them in high energy conformations.[35,36] They provide the high moduli characteristic of drawn fibers.

This stage of deformation continues until a draw ratio of 9 to 10. At this point the microfibril is prevented from further extension by the intramicrofibrillar tie molecules formed.[34] However, a substantial amount of deformation can still occur since draw ratios greater than 30 have been obtained.

Deformation - Stage 3

The third stage of deformation involves drawing of the fibrous morphology. It is the latter stage of the necking process and corresponds to the increase in stress with increasing strain at the end of the stress-strain curve. At its completion the neck will have reached its final diameter.

Further deformation proceeds by fibrillar and not microfibrillar slip for several reasons. The microfibrils have aspect ratios of approximately 1000, ~10 times that of the fibril. This increases their frictional resistance to shear displacement tenfold relative to that of the fibril. Adjacent microfibrils within a fibril are better packed, due to having the same draw ratio, than adjacent fibrils which have different draw ratios. There are few tie molecules at the ends of fibrils to transmit axial stress to the next fibril.[23] This also facilitates their longitudinal displacement. Therefore, although a limited amount of microfibrillar elongation and shear does occur, the majority of further deformation is due to interfibrillar shear.

The final diameter of the neck is limited by the morphological changes which occur during fibril displacement. Shear displacement between adjacent fibrils smooths their interfacial surface promoting

adhesion and giving a small increase in resistance to further shear. Interfibrillar shear also produces a relatively small amount of inter-microfibrillar shear and crystalline block deformation by transmission of the shear force into the fibril. However, this results in an enormous increase in the number of tie molecules per cross-sectional area through extension of existing tie molecules across more crystalline and amorphous regions.[23] Extended tie molecules in amorphous layers may coalesce to form crystalline bridges amplifying their enhancement of tensile modulus. However, this process is limited by their high surface-to-volume ratio and requires high undercooling. When sufficiently low temperatures are reached, the mobility needed to bring the separated tie molecules together is lost. Block deformation merges the crystalline and amorphous regions evolving a more uniform stress field and a more continuous crystalline structure. The result of these morphological changes is an increase in sample modulus and resistance to further deformation. Eventually the stress required for deformation will exceed carbon-carbon bond strength and molecular and bulk fracture occur.

Fracture

Fracture results in separate fibers of various length and thickness, reflecting inhomogeneity in the initial sample morphology and stress field. The inhomogeneities produce variations in draw ratio between adjacent fibrils which inhibit packing and lower adhesion. Fracture is initiated at vacancies located at the ends of individual microfibrils where there are few tie molecules spanning these vacancies to transmit axial stress.[37] Tie molecule scission occurs in the weakest region forming microcracks. Axial stress is transferred to adjacent microfibrils

through their adhesion to the affected microfibril. The total stress must now be borne by the remaining microfibrils causing failure at the next weakest vacancy. Lateral adhesion between fibrils, the product of the relatively few interfibrillar tie molecules formed during deformation and Van der Walls forces, is weak. Catastrophic failure occurs by fibril slippage after cracks have eliminated all end-to-end axial support in the sample.

Necking

Necking is initiated at an inhomogeneity in the sample such as a thinner section or a structural weakness. These regions deform and reduce their cross-sectional area more quickly than other areas of the sample. Stress increases more rapidly causing faster deformation, necking, until strain hardening strengthens the region and forces the neck to an adjacent region. However, the rapid increase in deformation in the neck cannot be accounted for by the decrease in cross-sectional area alone. Several theories have been developed to explain this phenomenon termed strain softening. (Recently the premise of these theories has been questioned by studies using improved instrumentation which has provided evidence that strain softening does not occur in polyethylene.[38])

Vincent[39] and Andrews[40] suggested that initial deformation reduces contact between elements, lamellae in polyethylene, in the sample. This reduces adhesion between the lamellae and lowers resistance to further deformation. Other theories have been reviewed by Capaccio et al[41] and Fatheringham and Cherry.[42] Adiabatic deformational heating proposed by Marshall and Thompson[43] has been eliminated as a possible cause by Vincent[39] and Lazurkin[44] who showed that necking occurs isothermally at

very slow draw rates. Robertson[45] proposed that strain changes the distribution of chain conformations to resemble the distribution found at higher temperatures. This allows deformation to occur more easily. Litt and Koch[46] hypothesized that uniaxial strain increases the free volume in polymers with Poisson's ratio less than 0.5. The extra free volume also lowers the resistance to deformation.

Drawing and high draw ratios can also be obtained without necking under selected conditions. Homogeneous drawing (without necking) can occur at high temperatures, low strain rates, or in the presence of plasticizers.[34] The general deformation mechanism is considered the same, but the three stages of drawing occur simultaneously and throughout the sample in homogeneous drawing. These conditions apparently reduce relative differences in resistance to deformation due to inhomogeneities in the sample. The drawing stress increases continuously with increasing strain as strain hardening gradually occurs. This contrasts with the plateau generated by localized strain hardening maintaining a constant stress as the neck propagates.

CHAPTER II

PROCESSING CONDITIONS AND EXTRUDATE PROPERTIES

Solid-State Extrusion of Polyethylene

Solid-state extrusion is a common metal processing technique[47] which has been applied to polymers with considerable success. High and low density polyethylene, polypropylene, nylon 6, nylon 66, polyethylene terephthalate, polyvinylchloride, polytetrafluoroethylene, and polyoxymethylene have all been successfully extruded.[48] The technique consists of forcing a solid billet through a tapered die under selected conditions of pressure, temperature, and lubrication. The polymer is deformed through shear and elongational flow to a morphology possessing significantly different properties than the original material. The magnitude of the change in properties is a function of the draw ratio, defined as the ratio of the cross-sectional area of the billet to that of the extrudate, and of extrusion conditions.

Comparison of Drawing and Solid-State Extrusion

The deformation mechanism above for drawing is applicable, with minor changes, to solid-state extrusion through conical dies.[34,39] Sample[15,50,51] properties and morphology are comparable and show similar trends with increasing draw ratio. The effects of initial morphology[19,23] and processing conditions also are analogous. Extrudate properties and the effects of extrusion conditions and initial morphology on the extrusion process will be discussed individually in this chapter.

Generally, drawing proceeds by necking. However, observations of the extrusion process during the course of this thesis have shown that extrusion proceeds by homogeneous deformation except when lubrication is used at high (>15) draw ratios. The billet follows the die geometry causing shear flow. This results in a mixing of straight and skewed microfibrils.[34] Peterlin suggested that the extrusion pressure enhances adhesion between fibrils and reduces the volume of vacancies at the ends of microfibrils.[34] This delays fracture allowing higher draw ratios to be achieved. It also should produce higher moduli in extrudates than in drawn samples at equivalent draw ratios. The elimination of light scattering voids at the ends of microfibrils by pressure also explains the transparency of extrudates.

Imada[16] observed that thermal shrinkage begins at lower temperatures for drawn samples than for extrudates. In both cases the strained tie molecules exert a retractive force on crystalline regions. He proposed that shrinkage was due to recovery of taut tie molecules in drawn samples and to thermal motion in crystals in extrudates. This implies that drawn tie molecules are not as closely associated with the crystalline phase as extruded tie molecules. Thus their mobility is not as dependent on mobility within the crystalline phase.

Peterlin[23] suggested that taut tie molecules relax at the higher temperatures used in extrusion by pulling out chain folds. However, as the extrudate exits the heated die, the additional contour length of the tie molecule crystallizes by chain folding onto established crystals. This reestablishes its rigidity and anchors it in the crystalline phase. Thus the extrudate attains high modulus, but shrinkage cannot occur unless the crystals melt. Support for this is provided by the observations that

shrinkage does not occur in drawn samples previously annealed with fixed ends[23] and does occur in samples extruded below the annealing temperature.[52]

Additional work has shown that shrinkage is also prevented by rigid intercrystalline bridges formed by the crystallization of extended tie molecules.[53] At low draw ratios, tie molecule concentration is low and they are widely dispersed. Crystallization is prevented and shrinkage occurs. At high draw ratios, the higher concentration and closer proximity of tie molecules allows crystallization. Intercrystalline bridges are rarely formed in samples drawn to high draw ratios[23] at low temperatures because the mobility required for alignment of the tie molecules is never achieved. The formation of intercrystalline bridges and close association of individual tie molecules with the crystalline phase results in a continuous crystalline morphology which exhibits the dead bend effect.[23] The extrudate forms microcracks and does not recover when bent.

Both drawn and extruded samples fracture into fibrils when drawn. However, fracture caused by extrusion at high draw ratios appears as breaks at oblique angles to the extrusion direction. This indicates shear fracture caused by shear or compressive stresses imposed by the die geometry. Causes of fracture during extrusion will be discussed extensively in Chapter VI. However, it can be concluded that at draw ratios at which unfractured samples can be obtained, the deformation process and properties produced by extrusion and drawing are similar.

Effect of Extrusion Conditions

Introduction

Extrudate properties are determined by draw ratio, extrusion temperature and pressure, lubrication, initial morphology, and die geometry. Extrusion rate and the maximum draw ratio obtainable are also controlled by these conditions. Knowledge of the effects of each of these variables is required to select a combination which would produce desired properties or attain the ultimate properties of the material. In this chapter the effects of these factors on maximum draw ratio and extrudate properties will be reviewed individually. To begin, the effect of draw ratio on extrudate properties will be reviewed to establish a point of reference.

Draw Ratio

The high density polyethylene used in this study, Alathon 7050 (DuPont), has previously been extruded under a variety of conditions by Porter and co-workers.[18-20,49] The effect of draw ratio on thermal and tensile properties, orientation, birefringence, and extrusion rate and pressure were measured. Extrusion rate decreases with increasing draw ratio at constant extrusion pressure.[18] Concomitantly, extrusion pressure increases with increasing draw ratio at constant extrusion rate. This behavior reflects the additional work required for greater deformation and to overcome strain hardening which increases with draw ratio.

Birefringence,[51] a gauge of chain isotropy, was measured along the fiber direction. It increases with draw approaching a limit at a draw ratio of ~15. Crystalline and amorphous orientation and rate of orientation were evaluated from c-axis (chain axis) wide angle x-ray (WAXS) and birefringence data. The crystalline phase is more highly

oriented, orients more rapidly, and reaches a constant orientation at a lower draw ratio than the amorphous phase. The lower orientation of the amorphous phase is predominantly due to chain ends, loose loops, and folds which comprise approximately 96%[53] of the amorphous phase. They cannot be oriented as well as tie molecules which are expected to have almost perfect orientation,[54] $f \simeq 1$, similar, indeed indistinguishable, from the crystalline phase. At higher draw ratios, amorphous orientation increases after crystalline orientation has become constant.[51] This supports Peterlin's model of deformation occurring by interfibril slip at high draw ratios. The number of tie molecules increases with draw ratio, raising their proportion in the amorphous phase and consequently increasing the average amorphous orientation. WAXS diffraction patterns also show monoclinic phase reflections which increase with draw ratio and an initial a-axis orientation perpendicular to the fiber axis also found in drawn samples.

Small angle X-ray (SAXS) was used to measure long period and scattering intensity.[51] Extrusion to a draw ratio of 30 decreases the long period approximately 60 Å. This may be caused by the preferential unfolding of lamellae with higher long periods due to their more uniform structure facilitating deformation. The long period is calculated from the scattering maximum. Greater reduction of higher long periods shifts the maximum to a shorter long period. However, the trend of decreasing long period with increasing draw ratio has not been universally found. Although Kojima et al[55] and Nakayama and Kanetsuna[56] showed similar results, Farrel and Keller[57] found no change in hydrostaticly extruded samples and Capaccio[41] showed a slight increase in long period with increasing draw ratio in drawn samples. This inconsistency may be

due to small real changes being obscured by experimental error.

The X-ray scattering intensity of the sample decreases with increasing draw ratio. This could occur by a reduction in chain fold concentration or dispersion of folds in a continuous crystalline-amorphous matrix. This supports Peterlin's contention that folded chains in the microfibril unfold under shear stress at high draw ratios and mix with the amorphous phase. The concentration of folds is reduced and boundaries between crystalline and amorphous regions are dissolved, forming a continuous matrix. The difference in density between the crystalline and amorphous phases is reduced decreasing the X-ray scattering.[58]

Thermal properties consist of melting point, per cent crystallinity, and melting peak width, all obtained from differential scanning calorimetry (DSC); linear expansion coefficient (α) below the melting point from thermal mechanical analysis (TMA); and per cent shrinkage measured by dimension changes after rapid melting. The width of the melting peak reflects diversity of morphology in the sample. The observed narrowing of peak width with draw ratio is the result of the transformation of crystals of various sizes into the more uniform microfibrillar structure. Both crystallinity and the melting point increased rapidly to a draw ratio of 15, then slowly reached a limit at higher draw ratios.[51] Peterlin[59] observed a similar trend in drawn polyethylene. He proposed that chain elongation during drawing is accomplished by transformation of gauche bond conformations to trans which exist at a lower energy state. Elongation promotes chain adhesion through increased surface area causing the formation of crystalline bridges from originally amorphous chains. The slow increase in melting point and crystallinity above draw ratio 15, the third state of deformation, indicates that microfibril formation is

responsible for the majority of the increase. It also suggests that interfibrillar slip does not significantly improve packing and there is either low crystalline bridge formation or a counteracting decrease in crystallinity through shear deformation of crystalline blocks.

Thermal expansion coefficients measured along the fiber axis were positive at low draw ratios, decreased, and became negative with increasing draw ratio.[60] The draw ratio at which α became negative increased with increasing extrusion temperature. Baughman and Turi[61] showed that the absolute value of the negative crystalline lattice coefficient is 5% of the positive amorphous coefficient. Therefore samples with amorphous fractions greater than 5%, such as extrudates, which are approximately 16% amorphous, should have an overall positive coefficient. Falender and Hansen[62] proposed that the negative α is due to retraction of strained tie molecules and a thermodynamic force to reduce the crystalline surface area, expanded by extrusion, to obtain a surface-to-volume ratio of lowest energy. Kojima[55] suggested that α decreases as the morphology becomes more similar to that of a perfect crystal with increasing draw ratio. However, the decrease in α with decreasing extrusion temperature indicates the amorphous phase determines α since crystalline perfection decreases and tension in the tie molecules increases at lower extrusion temperatures. Mead et al[60] observed a plateau in α at high draw ratios and Kojima showed only a linear increase in α with draw ratio. Therefore, α appears to be more dependent on extension of tie molecules which should increase linearly with draw ratio than the number of tie molecules per cross-sectional area which increases more rapidly. However, the correct mechanism is unclear.

Shrinkage is a measure of the efficiency of the deformation process relating elongation by chain extension to total sample elongation. Deformation can occur by chain unfolding and extension, chain scission, and viscous dissipation. However only chain extension maintains a retractive force which acts to return the sample to its original length upon melting. Therefore, increased shrinkage indicates greater morphological continuity which should correlate with higher moduli, as has been found.[63] Morphological changes should produce analogous results in α and in shrinkage, barring viscous dissipation during retraction in shrinkage. Per cent shrinkage was indeed found to decrease at higher extrusion temperatures corresponding to the higher α found at higher extrusion temperatures. However, no change in per cent shrinkage was found among extrudates of draw ratio 12, 24, and 36 although the samples shrunk less than 50% in length. Since considerable viscous dissipation does occur, it is expected that more would occur at higher draw ratios. A possible explanation is that all dissipation occurs during microfibril formation which is nearly complete at a draw ratio of 12. Fibril slip would then have to be completely elastic, which is unlikely. Capaccio[41] observed greater per cent shrinkage at a draw ratio of 10 than at a draw ratio of 20. Further studies are needed to draw valid conclusions.

Tensile modulus and strength are the final properties to be discussed in this section. Modulus increased slowly until approximately a draw ratio of 15 and then more rapidly and linearly with increasing draw ratio.[60] Capaccio[41] obtained similar results from hydrostaticly extruded and drawn samples. This implies that modulus is predominantly determined by taut tie molecules and not the folded-chain crystalline region. Melting point, crystallinity, total birefringence, and crystalline orientation,

all functions of the crystalline phase, reach plateaus at a draw ratio of ~15. The transition to a more rapid increase in modulus represents the conversion to deformation by fibril slip which greatly increases the concentration of tie molecules and consequently the resistance to further deformation.

Tensile strength increased with draw ratio reaching a limit at a draw ratio of ~15.[64] Peterlin proposed that the few axial tie molecules at the ends of microfibrils are the weak links which limit tensile strength. However, they have little effect on modulus.[65] The increase in tensile strength to draw ratio 15 is due to the formation of more microfibrils which increases the number of axial tie molecules.[66] This lowers the tensile stress imposed on each individual axial tie molecule and higher tensile strengths are obtained. Stress concentration factors at the tips of microcracks may also be reduced through the decrease in crystallite width and increase in distance between crystallites with higher deformation.[67] Deformation beyond draw ratio 15 is through interfibrillar slip. This increases the concentration of tie molecules but the number of axial tie molecules remains constant. Thus modulus continues to increase with draw ratio, but tensile strength becomes constant.

The effects of extrusion pressure, temperature, and rate, initial morphology, lubrication, and die geometry on extrudate properties will be examined individually in the following sections. However, it will be seen that these factors are interrelated. A change in one will induce changes in the other variables making it difficult to unambiguously identify cause and effect relationships. In addition to these subjects, variation in properties across the extrudate's diameter and pultrusion, a modification of the extrusion process in which a pulling force is attached to the

emerging extrudate, will be discussed.

Extrusion Temperature

Several researchers have obtained similar results and reached conclusions concerning the effect of temperature on the extrusion process. Generally higher temperatures enable higher draw ratios to be obtained. However, there is an optimum temperature, believed to be associated with the α-transition, which yields the highest modulus even though higher draw ratios can be obtained at higher temperatures.

In a study of polyethylene, Mead et al[66] observed an increase in crystalline orientation, crystallinity, and maximum draw ratio with increasing extrusion temperature. However, amorphous orientation decreased, the thermal expansion coefficient increased (became less negative), and modulus at constant draw ratio decreased. The highest modulus was found on extrusion at draw ratio 40 at 132°C, greater than that of an extrudate of draw ratio 46 extruded at 136°C. An optimum temperature for obtaining the highest modulus was observed by Peiffer[68] and by Farrell and Keller[57] in extruded polyethylene, by Taylor and Clark[69] in superdrawn acetal resin, and by Cansfield et al[70] in drawn and by Muruyama[71] in extruded polypropylene. They also concurred on the mechanism through which temperature affects the deformation process. Each author associated the optimum temperature with the α-transition of their respective polymer. Mead's results show that modulus is determined mainly by the amorphous phase (containing taut tie molecules) as crystalline properties increase but amorphous properties and modulus decrease with increasing temperature at constant draw ratio. Below the α-transition, deformation is confined to the amorphous phase. Modulus at constant draw ratio increases as temperature decreases but only low

draw ratios can be obtained. Stress is concentrated on the few amorphous tie molecules, causing fracture at low deformation. As temperature increases above the α-transition, mobility in the crystalline phase increases enabling higher draw ratios to be obtained. However, the increased mobility allows taut tie molecules to relax by slipping through their crystalline anchors. Shear stress is less efficiently transferred to microfibrillar crystalline blocks resulting in less chain extension and only a small increase in tie molecule concentration. Thus modulus does not increase linearly with draw ratio at high temperatures.

At the α-transition, crystalline motion begins. Extrusion at this temperature allows higher draw ratios and consequently greater concentrations of tie molecules to be obtained with the minimum loss of amorphous orientation. Thus the highest modulus is obtained at this temperature. In polyethylene the α-transition has been reported in the range of 80 to 110°C.[68,57,15] Although the optimum temperature of 132°C from Mead's study is high, his conclusions are the same as just presented. Additional evidence for the influence of the α-transition on the deformation process was given by Mead and Porter[18] who found a sharp decrease in the activation energy required for the deformation process above 110°C. This was attributed to a change in the molecular mechanism for deformation. This can now be explained as the shift from amorphous chain stretching to large scale crystalline chain axis slip as the predominant deformation mechanism.

Extrusion Pressure

Extrusion pressure affects both the properties of the billet and the subsequent extrudate. It may act as either a hindering or an activating

force for deformation, depending on other extrusion conditions. Several authors have studied the effects of hydrostatic pressure on the drawing of polyethylene.[72-77] Spitzig and Richmond[76] observed a linear increase in tensile yield stress and modulus with increasing pressure which could be mathematically represented by equations similar to the Coulomb yield criterion. They showed that yield stress is equivalent in tension and compression. The experimentally found higher compressive yield stress is due solely to the pressure dependence of yielding. The tensile modulus and strength of extrudates[78] and shear yield stress of undeformed polyethylene[77] also have been shown to increase with hydrostatic pressure. Pressure reduces the macroscopic volume and free volume[72] which increases secondary forces and hinders motion. Thus greater stress is required to initiate and sustain any molecular motion. This is also reflected in the increase in the γ, β, and melting transitions of 5, 16,[79] and 20°C[80] per 1000 atm. respectively. The greater effect of pressure on the amorphous phase than on the crystalline phase was also shown by Silano et al[81] who found a greater increase in modulus in low density polyethylene than in high density polyethylene.

Pugh[74] found a 920% increase in fracture stress but only a 290% increase in yield stress at constant pressure while the stress-strain diagrams of Mears et al[82] showed comparable increases in fracture and yield stresses. Mears also observed that pressure altered the deformation pattern and decreased elongation at fracture. Localized necking continued, producing a very narrow neck which then fractured, instead of propagating along the sample as at atmospheric pressure. Spitzig and Richmond[76] and Trent et al[83] attributed this behavior to the pressure medium used. They found no change in deformational behavior or elongation at fracture

when the sample was jacketed, separating it from the pressure medium. They concluded that fluids which are inert at atmospheric pressure can act as stress cracking agents at higher pressures. Therefore, although hydrostatic pressure makes deformation more difficult, it does not appear to affect the maximum draw ratio.

Pressure may also act as an activating agent for deformation. Mead and Porter[18] have shown that the elongational viscosity, the ratio of extrusion pressure to extrusion rate, decreases with increasing pressure. Shimada et al[84] found a linear increase in ln (extrusion rate) with increasing pressure. This behavior is consistent with the yield theory of Eyring[85] who proposed that flow occurs when a molecular segment acquires sufficient energy to surmount a potential energy barrier. Shear stress lowers the barrier by raising the initial energy state and Eyring predicted a logarithmic relationship between viscosity and shear stress. Deformation profiles show that extrusion does proceed predominantly through shear flow.

Additional support for the application of Eyring's theory to solid state extrusion is provided by the occurrence of slipstick extrusion at low draw ratios under high pressure. Pressure builds, increasing the extrusion rate, and then drops sharply accompanied by a surge of opaque, curled extrudate. Distortions in the extrudate, melt fracture, are also observed when melts are extruded rapidly. Blyer and Hart[86] proposed that this occurs when the critical value of the melt elastic strain energy is exceeded causing deformation between layers of polymer near the die wall. The similarities in extrusion behavior suggest that crystalline slipstick extrusion may be due to at least some segments acquiring the energy and mobility of segments in the melt through high shear stresses created in

the extrusion die.

Whether pressure activates or inhibits flow depends on other extrusion conditions. Shimada[84] observed that decreasing the extrusion temperature diminished the accelerating effect of increasing pressure on the extrusion rate. Mead and Porter[18] found a sharp increase in elongational viscosity at approximately draw ratio 15 where strain hardening begins. It also has been observed in this study that increased extrusion pressure has no effect on rate at high draw ratios. Thus, as extrusion conditions become more difficult, extrusion pressure appears to transform from an activating shear stress to a predominantly inhibiting hydrostatic pressure. A higher percentage of the extrusion pressure must be exerted toward overcoming the increased flow stress and billet-die friction. Hence less pressure is available to increase the extrusion rate.[87] Shimada[84] calculated activation energies for flow at various pressures at a draw ratio of 30. He found an increase in the activation energy needed for flow with increasing pressure indicating that the pressure acted as an inhibiting force. This trend may be reversed at low draw ratios before strain hardening has occurred.

The effect of pressure on extrudate properties is obscured by its concomitant effect on the extrusion rate and by its possible effect on the actual extrusion temperature in the die. It is unknown whether pressure is acting as an accelerating or an inhibiting force. The pressure drop and distribution within the die are also unknown. Capiati and Porter[88] observed an increase in modulus with pressure. This may be due to a decrease in the actual extrusion temperature through undercooling or to the faster extrusion rate decreasing relaxation of tie molecules by decreasing annealing time at the high extrusion temperature. Mead and

Porter[89] found that the tensile properties of an extrudate decreased after annealing. The observed increase in total birefringence and more negative thermal expansion coefficient with increasing pressure may also be explained by either of the mechanisms. Peterlin proposed that extrudates have higher moduli than drawn samples of the same draw ratio due to better fibrillar packing with increased pressure.[34] In conclusion, of the several possible mechanisms through which pressure improves tensile properties, the true cause or combination of causes is not clear.

Peterlin[34] proposed that pressure allows higher draw ratios to be achieved by extrusion than by drawing. Buckley and Long[90] reported that ductility in the amorphous phase increased under hydrostatic pressure. However, the maximum draw ratio obtained by both drawing and extrusion is dependent on initial morphology[19,91] and processing conditions.[60,41] Drawn and extruded samples of the same polymer processed under identical temperature and strain rate have not yet been prepared. Furthermore it is possible that higher draw ratios will be obtained by both processes through additional modifications. Therefore, no conclusions can be drawn concerning the effect of pressure on the maximum draw ratio at this time.

Lubrication

The effect of lubrication between the die and billet surfaces has been widely investigated. Lubrication can be accomplished in ram extrusion by coating the die and/or billet and by hydrostatic extrusion in which the pressure medium acts as a lubricant. Perkins,[48] using Teflon spray as a lubricant, achieved higher draw ratios without loss of properties. Pradecki and Statton[17] also obtained higher draw ratios and reduced extrusion pressures again using a fluorocarbon lubricant.

However, they observed a decrease in modulus and transparency. They concluded that lubrication reduces friction which decreases shear flow and increases elongational flow. The total deformation process becomes less efficient resulting in a reduction in properties. Reduced friction would be expected to decrease shear stresses and change the billet deformation pattern. However, Kanamoto et al[92] did not find an increase in extensional flow in the deformation profile of extruded polyethylene using lubrication.

The pressure medium in hydrostatic extrusion can act as a lubricant and as a plasticizer. Davis and Pampillo[75] found that the tensile properties of polyethylene under hydrostatic pressure varied with the pressure medium used. They concluded that the medium is absorbed and plasticizes the sample altering its tensile properties. Williams[93] reported that hydrostatic extrusion gives smoother extrudate surfaces than ram extrusion and Davis[94] found that die lubrication also improves the surface appearance of hydrostaticly extruded samples. Gupta and McCormick[95] and Nakayama and Kanetsuna[96] observed that friction between the die and billet and consequently the minimum pressure required for extrusion were a function of the pressure medium.

The effect of lubrication on melt extrusion has also been examined. Shaw[97] reported that lubrication decreases the pressure drop in the die during extrusion. It also changes the balance of shear and extensional forces resulting in more extensional flow. He concluded, as did Everage and Ballman[98] in a related study, that increased extensional flow produces high tensile stresses which lead to fracture.

In conclusion, except for the loss of extrudate transparency observed by Pradecki and Statton, lubrication has been shown to improve extrudate appearance. It also reduces friction, which may enhance

extensional flow, and can act as a plasticizer. The effect on extrudate properties is uncertain. At constant extrusion pressure, lubrication increases the extrusion rate which may decrease annealing and improve properties. However, it also decreases deformation time which is necessary to obtain high draw ratios. (The effects of annealing and deformation time will be discussed extensively in the section on extrusion rate.) The increase in extrusion rate may also be due to the shift to increased extensional flow and may not be detrimental to the formation of high modulus structures. It is also unknown if extensional flow will similarly cause fracture in solid-state extrusion as it does in melt extrusion.

Morphology

The deformation process during solid-state extrusion and drawing is a series of morphological rearrangements, ultimately limited by morphologies which fail under the force necessary to continue deformation. Therefore, it seems likely that the initial morphology, determined by molecular weight, molecular weight distribution, and crystallization conditions, should influence the deformation process, maximum draw ratio, and modulus at a constant draw ratio. Porter and coworkers[19,99] have studied the effects of initial morphology on extrusion and extrudate properties whereas Ward[41] has concentrated on its effects on drawing.

Capaccio et al[41] have reviewed the work of Ward and coworkers on drawing. Initially, samples of various weight average molecular weight, M_w, which were either quenched or slow cooled from the melt, were drawn under constant conditions of temperature, strain rate, and time.[90] Higher draw ratios were obtained at equivalent drawing times from samples of lower M_w and from slow cooled samples at equivalent M_w. The

effect of crystallization conditions decreased as M_w increased. These results indicate that higher crystallinity obtained at lower M_w and by slow cooling promotes deformation. However, in a later study, a quenched sample annealed to approximately the same crystallinity as a slow cooled sample exhibited drawing behavior intermediate between the two extremes.[100] Furthermore, as M_w was increased, the effects of annealing were reduced. It was concluded that drawing behavior is determined primarily by coarse changes in morphological topology produced by initial crystallization conditions and secondarily by the level of crystallinity. Reducing both M_w and undercooling lowers the melt viscosity and allows more uniform crystallization. Deformation is facilitated by the more orderly structure and reduction of tie molecules[101,102] between crystalline regions and entanglements within amorphous regions. Highly crystalline, low molecular weight material in samples with a broad molecular weight distribution (MWD) may aid deformation by facilitating alignment[103,104] and by its comparitively easy deformation. However, the effect of number average molecular weight is relatively minor to that of M_w.[41]

As M_w is increased, the slower deformation of the amorphous fraction begins to control the overall drawing behavior and reduces the maximum draw ratio.[101,105,106] However, high draw ratios can be obtained by increasing the drawing time or temperature.[107-109] Therefore, it was proposed that the initial morphology is a network of semipermanent junction points consisting of crystalline regions and amorphous entanglements which have similar effects on drawing behavior.[41] This concept is supported by several findings. A correlation was found between increasing draw time to reach a constant draw ratio and decreasing melt flow index (MFI) of samples of various M_w and MWD.[106] Yield stress was found to be

independent of M_w. Capaccio and Ward[110] observed that crosslinks produced by sample irradiation had a comparable effect on drawing behavior as increasing M_w. Finally, several studies have associated the optimum drawing temperature for maximum modulus with the α-transition.[57,60,68] However, further work has shown that the optimum temperature is increased for ultra-high molecular weight samples[104] even though the α-transition probably decreases due to the less perfect crystalline structure of these samples. It was proposed that optimum drawing occurred at temperatures producing comparable levels of internal viscosity.[108] However, the maximum modulus at the optimum temperature decreased with increasing molecular weight, indicating less efficient deformation.

The effectiveness of the deformation process can be directly related to tensile modulus. Moduli of samples drawn to the same draw ratio and temperature were found to be independent of M_w and crystallization conditions.[106] This suggests that tie molecules formed during crystallization are an insignificant fraction of the total in the drawn sample. However, they may be the initiation sites for fracture which lowers the maximum draw ratio for higher molecular weights. The homogenizing effect of deformation was also reported by Meinel and Peterlin[111] who found equal crystallinity after a draw ratio of 5.0 in samples quenched and quenched-then-annealed. They also observed that the X-ray crystal long period is dependent only on the drawing temperature and independent of the initial long period.

Porter and coworkers have studied the effects of various initial morphologies, including different M_w and levels of crystallinity, single crystals, and extended chain crystals on extrusion and have reached conclusions analogous to those of Ward. Quenched and annealed samples could

be extruded to equal draw ratios and possessed similar moduli at equivalent draw ratios.[19] Bigg et al[112] also observed this behavior. Single crystals obtained from solution and extended chain crystals formed under selective temperatures and pressures both extruded at faster rates and achieved higher draw ratios than folded chain crystals.[99] Again this implies that fewer entanglements and a more regular structure promotes deformation. However, extended chain crystals produced unfractured extrudates only at $M_w \geq 147 \times 10^5$ possibly due to stress concentrations caused by segregation of low molecular weight material to spherulitic boundaries and a reduction of interspherulitic tie molecules. Tie molecule concentrations sufficient to transfer stress and prevent brittle fracture between spherulites are produced during crystallization of high molecular weight samples.[113-116] The highest moduli were obtained from samples with an optimum combination of folded and extended chain crystals. This suggests that crystals act as junctions able to transfer stress between extended chains more efficiently than Van der Walls forces.

Several authors have studied the effects of M_w on extrusion. Perkins et al[117] reported that extrusion rate decreased but modulus was unaffected by increasing M_w. Hope et al,[118] performing a similar study, found that the maximum draw ratio decreased but modulus again was independent of increasing M_w except at ultra-high M_w where it decreased. They found that extrusion rate decreased with decreasing MFI and that maximum properties are produced at an optimum MFI and extrusion temperature. Gibson and Ward,[119] in conventional extrusion, and Zachariades et al[120] coextruding two different molecular weights, also found a similar correlation between extrusion rate and MFI.

In conclusion, it has been shown that deformation by both drawing and extrusion is controlled by a network of junctions represented by an MFI. Crystalline regions dominate deformation at low M_w whereas amorphous entanglements are ascendant at higher M_w. Properties are independent of M_w in the range 60,000 to 250,000[41] and of initial crystallinity. Ultra-high M_w and extended chain crystals do affect the deformation process but, in general, properties are determined by morphologies, microfibrils, produced by the deformation process which are insensitive to the initial morphology.

Die Geometry

Extrusion dies used here are composed of a cone leading into a cylindrical capillary. Extrusion rate and pressure and extrudate properties are all affected by die geometry. Several approaches to metal extrusion analysis have been developed which predict the effects of die angle and surface, capillary length, draw ratio, and pultrusion on frictional and redundant work and consequently extrusion pressure. They include pressure balance, slip line, and upper and lower bound analysis. Numerous authors have quoted and adapted original work in this field. Direction to the original work may be found in references 47 and 121-123. Discussion of individual methods is beyond the scope of this thesis. Therefore, only their predictions, which are generally consistent, will be presented and explained through upper bound analysis. Metal extrusion analysis techniques have been adapted to polymer extrusion with modifications for the effects of strain rate, strain hardening, and hydrostatic pressure, as will be discussed.

In upper bound analysis, the work imparted to the system by the extrusion pressure must equal work expended during extrusion consisting

of billet deformation, overcoming billet-die and billet-barrel friction, and redundant strain, changing the direction of flow at the cone entrance and exit. The effect of die geometry on extrusion pressure can be understood by examining its individual influence on each of these three components. Pressure is predicted and experimentally found to be proportional to true strain and increases linearly with the logarithm of draw ratio in non-strain hardening materials.[123]

Friction is also increased by the larger die surface area at higher draw ratio. Work lost to friction can be modified by lubrication,[98] die material, and extrusion temperature. Hardened steels and tungsten carbide can be more highly polished than softer metals such as brass and have lower coefficients of friction. Capillary length has a negligible effect on extrusion pressure when well polished dies are used.[47] Higher extrusion temperatures have also been found to reduce friction.[98] Larger die angles reduce die surface area and friction. However, work lost to redundant strain is increased.

Pugh[123] showed that the pulling stress in pultrusion reduces compressive stresses in the die and consequently billet-die friction. Thus less work is consumed per unit volume of extrudate in pultrusion than in extrusion. Pressure not consumed by friction can be used to increase the extrusion rate explaining the higher extrusion rates obtained by pultrusion than by extrusion at equivalent total pressures. Pugh's analysis also predicts that the effect of pulling will increase with increasing draw ratio and coefficient of friction and that pulling and pushing stresses should produce equal extrusion rates in the absence of friction. These predictions are based solely on billet-die friction and not on the increase in yield stress with hydrostatic pressure.

Shimada et al[84] reached similar conclusions in an analysis of pultrusion.

Metal extrusion analysis has been adapted to the extrusion of polymers. Imada et al applied pressure balance,[124-126] slip line,[125] and upper bound analysis[71] using the stress-strain characteristics of the polymer during drawing to compute the work of deformation. Strain hardening was also accounted for except in slip line analysis. Agreement between calculated and experimental values of extrusion pressure with increasing draw ratio was good in all analyses. However, only slip line analysis correctly predicted pressure to increase with increasing die angle. Kolbeck and Uhlman,[127] following Imada's upper bound analysis and neglecting friction, were able to predict the increase in pressure with die angle and maintained reasonable agreement with experimental extrusion pressures. Snelling and Lontz[128] successfully calculated extrusion pressures including only terms for strain hardening and strain rate effects.

Coates et al[87] reported an analysis employing the lower bound method modified to account for the effects of strain rate, strain hardening, hydrostatic pressure, and redundant strain on the flow stress. They showed that extrusion pressure increased more than linearly with the logarithm of draw ratio due to increasing strain hardening and strain rate and proposed that a trumpet shaped die would enhance extrusion rates by maintaining a constant strain rate with increasing draw ratio. Redundant work was negligible at a die angle of 15^{o} and friction became increasingly important as draw ratio increased. Under circumstances in which pressure does not increase the extrusion rate, such as high draw ratio, increases in pressure are completely absorbed by the additional pressure required to overcome the accompanying increase in surface friction and flow stress.[87] Gupta and McCormick[95] used a similarly

modified upper bound approach. They predicted an optimum angle of 16^{o}, which could be shifted by lubrication, at a draw ratio of 6.75 and an extrusion rate of 1 mm/min. Their results are similar to those of Coates except for a higher level of work expended for redundant strain.

In summary, the different methods of analysis are surprisingly predictive considering the variation in assumptions made and differences in the relative contributions of deformation, friction, redundant work, strain hardening, strain rate, and hydrostatic pressure to the total extrusion pressure. However, the best results are obtained when all of these factors are taken into consideration.

Studies of the effect of die geometry on extrudate properties have centered on the effects of die angle. Nakayama and Kanetsuna[129] observed that density increased but orientation was constant with increasing die angle. They also experimentally found that the die angle requiring the lowest extrusion pressure decreased with increasing draw ratio to the lowest angle used of 20^{o}. Pradecki and Statton[17] observed that higher draw ratios could be obtained at lower angles but that modulus and transparency were reduced. They proposed that low angles and lubrication increased elongational and decreased shear flow. However, maximum properties are obtained by an optimum combination.

Perkins[48] conducted an extensive study of die angle on extrusion characteristics and extrudate properties. He proposed that elongational flow is enhanced at large die angles. However, deformation profiles from low angle dies[60] and lubricated dies in both solid[83] and melt[97] state extrusion show that elongational flow is enhanced at smaller angles. Deformation profiles during drawing, corresponding to a 0^{o} angle, of course exhibit purely extensional flow.

Perkins observed a decrease in extrusion rate but an increase in maximum draw ratio with increasing die angle. Birefringence, tensile modulus, and tensile strength were at a maximum between 20 and 30°. The thermal expansion coefficient was at a maximum between 30 and 90° while melting point and crystallinity were constant except for a decrease at 120°. Higher molecular weight shifted the optimum angle to a lower value for all characterizations. This evidence, considered with the previously presented results, indicates that lower angles allow faster extrusion rates and higher draw ratios through either greater elongational flow or a lower strain rate. It will also be shown in Chapter VI that the angle between the cone and capillary is a major cause of extrudate fracture. Biggs[15] proposed this was due to high localized elongation at this corner as illustrated by slip line analysis.

The increase in maximum draw ratio in Perkins' study is in disagreement with observations by Kolbeck and Uhlman,[127] Pradecki and Statton,[17] and in this thesis and is unexplained. An optimum combination of shear and elongational flow, dependent on molecular weight and the property, may be necessary to obtain optimum properties. Shear stress may be transferred to microfibrillar crystalline blocks resulting in an increase in tie molecule concentration and improved properties. However, high shear stress at large angles may cause chain fracture and reduce properties before becoming evident as macroscopic fracture.

Pultrusion

Pultrusion is a variation on the extrusion process in which a pulling force is attached to the emerging extrudate. The method has been demonstrated by Shimada[84] and by Hope.[118,130] A similar approach,

die drawing, in which only a pulling force is used to draw a billet through an extrusion die, has been developed by Ward and coworkers.[131,132] These processes offer advantages over the conventional extrusion process. Pultrusion will be discussed here and in the experimental section.

Both Shimada and Hope showed that the extrusion rate increased with the addition of a pulling force. Shimada observed that λ, the ratio of pushing to pulling pressures which produce equivalent extrusion rates, was 2.9. Thus, pressure when applied by pulling is a more effective deformational force than when applied by pushing. This relationship was valid at all extrusion rates and combinations of pushing and pulling pressures and allowed superposition of plots of extrusion rate versus various combinations of pushing plus pulling pressures. Pultrusion allowed the achievement of higher extrusion rates without fracture than could be obtained by extrusion, indicating that stress concentrations associated with high strain rates are reduced. There was no significant difference in tensile moduli between extruded and pultruded samples implying similarity in final morphology. This is expected since Peterlin found little morphological difference between drawn and extruded samples. Shimada also found extrudate modulus to be independent of the total applied extrusion pressure. This indicates that extrusion pressure does not act as a hydrostatic force by lowering the effective extrusion temperature. If this were the case, an equivalent total effective pressure, pushing plus 2.9 times pulling pressure, consisting of a higher percentage of pulling pressure should produce a higher extrusion rate but a lower modulus since undercooling is reduced. The independence of modulus from pulling pressure also implies that annealing is completed while the sample length is maintained by compressive stress. Therefore it appears

that a pulling force acts as an independent and more effective deformational force than a pushing force.

The ability of a pulling pressure to produce faster extrusion rates than an equivalent pushing pressure has been mathematically explained by Pugh[123] and by Shimada by a reduction in billet-die friction. Several intuitive explanations will be given here. Polyethylene's folded chain structure can be roughly compared to a rope folded or coiled in a regular pattern with limited adhesion between adjacent sections of rope. Conceptually, it is easier to break the adhesion, unfold, and pass the rope through an orifice smaller than the diameter of the entire structure by pulling than by deforming and forcing the structure through by pushing. In pultrusion, the structure is pulled and compressed against the die wall. Folds away from the die exit partially deform and partially act as a fixed end promoting a more tensile deformation of folds in a zone closer to the exit. Application of the pulling force has been observed to cause necking in experimental work for this thesis. Less work is lost to structural transformations and compression, modes of deformation which do not contribute to the extrusion rate. The net result is a more efficient use of pulling force than pushing force for deformation which produces higher extrusion rates. Although the ends of individual chains cannot be grasped and pulled, a similar deformation process is expected to occur during pultrusion of polyethylene.

The greater effectiveness of a pulling pressure can be visualized in other ways. During extrusion the effective pressure decreases as the die exit is approached. Thus there is less deformational force at higher draw ratios where strain hardening and increased strain rate have increased the stress needed for deformation.[87] Pulling places the greatest

deformational force at the die exit. A decrease in pulling pressure proceeding into the die is not as detrimental to the deformation process because deformation is becoming increasingly easier. Motion is more continuous throughout the die and the extrusion rate is increased.

Pugh showed that pulling stress decreases compressive stresses in the die which reduces work diverted to overcoming friction and allows the total pressure to be used more efficiently for billet deformation. Reduction in compressive stress also reduces the increase in flow stress with pressure.

With these mechanisms in mind, predictions can be made concerning the effect of extrusion conditions on λ. It is expected that λ will increase with draw ratio. Necking, caused by the pulling force, should occur at the same strain in the die independent of the die draw ratio. As the die draw ratio increases, greater deformation will occur without a corresponding increase in friction or pressure acting as a hydrostatic force inhibiting deformation. Therefore λ should increase. Larger die angles should also enhance λ. Pultrusion combines the deformational flow patterns of shear from the die geometry and elongation from drawing. Extrusion becomes more difficult at higher angles because greater shear flow is required. Therefore, the addition of the more facile elongational flow from pulling will have a greater effect. A less crystalline initial morphology is expected to decrease λ since the advantage of pulling is thought to be partially derived from the regularity in structure. Higher temperatures may also reduce λ. Deformation occurs more easily as the temperature is increased. This reduces the difference in deformational efficiency between pushing and pulling. It also prevents the structure from acting as a fixed end. The predictions on the effect of temperature,

die angle, and draw ratio on λ will be examined in the experimental section.

In conclusion, pultrusion has been experimentally shown to be a more effective deformation process than straight solid-state extrusion. These results show that the deformation rate can be increased without a loss of properties and that extrusion pressure does not have a significant undercooling effect, contrary to previous studies on extrusion pressure.[88] Several mechanisms have been offered here to account for the greater effectiveness of a pulling pressure based on the more efficient use of force for deformation by pulling than by pushing. Predictions on the effect of extrusion conditions on λ based on this model will be tested in Chapter V.

Extrusion Rate

In the preceding sections the extrusion rate has been shown to be influenced by pressure, temperature, lubrication, initial morphology, die geometry, and addition of a pulling force. Each of these factors has its own effects on deformation, and consequently extrudate properties, which act in conjunction and obscure the effects of strain rate and annealing time associated with the extrusion rate. However, the influence of extrusion rate can be estimated by drawing samples at different strain rates and annealing extrudates for various times.

A study of extrudate dimensional changes by Mead and Porter[89] showed that annealing begins between 86 and 93^{o}C; Gibson and Ward[133] observed irreversible dimensional changes at 70^{o}C. Large scale structural reorganization occurs above 125^{o}C and splits the DSC melting curve into two peaks. One peak has the same melting temperature as the original

curve and the other is lower. An increase in the total area of the new curve correlates with a decrease in modulus. Annealing also reduces the total birefringence but increases the crystallinity.[108] These results indicate that annealing relaxes taut tie molecules and removes defects from the crystalline region. Slower extrusion rates allow more annealing and consequently should decrease the modulus.

Annealing is reduced by laterally constraining the extrudate.[89] The variation in pressure in the die is unknown. However, high pressures must still exist at the exit of the conical region since deformation occurs. Therefore, higher extrusion pressures may reduce annealing. However, it would be difficult to distinguish between reduction of annealing and increase in tie molecule concentration which may also be promoted by higher extrusion pressures. Increasing the pressure may lower the effective extrusion temperature by increasing undercooling, causing more microfibrillar crystalline block deformation and consequently increasing the tie molecule concentration.

Annealing likely occurs in the die capillary where compressive forces may be low. However, the temperature in the capillary is lower than that in the die due to its exposure to the ambient temperature.[127] This would reduce annealing. Property losses in the capillary region may be reduced by using a pulling force on the emerging extrudate. Annealing with fixed ends has been shown to increase the modulus of drawn samples.[23] The fixed ends prevent the sample from shrinking, but tie molecule relaxation occurs by chain slip through crystalline blocks. However, on cooling, the tautness is recovered by crystallization of the additional conformation length by chain folding onto existing crystals. Shimada[84] did not find an increase in modulus by adding a pulling force

in his pultrusion experiments. However, he also did not observe the normally found increase in modulus with increasing pressure. Therefore his results cannot be unequivocally construed as evidence against the ability of a pulling force to improve tensile properties.

The effect of extrusion rate on deformation can be considered applying the time-temperature superposition principle. Analogous to increasing the temperature, both deformation to high draw ratios and relaxation of tie molecules occur more easily as the strain rate decreases. Above the α-transition, the relaxation process dominates. Although higher draw ratios can be obtained, modulus decreases with increasing extrusion temperature. At lower strain rates, the predominant effect appears to be the deformation process. As stated earlier, longer drawing times are required to draw quenched samples to the same draw ratio as slow cooled samples. However their moduli are equivalent.[134] Farrell and Keller[57] reported a decrease in modulus at constant draw ratio for polyethylene extruded at higher strain rates by increasing the crosshead speed. Modulus decreased even though presumably extrusion pressure increased, due to the higher flow stress at higher strain rates, which should increase modulus. Taylor and Clark[69] found that low strain rates are required to superdraw, i.e., post-neck drawing, polypropylene. Tensile strength and modulus also increased with decreasing strain rates. Capaccio et al[108] also observed a decrease in modulus with increasing strain rate in drawn polyethylene. This evidence indicates that lower strain rates increase the percentage of deformation occurring by crystalline chain unfolding and reduces deformation by crystalline block slip. Stress degradation may be decreased by reduction of stress concentrations in the amorphous phase. The slower deformation increases tensile properties by reducing

chain fracture and more efficiently transferring stress to and deforming microfibrillar crystalline blocks. Thus more deformation occurs through mechanisms which increase tensile properties.

Variations in Properties As a Function of Position

The variation in polyethylene deformation profiles demonstrates the existence of complex stress fields during extrusion which are dependent on molecular weight.[92] The possibility that a nonuniform stress field produces variations in properties has been investigated. Farrell and Keller[57] measured the concentration of folds at a given fold length in extruded polyethylene by the longitudinal acoustic mode of Raman spectroscopy. A correlation was found between decreasing fold concentration, indicating increasing deformation, with increasing modulus. Fold concentration was also measured at five points across the diameter of an extrudate of draw ratio 12. The lowest fold concentration was found at the extrudate's center followed by the outer edge at the billet. Points at one half the distance between the edge and center showed the highest concentration. This pattern, ∼, is the inverse of the deformation profile of a polyethylene of similar molecular weight extruded at the same temperature and draw ratio by Kanamoto.[92] If the relation between these two profiles is valid, it indicates that slower deformation rates, manifested by reduced motion in the deformation profile, increases chain unfolding and modulus. Farrell and Keller also found that modulus decreases with increasing extrusion rate, consistent with this concept. Slip line analysis showed that high, localized elongation occurs at the corner of the cone and capillary in dies with large entrance angles.[15] Williams,[93] however, found no change in birefringence across the diameter

of a hydrostaticly extruded polypropylene. The draw ratio used was not specified but was between 5 and 15. He reasoned that strain hardening strengthens the deformed region which transfers stress to an undeformed region. Thus, all regions are eventually deformed to the same extent. These results are contrary to those of Farrel and Keller unless Williams' sample was near draw ratio 15 where birefringence is independent of draw ratio.

A study utilizing wide angle and small angle X-ray techniques was done on polyethylene samples drawn to draw ratio 7.5 by Kasai and Kakuda.[135] Deformation profiles at drawn samples show uniform elongational flow. Although variations in the diffraction patterns as a function of position were observed in the neck, there was no variation in the final extrudate, as expected.

These three studies indicate there may be a correlation between deformation profiles and extrudate properties. It is uncertain whether extrudate properties vary significantly along the extrudate diameters. Additional studies are needed to clarify these issues.

CHAPTER III

EXPERIMENTAL METHODS FOR DRAW RATE AND PROPERTIES STUDY

Research Plan

The experimental work in this thesis is divided into three sections: (1) the effect of extrusion conditions on extrudate properties, (2) the effect of draw ratio, die angle, and extrusion temperature on λ, the ratio of pushing to pulling pressures which produce equivalent extrusion rates during pultrusion, and (3) methods to increase draw ratio and tensile modulus.

The Effect of Extrusion Conditions on Extrudate Properties

Billets were crystallized under pressures ranging from 30 to 121 MPa to study the effects of initial morphology on extrusion rate. The billets were extruded at 213 and 182 MPa pushing pressure (P_E) and pultruded at 182 MPa P_E plus 4.0 MPa pulling pressure (P_L). Unexpectedly, a 600% variation in extrusion rate was found at constant extrusion temperature and pressure which was unrelated to crystallization pressure. Extrusion rate also varied widely at constant crystallization pressure. It is now believed that the range in extrusion rate was caused by variations in lubrication between billets. The billets were unintentionally lubricated from handling during their preparation from extrusion. Evidence for this theory is given in Chapter VI. Although lubrication masked the effects of crystallization pressure on extrusion rate, it provided an

opportunity to determine the effects of pultrusion and extrusion pressure unconfounded by the effects of extrusion rate.

Studies correlating lubrication, pressure, and pultrusion with extrudate properties have not been conclusive in terms of their effects or mechanisms. Increasing pressure has been found to increase[88] and have no effect[83] on modulus. The increase in modulus may be due to either greater undercooling or reduced annealing at the faster extrusion rates produced by higher pressures. A pulling force was observed to have no effect on modulus[84] although a decrease in modulus has been found in extrudates annealed with loose ends.[89] Lubrication has been observed both to decrease[17] and to have no effect[48] on modulus; increased drawing speed has been shown to decrease modulus.[57]

The purpose of this study is to determine the effects of extrusion rate, lubrication, extrusion pressure, and pultrusion on extrudate properties and morphology and thus attempt to explain changes in the deformation process induced by these parameters. Samples have been characterized by differential scanning calorimetry (DSC), tensile testing, shrinkage, and density. A series of extrudates of increasing extrusion rate produced at the three processing conditions have been characterized to determine the effect of extrusion rate and/or lubrication at each condition (Table 1A). Utilizing the range of extrusion rates produced under the three conditions, the effect of extrusion rate was eliminated. To isolate the effect of pressure from deformation time, properties of extrudates produced at P_E = 213 and 182 MPa having similar extrusion rates were compared (Table 1B). The same comparison was made between extrudates produced at P_E = 182 and P_E = 182 plus P_L = 4.0 MPa to determine the effect of pulling pressure (Table 1C). For control, the

properties of extrudates having similar rates at each extrusion condition were compared. It is possible that the initial billet morphology influenced extrudate morphology. Therefore, extrudates produced from billets crystallized under the same (Table 2A) and different (Table 2B) crystallization pressures which have similar extrusion rates have been compared.

The Effect of Draw Ratio, Die Angle, and Extrusion Temperature on Pultrusion

A pulling pressure produces faster extrusion rates than an equivalent pushing pressure during pultrusion. The ratio between pushing and pulling pressures which produce equivalent extrusion rates is given by λ. In Chapter III-C-8 on pultrusion, mechanisms explaining the greater effectiveness of a pulling pressure and expected effects of draw ratio,

Table 1

Characterized Polyethylene Extrudates

A. Effects of Extrusion Rate on Extrudate Properties

Extrusion Pressure	P_E = 213 MPa	P_E = 182 MPa	P_E = 182 + P_L = 4.0 MPa
Extrusion Rate, cm/min.	4.31	3.60	2.84
	2.82	1.90	2.17
	1.83	1.83	2.12
	1.81	1.49	1.52
	1.55	1.48	1.06
	1.03	1.05	0.59
	0.94	0.66	
	0.93	0.54	
	0.71		

B. Effects of Extrusion Pressure on Extrudate Properties Prepared at Constant Extrusion Rate

Extrusion Pressure	P_E = 213 MPa	P_E = 182 MPa
Extrusion Rate, cm/min.	1.83	1.83
	1.55	1.49
	1.03	1.05

C. Effect of Pultrusion on Extrudate Properties Prepared at Constant Extrusion Rate

Extrusion Pressure	P_E = 182 MPa	P_E = 182 + P_L = 4.0 MPa
Extrusion Rate, cm/min.	1.49	1.52
	1.05	1.06
	0.54	0.59

Table 2

Polyethylene Extrudates Characterized as Controls

A. Comparison of Extrudate Properties Prepared at Constant Extrusion Rate Crystallized Under the Same Pressure

Extrusion Pressure	P_E = 213 MPa	P_E = 182 MPa
Extrusion Rate, cm/min. - Billet Crystallization Pressure, MPa	0.94 - 51	1.90 - 30
	0.93 - 51	1.83 - 30

B. Comparison of Extrudate Properties Prepared at Constant Extrusion Rate Crystallized Under Different Pressures

Extrusion Pressure	P_E = 213 MPa	P_L = 182 MPa	P_E = 182 + P_L = 4.0 MPa
Extrusion Rate, cm/min. - Billet Crystallization Pressure, MPa	1.83 - 91	1.49 - 30	2.17 - 30
	1.81 - 121	1.48 - 61	2.12 - 121

extrusion temperature, die angle, and molecular weight on λ, derived from these mechanisms, were proposed. The purpose of this study is to

determine the effect of extrusion temperature, draw ratio, and die angle on λ and thus determine the validity of the proposed mechanisms. Various methods of calculating λ and the effect of pultrusion on deformation profiles also are discussed.

Methods to Increase Draw Ratio and Tensile Modulus

In the course of the experimental work for the previous two sections it was noted that lubrication and possibly pulling pressure affected deformation profiles and the maximum draw ratio achieved before fracture. From these observations, mechanisms explaining the effects of lubrication, pulling pressure, and die geometry on the maximum draw ratio obtainable were developed. In this section, methods to achieve higher draw ratios based on these mechanisms were tested. Samples of high draw ratio produced by two of the methods were characterized and compared with samples of lower draw ratio to determine the efficiency of the deformation process.

Billet Preparation

Billets were prepared for extrusion as follows. An Instron capillary rheometer, Model A70, was heated to 120°C and the bottom of the capillary blocked. Prior to filling with the sample, pellets of high density polyethylene (DuPont Alathon 7050, M_W = 59,000, M_N = 19,000, MFI = 17.5), a short Teflon plug was inserted into the capillary. The pellets were then packed under 242 MPa for 1 min. with the extrusion plunger. The capillary was refilled and capped with a Teflon plug and the pellets packed under 242 MPa for 30 min. Maintaining the pressure at 242 MPa, the temperature was raised to 150°C and held for 5 min.

Pressure was then reduced to the desired crystallization pressure and held for 15 min. Next the temperature was raised to 170°C, while maintaining constant pressure, and held for 10 min. The heaters were then turned off and cooling under the crystallization pressure occurred. Billets were crystallized under 30, 51, 61, 71, 91, and 121 MPa. When the capillary had cooled to 80°C, ~95 min., the billet was removed. The billet, 0.95 cm in diameter, was cut into sections 7 cm in length, tapered at one end, and split longitudinally. The interior of the split halves was sanded with fine grained sandpaper to a smooth surface to complete billet preparation. The billet was unlubricated except as acquired during handling.

Billet Characterization

Crystallinity

The effects of crystallization pressure on billet morphology were characterized by density, differential scanning calorimetry (DSC), and small angle X-ray scattering (SAXS).

Density was measured at room temperature by placing billet slices, ~1 mm thick, in a density gradient column of diethyleneglycol and isopropyl alcohol. A gradient of 1.9 $g/cm^3/cm$ column length was calibrated using density floats calibrated to ± 0.0001 g/cm^3. The crystalline mass fraction was calculated from the equation:

$$X_M = [(P-P_a)/(P_c-P_a)](P_c/P)$$

Where X_M = crystalline mass fraction

P = sample density

P_c = density of the crystalline phase assumed to be 1.000 g/cm^3[6]

P_a = density of the amorphous phase assumed to be 0.855 g/cm^3[6]

Differential Scanning Calorimetry

DSC was performed on a Perkin-Elmer DSC-1B at a heating rate of 10^{o}C/min. Temperature was calibrated with indium and lead standards and heat of fusion with an indium standard. Thin slices of billet were laid flat in the sample pans to promote heat conduction. Pre and post-melting baselines were offset from each other. Therefore the fusion curve baseline was drawn as shown in Fig. 2. Crystallinity was calculated assuming a value of 69 cal/g[136] for the heat of fusion for a perfect extended chain crystal. Melting temperatures were read at the peak of the fusion curve and at the point where the curve broke away from the premelting baseline. The peak width was measured at one half the peak height.

Small Angle X-ray Scattering

SAXS diffraction was measured using a Kratky Small Angle X-ray Camera equipped with a Tennelec PSD 1100 one dimensional position sensitive detector. Fold period was calculated by substituting the scattering angle of peak scattering intensity into Bragg's equation. The Lorentz correction, which adjusts for the effects of sample isotropy, was not applied. However, a rough estimate of the corrected fold period is presented.

Extrusion Processes

The billet was heated in the capillary rheometer for 5 min. prior to the application of extrusion pressure, allowing it to equilibriate at the extrusion temperature of 120^{o}C. An unlubricated conical brass die with a 20^{o} cone angle and a 0.95 cm capillary length was used. The die draw ratio, defined as the ratio of the inlet to the outlet cross-sectional areas was 29.1 at room temperature. Heating the die to 120^{o}C

FIG. 2. DRAWING OF DSC BASELINE FOR CALCULATION OF CRYSTALLINITY

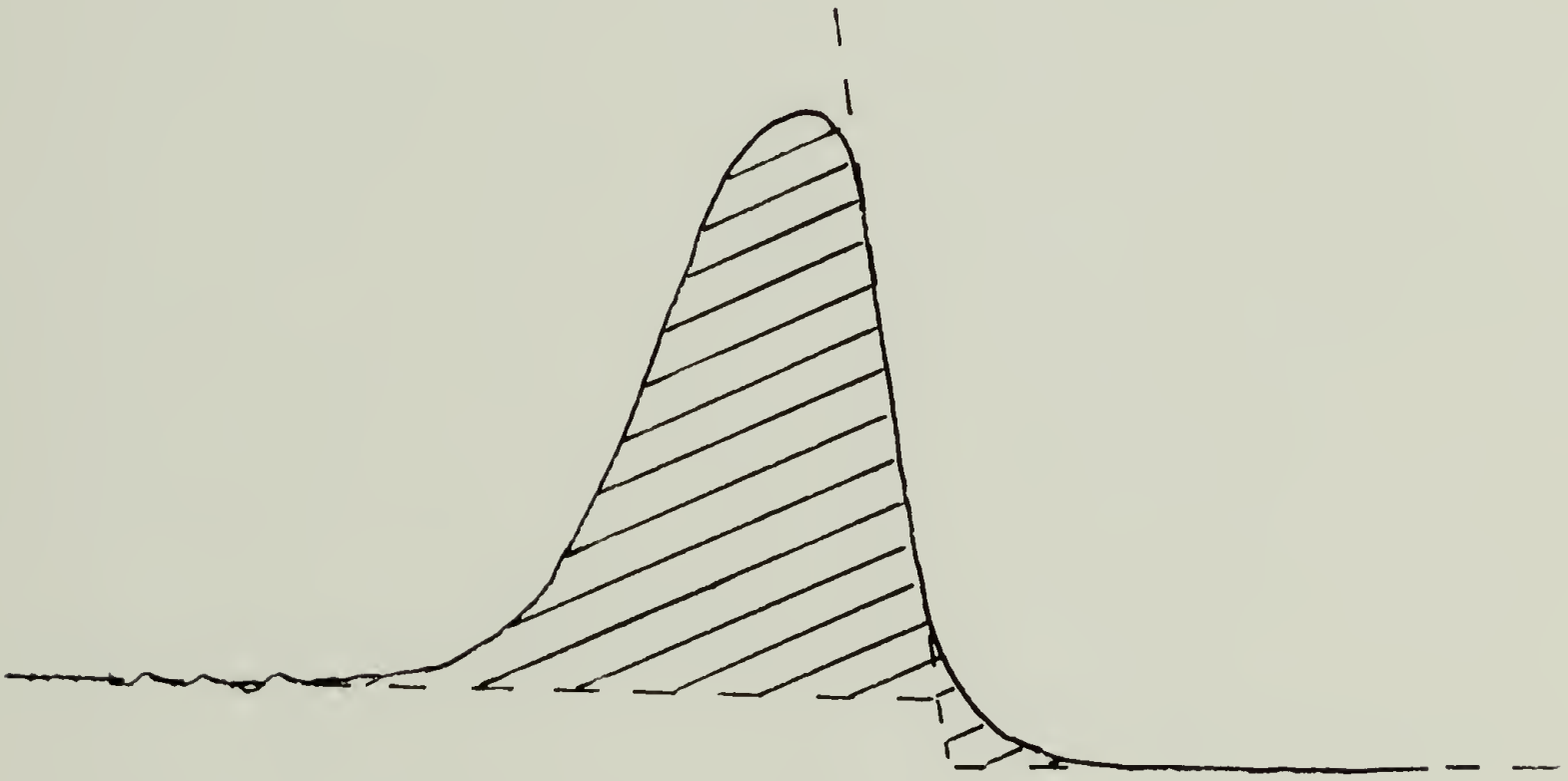

▨ - AREA USED FOR CALCULATION OF CRYSTALLINITY

reduced its draw ratio to 29.0. Extrusion was begun by applying a constant pressure of 213 MPa (2100 atm.). Extrusion rate was measured by employing a cathetometer to follow the movement of a mark taped to the extrudate. Curling was prevented by extruding the sample into a narrow tube. The extrusion rate was not recorded until a constant rate was maintained corresponding to complete extrusion of the volume of the tapered section of the billet. The rate was checked several times to ensure that it was constant. After approximately 15 cm of extrudate were obtained, the pressure was lowered to 182 MPa. The extrusion rate was again recorded.

The same billet was then pultruded by attaching 4.0 MPa (1 kg) pulling pressure to the emerging extrudate through the pulley system shown in Fig. 3. Extrusion rate was measured through a recorder calibrated to measure extrudate length, followed by revolutions in a gear attached to a potentiometer, as a function of time. A straight recorder trace represented a constant extrusion rate.

Extrudate Characterization

Density

Crystallinity was determined from density measurements employing the same method used for billet characterization. One cm lengths of extrudate were used and their midpoint was taken as their equilibrium position in the column.

Differential Scanning Calorimetry

DSC measurements were made on a Perkin-Elmer DSC-2 which provides greater sensitivity to morphological differences than the DSC-1B.

FIG. 3. PULTRUSION APPARATUS

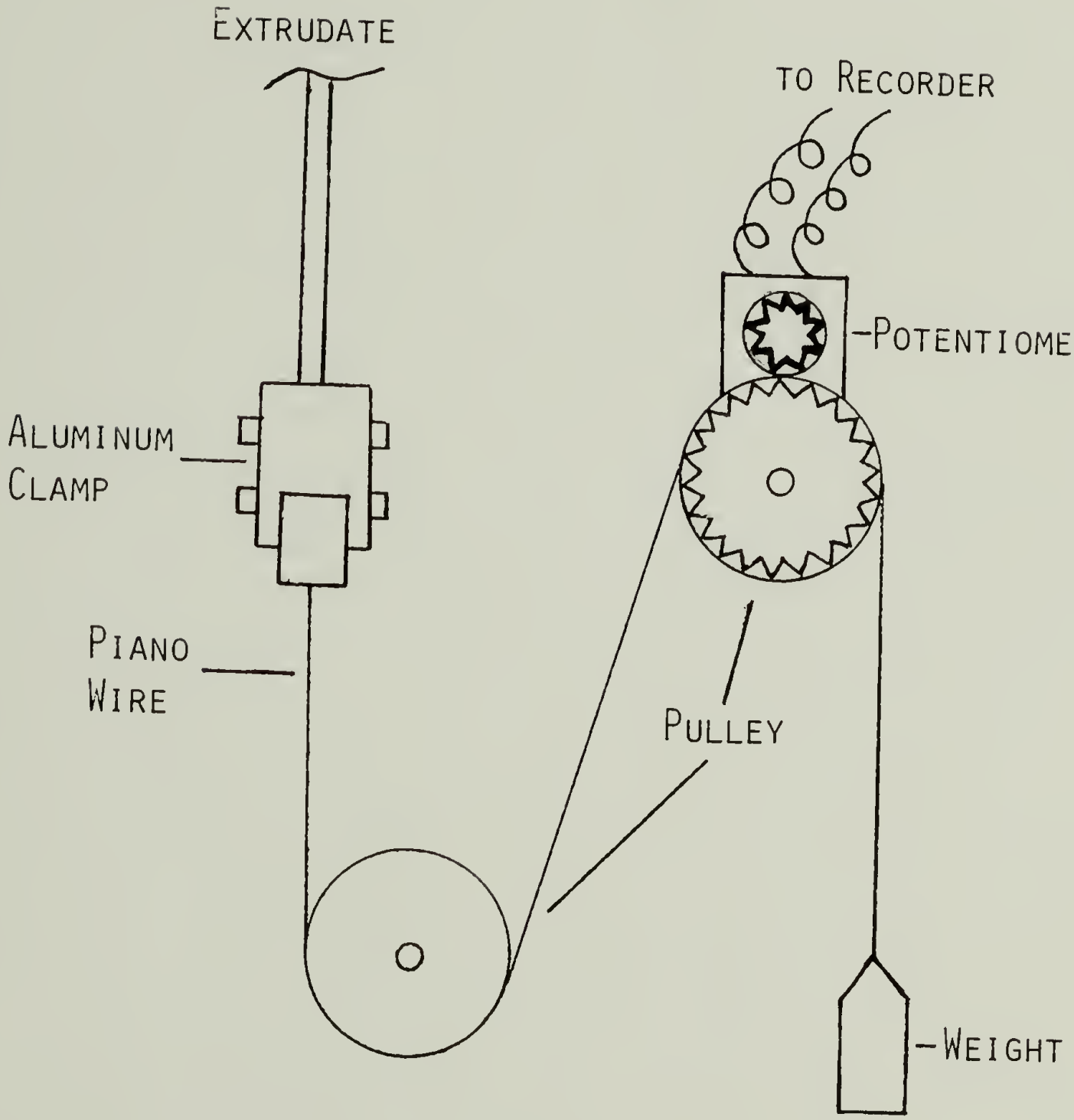

Variations in sample weight were held to ± 0.03 mg for sample sizes of 2.5 mg to eliminate any effect of sample weight on peak melting temperatures. Several samples from the same extrudate were run to obtain an empirical measure of error due to procedural errors and variations along the extrudate. The same sample of indium was run several times to determine machine reproducibility. Calibration and calculations employed with the DSC-2 are identical to those used with the DSC-1B.

Shrinkage

Shrinkage measurements for the stored elastic energy in the extrudate were made to determine the efficiency of deformation. Samples 0.40 ± 0.02 mm thick and approximately 1 cm long were sliced from the base of the semicircular extrudates. These dimensions are an optimum geometry for the shrinkage test. Melt shrinkage patterns show that the edges and ends of the sample melt before the interior. The interior acts as a rigid support inhibiting shrinkage and decreases the measured efficiency of deformation. Thinner samples are heated at more even rates but curl upon melting preventing accurate measurements. Thicknesses outside of ±0.02 mm range produced significant differences in shrinkage values. Previously no change was found for thicknesses between 0.30 and 0.50 mm.[63] Longer samples reduce end effects and measurement errors but also curl upon melting.

Before being placed in the shrinkage bath, the sample length was measured with a micrometer to ±0.005 mm. The sample was then immersed in silicone oil at 180°C (Arthur Thomas Co., Catalog #6428-R15) in a beaker approximately 6.5 cm tall. As a solid, the sample sank in the oil enhancing heat transfer and even melting. It melted before reaching

bottom and floated to the surface allowing it to be removed without deformation. After crystallization, the sample length was again measured. Molecular draw ratio (MDR), representing deformation due to elastic bond deformation, was calculated from:

$$MDR = \frac{L_T - L_S + L_O}{L_O}$$

Where L_T = sample length after extrusion

L_O = sample length before extrusion = $\frac{L_T}{\text{Die draw ratio}}$

L_S = sample length after melting

At a bath temperature of 180°C the sample melted completely in approximately 6 sec. However, shrinkage continued with time the sample was left in the bath until 8 min. at which point the sample became circular. This conformation is due to thermodynamic forces converting the melt to an equilibrium shape of lowest energy and not elastic forces incurred by deformation. Therefore, a study of MDR as a function of shrinkage time was undertaken to determine the shrinkage point corresponding to maximum elastic recovery and minimum viscous flow to the equilibrium state. This time, 2 min., was used for the MDR and extrusion rate study.

Mechanical Properties

Tensile modulus measurements were made from grip displacement on an Instron tensile testing machine, Model TTCM. The grips, specifically designed for the sample geometry, prevented slippage yet did not crush the sample.[88] Since only one sample was made at each extrusion rate and the aspect ratio, 42, was below that necessary to eliminate end effects,[137-139] the reproducibility of a single measurement, the variation

in modulus in samples taken from a single extrudate, and the effect of aspect ratio on sample modulus were determined. The procedure given here and interpretation of further experiments were based on these results. Four consecutive tests were run on each sample with a 5 min. interval between each test. Tests were run at room temperature on a sample 8 cm in length at a strain rate of 1.25×10^{-3}. Modulus values are reported for the first test and the average of the other three.

The interior surface of many of the extrudate halves was irregular, producing a variation in cross-sectional area. However, since modulus is a bulk property, the average cross-sectional area can be used to calculate modulus. This was determined from the following fraction: (Sample weight)/(Density)(Sample length). The density used for each sample was as determined previously by density gradient column.

Previous studies have shown that an aspect ratio of approximately 100 is necessary to eliminate end effects found during tensile testing of anisotropic materials.[139] Tensile force is transmitted only to the sample's exterior by the grips. It is then gradually conveyed to the interior through shear stresses. Samples with low aspect ratios do not allow the force to reach the interior and produce lower moduli. To determine the effect of aspect ratio, the same sample of draw ratio 29.1 was tested at lengths of 26.8, 13.4, and 6.7 cm. This corresponds to aspect ratios of 150.6, 75.3, and 37.7 respectively. The strain rate was kept constant by varying the crosshead speed. The sample had a smooth surface and a constant diameter. Five tests were run at each length and the average of tests 2 through 5 is plotted versus aspect ratio.

The constancy of modulus along an extrudate was determined by testing four samples from the same extrudate. The average cross-sectional area of the samples was different due to the unevenness of the interior surface. Six tests were run on each sample and the average of tests 2 through 6 is reported.

Variation in Properties as a Function of Radial Position in the Extrudate

Variation in properties as a function of radial position in the extrudate was determined by DSC and shrinkage measurements made on individual sections of the extrudate. DSC was done in triplicate on each sample and shrinkage tests were done as many times as necessary to obtain consistent values. Averages were then taken. In some cases, one DSC value was excluded from the average when it was judged to be inconsistent with two other similar values. Since only three measurements were taken, judgement was not based on statistics, but on reproducibility of six samples taken from the same extrudate. This method lowered standard deviations but did not affect the sections' relative rankings or the conclusions. The sections were then ranked from highest to lowest in crystallinity, temperature at the start and peak of the melting curve, and MDR. Similar values were placed together. Ranking was not statistical.

CHAPTER IV

RESULTS AND DISCUSSION OF EXTRUSION RATE AND EXTRUDATE PROPERTIES STUDY

Billet Characterization

Billet crystallinity was determined as a function of crystallization pressure and position along its length. Billets are identified by pressure and position, for example 51-A, see Table 3. This indicates that the billet was crystallized under 51 MPa (500 atm.) and that this section was adjacent to the bottom end of the barrel during crystallization. The effect of position was investigated because of a likely pressure drop in the capillary during crystallization due to adhesion between the billet and the barrel. A sudden decrease in pressure occurred often during crystallization at temperatures below which crystallization should have been completed. This is interpreted as a sudden breaking of adhesion formed during crystallization between the billet and the barrel by contraction of the billet with further cooling.

Density

The billet crystallized at 51 MPa showed no significant change in crystallinity, determined by density, with position (Table 3). This allowed billets from different positions to be compared as a function of pressure (Table 4). These results also show that density is at least a precise analysis of crystallinity. Crystallinity increased slightly, ~1.4%, with crystallization pressures between 30 and 91 MPa, similar to results of Wunderlich and Arakawa.[140]

Table 3

Effect of Billet Position on Crystallinity Measured by Density

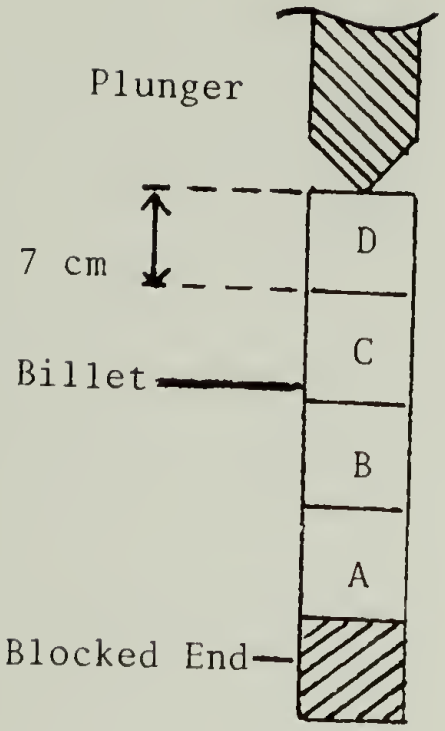

Crystallization Pressure = 51 MPa

Position	Density, g/cc	Crystallinity, %
A	0.9716	82.76
B	0.9726	83.10
C	0.9719	82.96
D	0.9719	82.96

Table 4

Effect of Crystallization Pressure on Billet Crystallinity

Billet Crystallization Pressure, MPa - Position	Density, g/cc	Crystallinity, %
91-D	0.9721	83.08
71-C	0.9709	82.33
61-C	0.9711	82.45
51-D	0.9719	82.96
30-D	0.9707	82.20
30-C	0.9698	81.64

Differential Scanning Calorimetry

The average crystallinities, starting (Tms) and peak (Tmp) melting points, and fusion curve widths determined by DSC-2 as a function of crystallization pressure and position are listed in Tables 5 and 6. There was no systematic change in values with position indicating again,

Table 5

Thermal Analysis of the Effect of Crystallization Pressure on Billet Morphology Measured by DSC-1B at 10°C/Min.

Crystallization Pressure, MPa	Crystallinity, %	Tms,[1] K	Tmp,[2] K	Peak Width,[3] mm
30	75.4±2.0	392.3±2.0	409.4±1.2	21.0±2.3
51	75.0±3.0	393.3±4.1	409.1±0.6	19.3±4.6
61	80.2±1.5	391.1±1.4	409.2±0.4	22.4±2.3
71	77.6±4.1	392.1±2.0	408.5±0.4	20.8±2.0
91	76.8±3.7	391.4±2.5	409.1±0.8	22.5±3.0
121	76.8±2.8	392.9±2.4	411.1±1.4	22.8±2.5
Average	77.0±2.9	392.2±2.4	409.4±0.8	21.5±2.8

Table 6

Thermal Analysis of the Effect of Position on Billet Morphology Measured by DSC-1B at 10°C/Min.

Position	Crystallinity, %	Tms, K	Tmp, K	Peak Width, mm
A	77.5	392.7	409.5	20.1
B	78.3	389.6	409.3	24.0
C	76.6	392.6	409.2	20.8
D	74.8	393.5	409.8	21.0

[1]Tms = Temperature at the beginning of the fusion curve

[2]Tmp = Temperature at the peak of the fusion curve

[3]4 mm = 1 K

as in density measurements, that any pressure drop along the barrel during crystallization caused no effect. Crystallization pressure also exhibited no systematic effect on these values. However, this does not contradict the density results. The standard deviations show that the precision of the DSC is below that required to detect the small differences between billets found by density. These results also show that Tmp is the most reproducible measurement obtainable from DSC.

The large standard deviations in DSC values may be partially due to the unselective method of collecting the sample from any part of the billet. A later study (Table 7) showed that the core had higher crystallinity and, as expected, higher melting points than the billet sheath. This is probably caused by faster crystallization rates in the sheath than in the core. An additional study (Table 8) showed that faster crystallization rates, induced by blowing ambient air, or air cooled by dry ice or cooled by liquid nitrogen into the insulation surrounding the rheometer, produced slightly lower crystallinity but had no observable effect on melting points. Therefore, the large deviations are likely due to the average consisting of values from samples containing material only from the core and others only from the sheath. The range in Tms is due to the irregular baseline making it difficult to determine where the slowly rising melting curve departs from the baseline. The variation in peak width, reflecting differences in morphology, is unaccounted for. The difference in crystallinity measured by density and DSC will be discussed later.

Small Angle X-ray Scattering

SAXS was run on the 121 D and 30 D billets. Long periods, uncorrected for the Lorentz effect, of 453 and 416 Å were obtained for the 121 D and

Table 7

Thermal Analysis of Core and Sheath of Billet by DSC-1B

Section	Crystallinity, %	Tms, K	Tmp, K	Peak Width, mm
Sheath	73.0±0.7	391.5±2.3	408.6±0.7	21.3±0.1
Core	76.1±0.4	393.3±1.8	409.1±0.7	19.7±1.9

Table 8

Thermal Analysis of the Effect of Crystallization Time on Billet Morphology by DSC-1B

Crystallization time, min.	Crystallinity, %	Tms, K	Tmp, K	Peak Width, mm
95	75.2	393.9	408.4	19.6
66	74.9	389.8	407.8	22.2
46	74.5	390.5	408.1	21.5
34	72.1	390.4	408.4	22.4
27	70.9	395.0	408.3	17.0
14	73.6	390.2	408.2	22.6

Crystallization pressure for all billets = 91 MPa

30 D samples respectively. The corresponding estimated corrected long periods are between 300 and 400 Å.[151] Although direct comparisons cannot be made, the fold period values and slight increase in fold period with increasing pressure obtained here are consistent with other work.[152,153]

Annealing, which can increase crystallinity, melting point, and long period, has been observed in melt crystallized polyethylene from atmospheric to elevated pressures above 110°C.[144] During extrusion at 120°C,

rear portions of the billet may be annealed prior to extrusion which may affect extrusion rate and properties. Billets crystallized at low pressures should show the greatest change. Therefore, the unextruded portions of partially extruded billets were analyzed and compared with themselves prior to extrusion, Table 9. No consistent, significant changes were obtained indicating that the billet does not anneal in the short time at 120°C and high pressure prior to extrusion.

In summary, the initial morphology of billets crystallized from 30 to 121 MPa was analyzed to detect differences which may affect deformation and consequently extrusion rate and extrudate properties. Previous work had shown that higher long periods, produced by crystallization at higher pressures, yielded faster extrusion rates.[19] Slight increases in crystallinity, melting point, and long period were detected here with increasing pressure but should not affect deformation. Therefore, the initial morphology can be considered constant.

Extrudate Characterization

Table 9

Determination for Annealing During Extrusion

Billet	Crystallinity by Density, %	Crystallinity by DSC-1B, %	Tms, K	Tmp, K
Before Extrusion				
30-D		73.5	381.0	409.2
71-D		77.2	384.4	407.1
91-D	82.45			
91-D	83.39	77.6		
121-D		77.6	386.3	409.0

Billet	Crystallinity by Density, %	Crystallinity by DSC-1B, %	Tms, K	Tmp, K
After Extrusion				
30-D		74.2	390.4	406.4
71-D		78.2	384.5	407.0
91-D	82.64			
91-D	82.45			
121-D		75.7	380.5	408.6

Density

Extrudate crystallinity measured by density gradient column was independent of extrusion rate for all three extrusion conditions, Table 10. Indeed, the range in crystallinity produced by each condition was lower than that obtained from three samples cut from the same extrudate, Table 11. This allowed the average crystallinity from each condition to be used as a gauge of the effect of extrusion conditions on crystallinity. There was no change in crystallinity with extrusion pressure or through pultrusion. Extrudate crystallinity was only slightly, 0.9%, above billet crystallinity.

Several studies on the effect of deformation on density have produced conflicting results. Imada[16] observed no change in crystal lattice dimensions with deformation. He reasoned, therefore, that an increase in density must be due to an increase in crystallinity. However, Glenz and Peterlin[145] found that the crystalline block volume decreased with deformation. Smith et al,[146] using broadline NMR, observed an increase in crystallinity and in low molecular weight material with deformation. They attributed the latter increase to chain ends rejected from crystalline

Table 10

Extrudate Crystallinity Determined by
Density - Effect of Extrusion Rate and Pressure

Extrusion Conditions	Extrusion Rate, cm/min.	Density, g/cm^3	Crystallinity,%
P_E = 213 MPa	4.31	0.9731	83.72
	2.82	0.9725	83.33
	1.83	0.9732	83.77
	1.55	0.9732	83.77
	1.03	0.9731	83.72
	0.93	0.9727	83.44
	0.72	0.9730	83.64
Average ± Standard Deviation		0.9730±0.0003	83.64±.17
P_E = 182 MPa	3.60	0.9714	82.66
	1.90	0.9730	83.61
	1.83	0.9730	83.61
	1.49	0.9731	83.67
	1.48	0.9733	83.86
	1.05	0.9730	83.61
	0.66	0.9731	83.67
	0.54	0.9730	83.61
Average ± Standard Deviation		0.9729±0.0006	83.54±.36
P_E = 182 + P_L = 4.0 MPa	2.84	0.9722	83.23
	2.17	0.9724	83.40
	2.12	0.9725	83.17
	1.52	0.9723	83.34
	1.06	0.9726	83.28
	0.59	0.9724	82.12
Average ± Standard Deviation		0.9724±0.0001	83.26±.10

Table 11

Crystallinity Along an Extrudate Determined by Density

Extrusion Conditions: P_E = 182 MPa, Draw Ratio = 29.1, Die Angle = 20^o Extrusion Temperature = 120^oC, Extrusion Rate = 2.11 cm/min.

Sample	Density, g/cm^3	Crystallinity, %
1	0.9730	83.63
2	0.9727	83.46
3	0.9734	83.91
Average ± Standard Deviation	0.9730±0.0004	83.67±.23

domains during deformation. However, Glenz and Peterlin found no increase in paracrystalline disorder, caused by chain ends and kinks, due to the high molecular mobility during deformation allowing these morphologies to be incorporated within crystals.

Several other factors along with the changes in paracrystalline disorder and crystal lattice dimensions stated above may cause a change in density with deformation. Spherulites are destroyed and some chains are unfolded, but much of the spherulites' folded chain morphology is maintained in the microfibril. A slight decrease in density may result. Density may be increased by formation of intercrystalline bridges from tie molecules, orientation of amorphous chains, close packing of adjacent microfibrils, compression of voids by extrusion pressure, and crystallization of formerly amorphous chains allowed by their increased mobility during deformation. The relative contribution of each of these factors to extrudate density is unknown. Therefore, it cannot be predicted whether density should increase or decrease with deformation.

It is also difficult to predict, based on these factors, the effect of extrusion conditions on density. Higher extrusion pressure may produce closer chain packing and smaller voids but may lower the effective extrusion temperature and reduce crystallization of amorphous chains by decreasing chain mobility. Pultrusion may create more orderly flow and increase packing. If lubrication increases extrusion rate by creating a more orderly flow pattern, density may increase with extrusion rate. However, if lubrication only reduces friction, the higher extrusion rate may prevent uniform deformation and packing and density will be reduced.

The constancy of crystallinity with extrusion rate and pressure and with pultrusion indicates that these factors do not significantly affect the deformation process. However, overshadowing this conclusion is the result that extrudate crystallinity is only 0.9% higher than billet crystallinity, significantly lower than the 8 and 9% increases observed by Mead[60] and Imada[16] respectively. This result was unexpected since this study and Mead's used the same material and had similar billet crystallinity. The cause of this disparity is unknown at this point and will be further discussed with DSC results. This prohibits drawing any conclusions concerning the effect of extrusion rate or conditions on the deformation process.

Differential Scanning Calorimetry

Crystallinity, starting (Tms) and peak (Tmp) melting temperatures, and fusion curve width were measured with a DSC-2. There was no observable change in crystallinity with extrusion rate, pressure, or by pultrusion, consistent with density measurements. Preliminary tests showed that crystallinity values are reproducible within $\pm$ 1.5%.

Therefore, a real difference of ~3% is required to detect changes in crystallinity between samples.

Tms increased slightly with increasing extrusion rate for all three processing conditions, see Fig. 4, whereas Tmp decreased slightly, but less definitively, than Tms, Fig. 5. With the opposite trends of Tms and Tmp with extrusion rate, it is expected that the fusion curve width would increase with increasing extrusion rate. However, the difference between melting temperatures as a function of extrusion rate is scattered, Table 12. This is due to the combining of the scatter in the Tms and Tmp values. There also was no consistent change in crystallinity or curve width with extrusion rate, Table 13. No statistically significant differences were found between extrusion conditions in any category. Comparison of the controls showed that billet crystallization pressure had no effect on the extrudates.

Billet and extrudate crystallinity, Tms, Tmp, and fusion curve widths are compared in Table 14. Extrudate values are averaged over all extrusion rates and processing conditions and billet values are averaged over all crystallization pressures. Crystallinity decreased slightly during extrusion, 0.8%, to 76.2%. This does not conflict with the 0.9% increase found by density measurements because of the ± 1.5% precision of the DSC. Tms and Tmp increased approximately 6 and 3 K respectively and fusion curve width decreased 1.8 K. These results show that the transformation from spherulites to a packed microfibrillar structure occurred. However, the microfibrillar crystalline structure exactly compensated for the loss of spherulitic crystallinity resulting in no change in crystallinity measured by both DSC and density.

FIG. 4. T_{MS} VS. EXTRUSION RATE

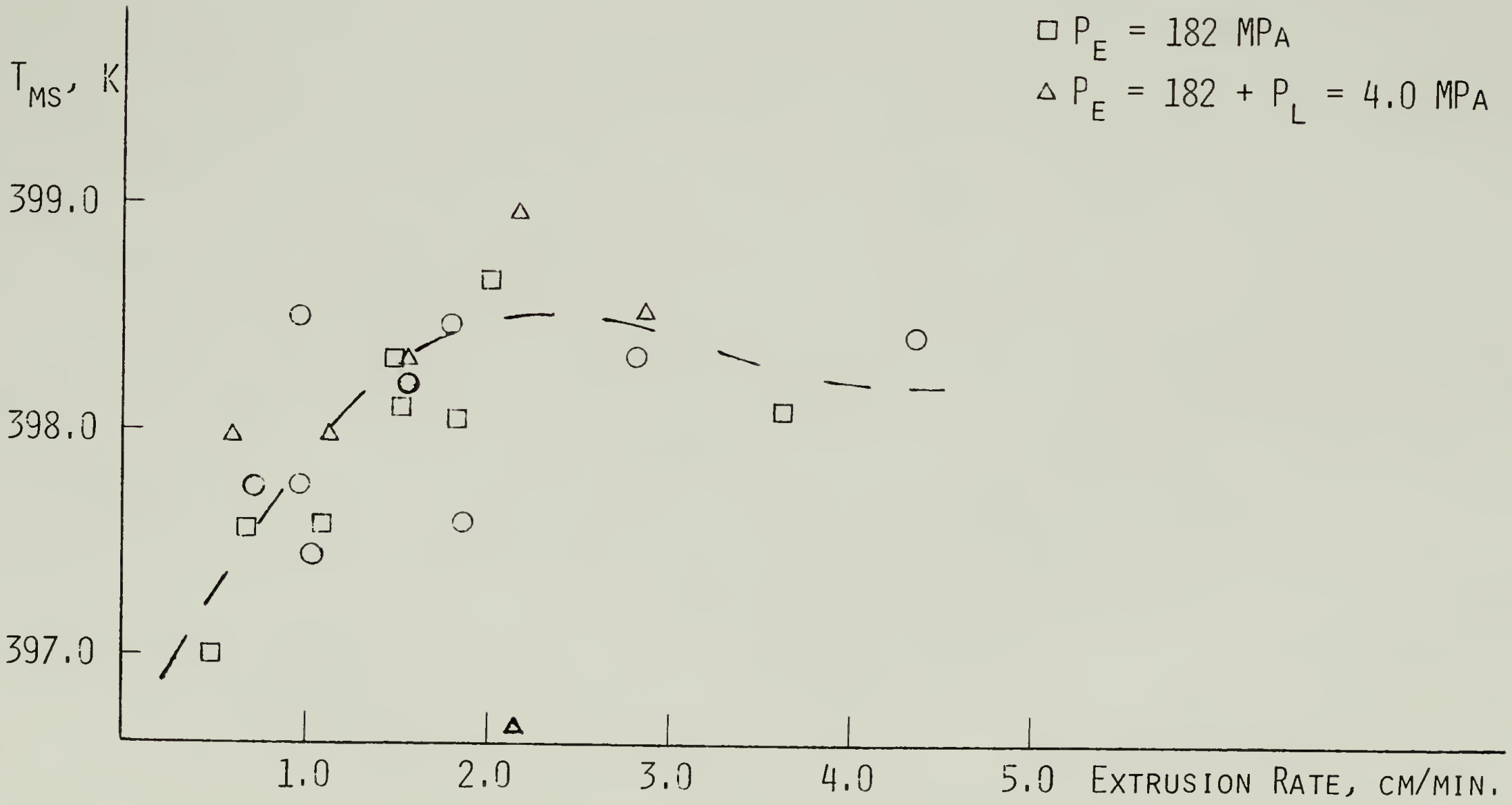

FIG. 5. T_{MP} VS. EXTRUSION RATE

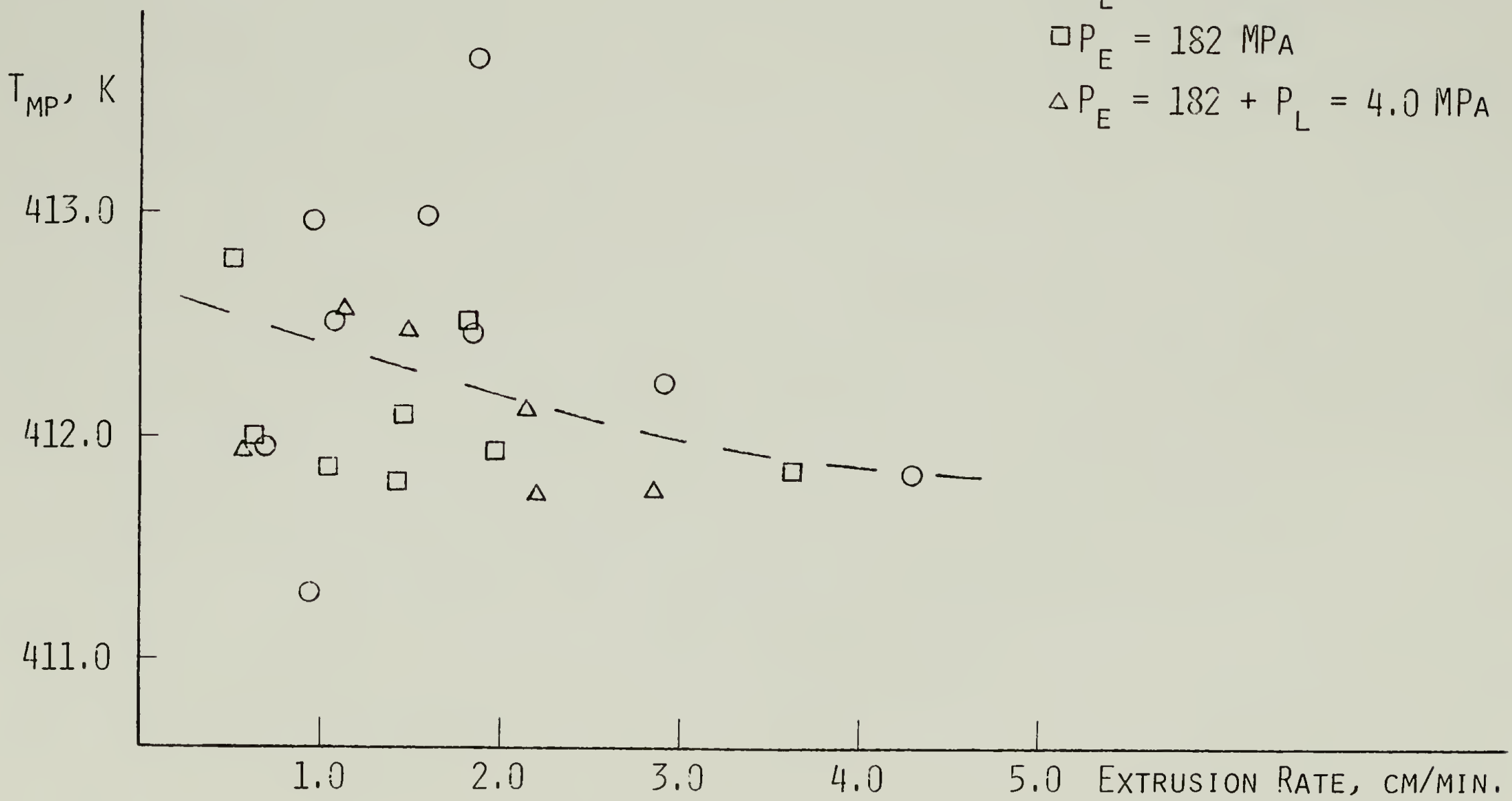

Table 12

Difference Between Extrudate Tms
and Tmp as a Function of Extrusion Rate

Extrusion Conditions	Extrusion Rate, cm/min.	Tmp - Tms, K
P_E = 213 MPa	4.31	13.44
	2.81	13.94
	1.83	14.86
	1.81	15.19
	1.55	14.75
	1.03	15.09
	0.94	13.56
	0.93	14.44
	0.72	14.19
P_E = 182 MPa	3.60	12.72
	1.90	13.25
	1.83	14.47
	1.49	14.03
	1.48	13.47
	1.05	14.27
	0.66	14.41
	0.54	15.88
P_E = 182 MPa + P_L = 4.0 MPa	2.84	12.50
	2.17	15.12
	2.12	13.19
	1.52	14.16
	1.06	14.37
	0.59	13.97

Table 13

Extrudate Thermal Analysis
by DSC-2 at 10°C/Min.

Extrusion Conditions	Extrusion Rate, cm/min.	Crystallinity, %	Peak Width, mm
P_E = 213 MPa	4.31	73.6	13.4
	" *	73.4	13.5
	2.81	73.0	13.9
	1.83	78.0	15.4
	"	74.1	14.9
	"	76.2	14.2
	1.81	75.1	15.2
	1.55	76.5	14.4
	"	78.0	14.3
	"	76.5	15.5
	1.03	75.4	15.7
	"	75.5	14.5
	0.94	74.8	13.6
	0.93	73.0	14.4
	0.72	76.5	14.2
	Average ± Standard Deviation	75.3±1.7	14.5±.8

*Ditto marks are replications of the same extrudate

Table 13

Extrudate Thermal Analysis
by DSC-2 at 10°C/Min.

Extrusion Conditions	Extrusion Rate, cm/min.	Crystallinity, %	Peak Width, mm
P_E = 182 MPa	3.60	75.3	12.1
	"	73.8	13.3
	1.90	74.9	13.4
	"	79.4	13.1
	1.83	76.1	14.4
	"	78.3	14.6
	1.49	76.0	13.1
	"	74.6	15.0
	1.48	74.1	12.3
	"	75.8	14.7
	1.05	76.2	13.7
	"	77.1	15.3
	"	78.0	13.9
	0.66	75.9	15.0
	"	76.9	15.1
	"	76.6	13.1
	0.54	77.3	16.7
	"	76.1	15.1
Average ± Standard Deviation		76.2±1.5	14.0±1.2

Table 13

Extrudate Thermal Analysis
by DSC-2 at 10°C/Min.

Extrusion Conditions	Extrusion Rate, cm/min.	Crystallinity, %	Peak Width, mm
P_E = 182 + P_L = 4.0 MPa	2.84	74.6	-
	"	-	-
	"	75.9	12.5
	2.17	78.8	15.1
	2.12	75.6	13.8
	"	75.2	12.6
	1.52	77.4	13.6
	"	76.9	14.7
	1.06	76.6	13.2
	"	77.5	-
	"	78.0	15.9
	"	79.7	14.1
	0.59	76.0	14.0
	"	76.3	13.9
Average ± Standard Deviation		76.8±1.5	14.2±1.0

Table 14

Comparison of Average Pre-Extrusion
Billet and Extrudate Thermal Properties

	Billet	Extrudate
Tms, K	392.2±2.4	398.1±0.7
Tmp, K	409.4±0.8	412.2±0.6
Peak Width, mm	21.5±2.8	14.2±1.0
Crystallinity, %	77.0±2.9	76.2±1.5

Mead[60] and Kojima[147] reported similar changes in thermal properties, excluding crystallinity, with deformation. They found increases in extrudate crystallinity of 15 and 20% respectively, both attaining approximately 83% extrudate crystallinity. This indicates that extrudate thermal properties are independent of small changes in billet morphology, similar to extrudate long period,[19] and are determined by the deformation process. It can be concluded from this study that thermal properties are also largely independent of variation in extrusion rate and the changes in extrusion conditions used and are controlled by the deformation process. Possible changes in the deformation process with extrusion conditions, detailed in the density discussion, should have similar effects on crystallinity measured by density and DSC. These changes are insignificant for the conditions studied.

The low extrudate crystallinity measured in this study may be related to the irregular interface between the two extrudate halves. A smooth interface extrudate showed a 10% increase in crystallinity and had a 4 K increase in Tmp, similar to the increase in Tmp found in this study.

Crystallinity measured by density was approximately 6% higher than that measured by DSC in both billets and extrudates. The cause of this is unknown but may be related to the assumed amorphous density of 0.855 g/cc. An amorphous density of 0.896 g/cc would give equal density and DSC crystallinity values. The higher amorphous density may be due to orientation in the amorphous phase. Amorphous orientation does occur to a low level in the extrudate[60] and was observed in the billet in WAXS diffraction patterns.[148] However, it is highly coincidental that the billet and extrudate have almost the same level of amorphous orientation. Therefore, no definite conclusions can be drawn.

Tensile Modulus

The reproducibility of a single modulus measurement was determined by running four consecutive tensile tests on the same sample allowing one minute between tests. Modulus was found to increase approximately 7% (Table 15) over the four tests analogous to behavior observed by Wilding and Ward[149] during creep tests. When the interval between tests was increased to 5 minutes, modulus was observed to increase between the first and second tests and then become constant. Since this procedure produced a consistent modulus, it was adopted for the extrusion rate - modulus study. Results of the first and the average of the three succeeding tests are reported.

The increase in modulus between the first and second tests may be due to the restraining of tie molecules that had relaxed during exposure to high temperatures in the die capillary. They remain taut after being reextended in the room temperature tensile test due to insufficient mobility to return to the relaxed state. No new tie molecules are formed.

Table 15

Extrudate Modulus as a
Function of Time Between Tensile Tests

Test Conditions: Draw Ratio = 29.1, Strain Rate = 8.2×10^{-4}, Aspect Ratio = 139

Interval Between Tests, Min.	1	5
Test	Modulus	
1	32.6	31.7
2	33.5	33.5
3	34.3	33.7
4	33.8	32.6

The increase in modulus observed only when one minute intervals are allowed between tests indicates a parallel coupling of viscous and elastic flows. Full elastic recovery of extended tie molecules is slowed by viscous forces. Modulus will be observed to increase if the next test is begun before the tie molecules have returned to their original state.

The stress-strain curves give insight into sample behavior and demonstrate that both elastic and viscous deformation occur during the tensile test. The applied force decreased approximately 15% when the sample was held in the strained state, characteristic of viscous flow. However, there was a similar reduction of force when the same load was applied to an undeforming steel bar implying that the sample's decrease was at least partially due to machine compliance. When the load was removed from the sample quickly, pressure slowly built to approximately 5 MPa, apparently through sample contraction. This did not occur with the steel bar establishing the existence of elastic sample deformation. When the load was removed slowly, a lower pressure recovery was observed. This signifies viscous deformation and may be due to flow of unstrained amorphous material such as chain ends. The overall observed behavior is a result of interaction between strained tie molecules and amorphous material.

The sample's behavior can be modeled by a spring (Sp) and dashpot (Dp) in parallel which together are coupled in series with a spring (Ss), Fig. 6. As the sample is stretched, Ss deforms giving an initial linear increase in stress with elongation. Stress is read from Ss only. Sp and Dp then begin to deform slowly causing a slower, curved increase in the measured stress. When the strain is held constant, Dp continues to deform until Sp attains complete extension. This allows Ss to relax slightly

FIG. 6 MODEL BEHAVIOR DURING TENSILE TESTING

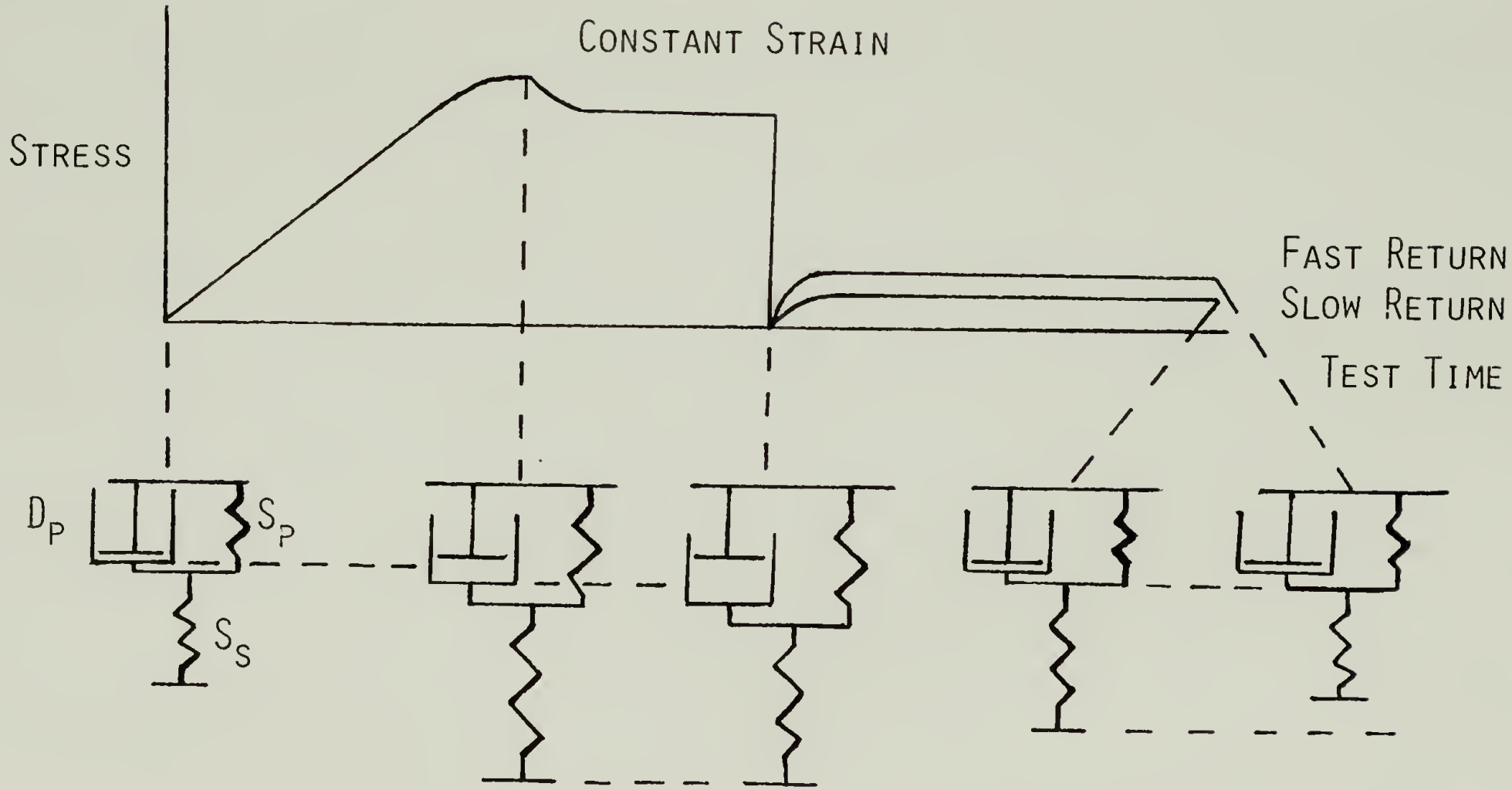

and decreases the measured stress. When Ss is relaxed quickly to give 0 load, the total apparatus remains slightly extended due to the sluggish movement of Dp. Sp slowly returns Dp to its original state and simultaneously extends Ss. This causes a small pressure to be registered by Ss. If the load is reduced slowly, Dp will be closer to its undeformed state by the time Ss is fully relaxed. The total system is less extended when Sp returns Dp to its original state and a lower stress is measured.

Fig. 7 shows that modulus increased significantly with aspect ratio. The precise form of the curve is uncertain. Previous work had shown that modulus becomes constant above aspect ratio 100.[139] Therefore, it is not known if the three points should be connected as shown or if modulus actually rises more sharply to aspect ratio 100 and then levels off. It is also unknown if higher moduli could be obtained at higher aspect ratios. However, the correct value, eliminating end effects, of the extrusion rate-modulus study samples with aspect ratio 42.3 can be estimated. From Fig. 7 the modulus at aspect ratio 42.3 is approximately 79% of the modulus at 150.6. Thus, the measured moduli of the extrudates are, at maximum, 79% of their actual value.

Table 16 presents the results of modulus measurements made on four samples cut from the same extrudate. The cross-sectional areas of the samples were unequal due to the uneven splitting of the billet from which they were extruded. There was an inconsistent increase in modulus between the initial test and the average of the three subsequent tests. However, the standard deviations of the initial and average tests were approximately equal. These results indicate that a 3.3 GPa difference in modulus will be necessary to conclude that two samples in the extrusion rate-modulus study have different moduli.

FIG. 7. TENSILE MODULUS VS. EXTRUDATE ASPECT RATIO

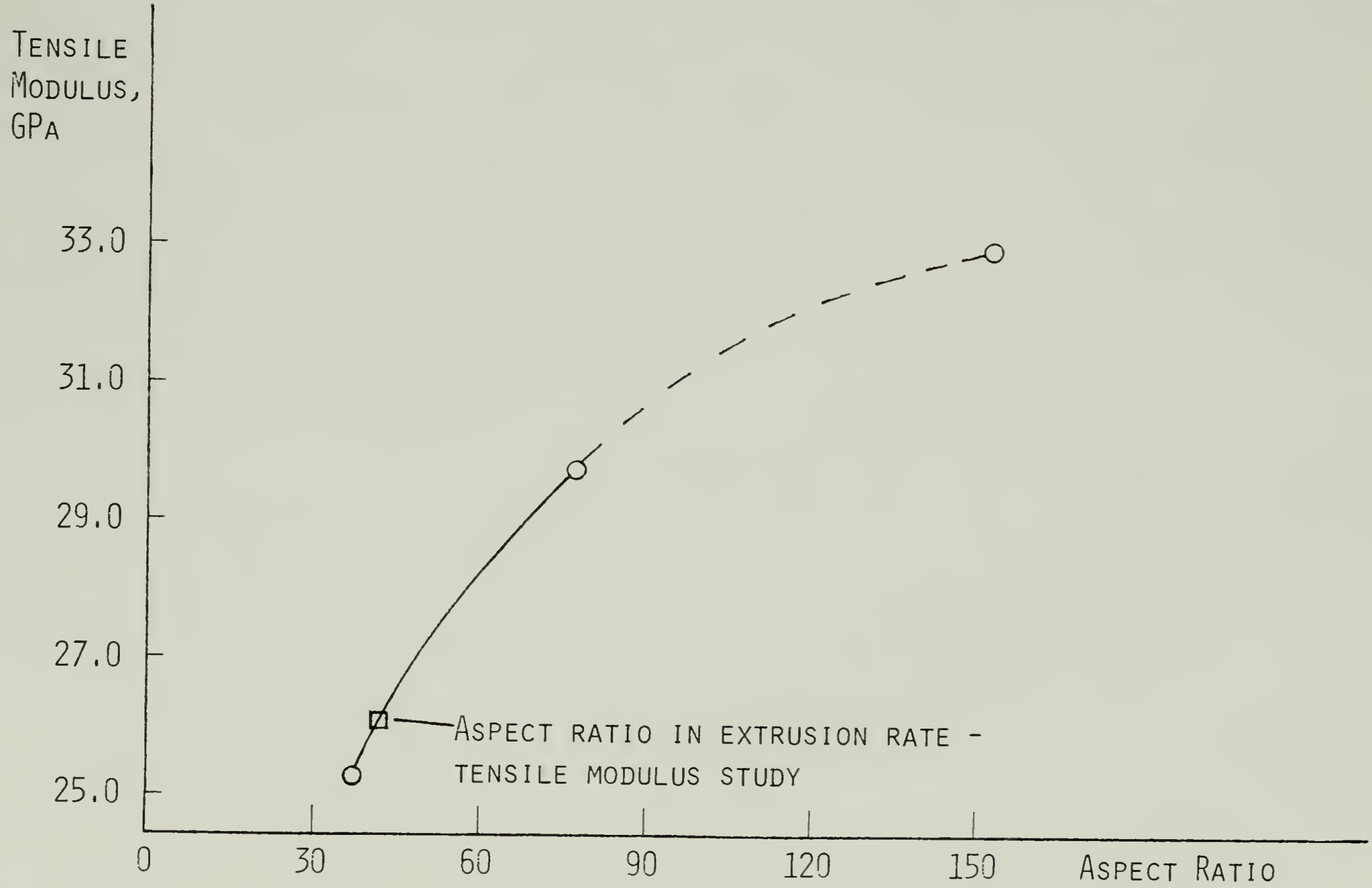

Table 16

Modulus of Samples Cut from the Same Extrudate

Extrusion Conditions: Draw Ratio = 29.1, Die Angle = 20^{o}, P_E = 182 MPa Extrusion Temperature = $120^{o}C$, Extrusion Rate = 1.57 cm/min.

Sample	Cross-Sectional Area, mm^2	Initial Modulus, GPa	Average Modulus, GPa
1	1.491	26.2	29.4
2	1.522	22.6	28.5
3	1.027	25.6	28.1
4	0.997	24.3	25.5
Average ± Standard Deviation		24.7±1.6	27.9±1.7

The effect of extrusion rate on modulus for the three extrusion conditions is shown in Fig. 8. The large scatter of moduli and small change in modulus with extrusion rate prevents statistically concluding that extrusion rate affects modulus. However, all three conditions exhibited a slight but measurable rise in modulus with decreasing extrusion rate.

Several statements, founded on this result, can be made about the deformation process. The increase in modulus may be due to two reasons. A lower extrusion rate allows deformation to occur more uniformly through unfolding of crystalline blocks instead of block slippage and chain fracture. This increases the concentration of tie molecules and consequently modulus. A lower extrusion rate also indicates that the pressure is acting more as a flow inhibiting compressive force and less as an accelerating force and lowers the effective extrusion temperature. This also increases the modulus. The data also shows that although lubrication may reduce friction and shear deformation, it does not affect modulus and

FIG. 8. TENSILE MODULUS VS. EXTRUSION RATE

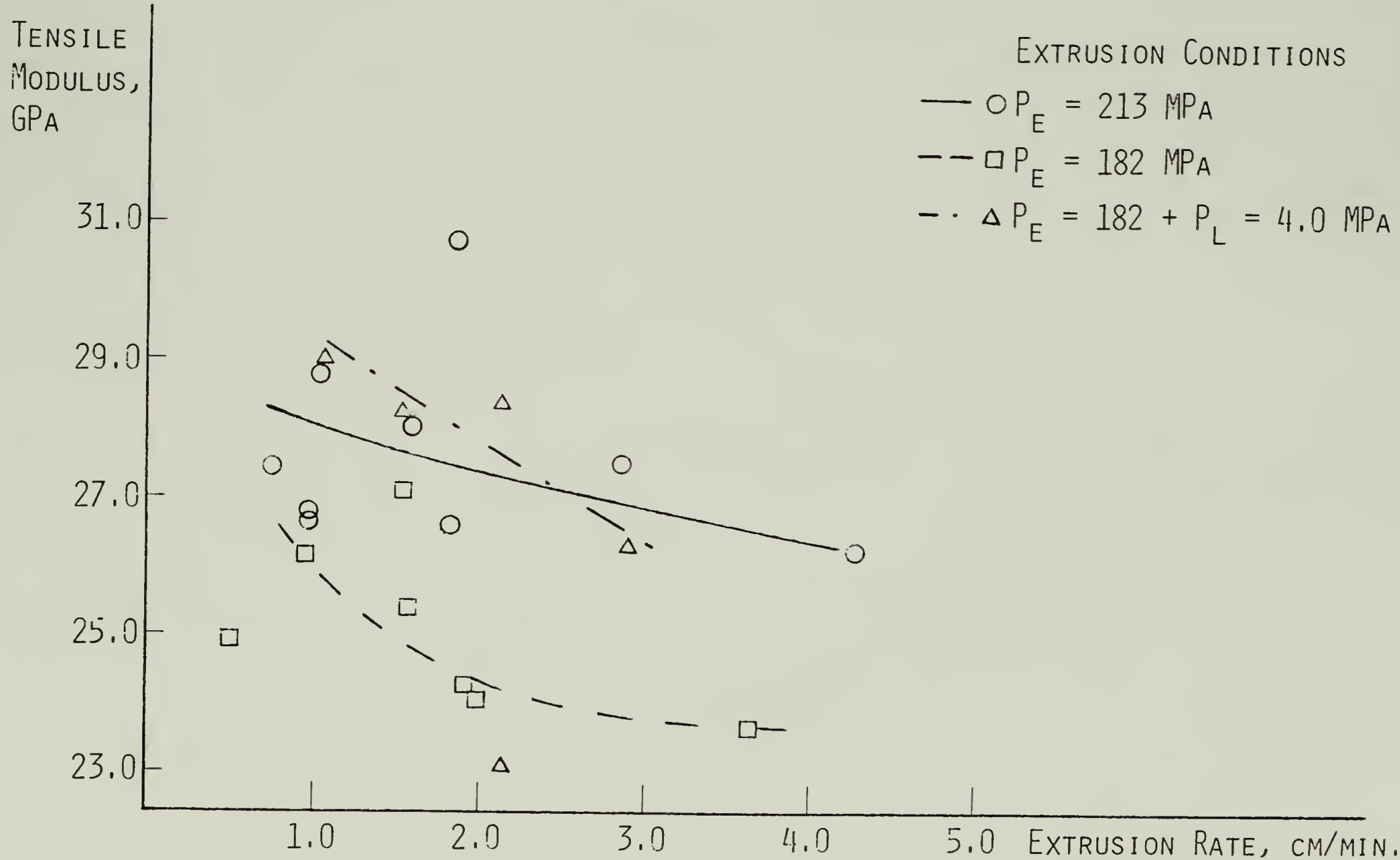

thus must have little effect on extrudate morphology. Annealing time increases as extrusion rate decreases and may lower modulus. If annealing occurred rapidly and to a significant extent, the difference in annealing time between extrudates should produce readily visible effects. Peterlin and Corneliusson[58] showed that annealing begins in drawn samples after less than one minute at 110°C. The small increase in modulus with decreasing extrusion rate, opposite to the trend predicted assuming significant annealing, indicates that little annealing occurs.

Adiabatic heating may occur during extrusion depending on billet size.[9] This raises the actual extrusion temperature and reduces tensile modulus. Faster extrusion rates would generate more heat and might be responsible for the observed decrease in modulus at higher rates. However, higher extrusion temperatures also produce higher extrudate crystallinity. Since crystallinity, measured very precisely by density gradient column, does not change with extrusion rate, adiabatic heating can be assumed to be insignificant. In general, it appears that all of the proposed mechanisms through which extrusion rate may affect the final morphology are nearly independent of variations in extrusion rate produced by lubrication in the range studied.

Samples extruded at 213 MPa had higher moduli than samples of similar extrusion rate extruded at 182 MPa. This increase is due exclusively to higher pressure acting as a hydrostatic force and lowering the effective extrusion temperature through undercooling. Any possible effect of less annealing time normally produced by extrusion at higher pressure has been eliminated by comparing samples with similar extrusion rates. Increased pressure also does not produce higher modulus through closer microfibril

packing because the 213 and 182 MPa extrudates have nearly identical average densities.

There was a distinct increase in modulus in samples pultruded at 182 MPa pushing pressure plus 4.0 MPa pulling pressure compared to samples extruded at 182 MPa pushing pressure alone. However, the mechanism through which pulling increases modulus is difficult to identify. Pulling does not improve microfibril packing since the average density of the pultruded samples is slightly lower than that of the extruded samples. It could act as a fixed end and reduce annealing, but the analysis of the effect of extrusion rate on modulus concluded that annealing does not occur significantly. The combination of pulling and pushing may produce more orderly deformation than pushing pressure alone. This would reduce stress concentrations and be manifested by improved appearance (a smoother interface between the two halves) as well as higher modulus. However, there was no discernable improvement in the pultruded samples' appearance.

Finally, it is possible that increased elongational flow, possibly induced by the pulling force, alters the final morphology to produce a higher modulus. This proposal cannot be evaluated with the present data. Its validity would mean that increased extrusion rate is more detrimental to the deformation process than is apparent from Fig. 8. Elongational flow is also increased by lubrication.[17] Thus, higher extrusion rates resulting from greater lubrication should produce samples with higher moduli. Since the opposite trend was found, the higher deformation rate must compensate for the increase in modulus caused by greater elongational flow as well as produce the decrease in modulus observed. Although this reasoning is logical, it is too far removed from verifying data to be conclusive. In summary, the mechanism or combination of mechanisms

through which a pulling force increases modulus is uncertain.

There was no correlation between modulus and billet crystallization pressure or crystallinity. The minor differences in billet crystallinity were too small to have a significant effect on the deformation process.

Variations in modulus with extrusion rate and processing conditions were also not reflected by changes in sample crystallinity. As stated earlier, Zachariades et al[51] reported that crystallinity as well as modulus increased with increasing draw ratio. However, crystallinity began to level off above a draw ratio of 15, signifying that crystallinity is increased through spherulitic deformation but not through microfibrillar shear deformation. Samples extruded at lower rates have higher moduli. However, this is probably due to differences in deformation occurring at the microfibrillar level and thus are not reflected by crystallinity.

Zachariades and coworkers also found that raising the extrusion temperature increased crystallinity but decreased sample modulus at constant draw ratio. This indicates that tie molecule concentration and not crystalline perfection determines modulus. If higher extrusion pressure increased modulus by lowering the effective extrusion temperature, it should also decrease crystallinity. Extrusion pressure was found to have no effect on crystallinity. However, crystallinity attained only about 10% of its expected increase relative to Zachariades' results. Therefore it is reasonable that it would not be affected by the, at maximum, $6^{o}C$ change in the effective extrusion temperature. Although a direct comparison cannot be made because of differences in strain rate and aspect ratio, the moduli found here and in Zachariades' study are approximately the same.

Shrinkage

The effect of shrinkage time was studied on three samples: the two halves of an extruded sample and one half of a pultruded sample of a similar extrusion rate as the extruded samples. This allows reproducibility of results and differences between extrusion and pultrusion to be determined unconfounded by possible effects of extrusion rate. A plot of molecular draw ratio (MDR) versus shrinkage time (Fig. 9) shows a steep, linear increase in MDR to three minutes, then a slower, curved increased at longer times for all three samples. The change from a linear to a curved increase in MDR with time signifies a transition from elastic recovery of bonds deformed by extrusion to viscous flow to an equilibrium state in the melt as the dominant recovery force. An MDR due exclusively to elastic recovery is impossible to obtain using this procedure because both modes of recovery are always operating simultaneously to some extent. However, samples can be compared by selecting a sample thickness and a shrinkage time near the transition since both modes are operating approximately equally in a small range of time near the transition.

Two minutes was chosen as the shrinkage time because it had the lowest standard deviation, good shape retention, and an MDR within 5% of the MDR at three minutes. The MDR's of the two halves of the extrudate are significantly different below two minutes. Although the general shape of both curves are similar, it was expected that the individual points at each time would be closer. The intersection of the curves at two minutes was another reason to choose it as the shrinkage time.

Sample shape also changed with shrinkage time from initially rectangular, becoming dogbone-shaped at 0.5 min., rectangular at 2 min., and circular at 8 min. as it assumed its final equilibrium melt shape, Fig. 10.

FIG. 9. SHRINKAGE TIME VS. MDR

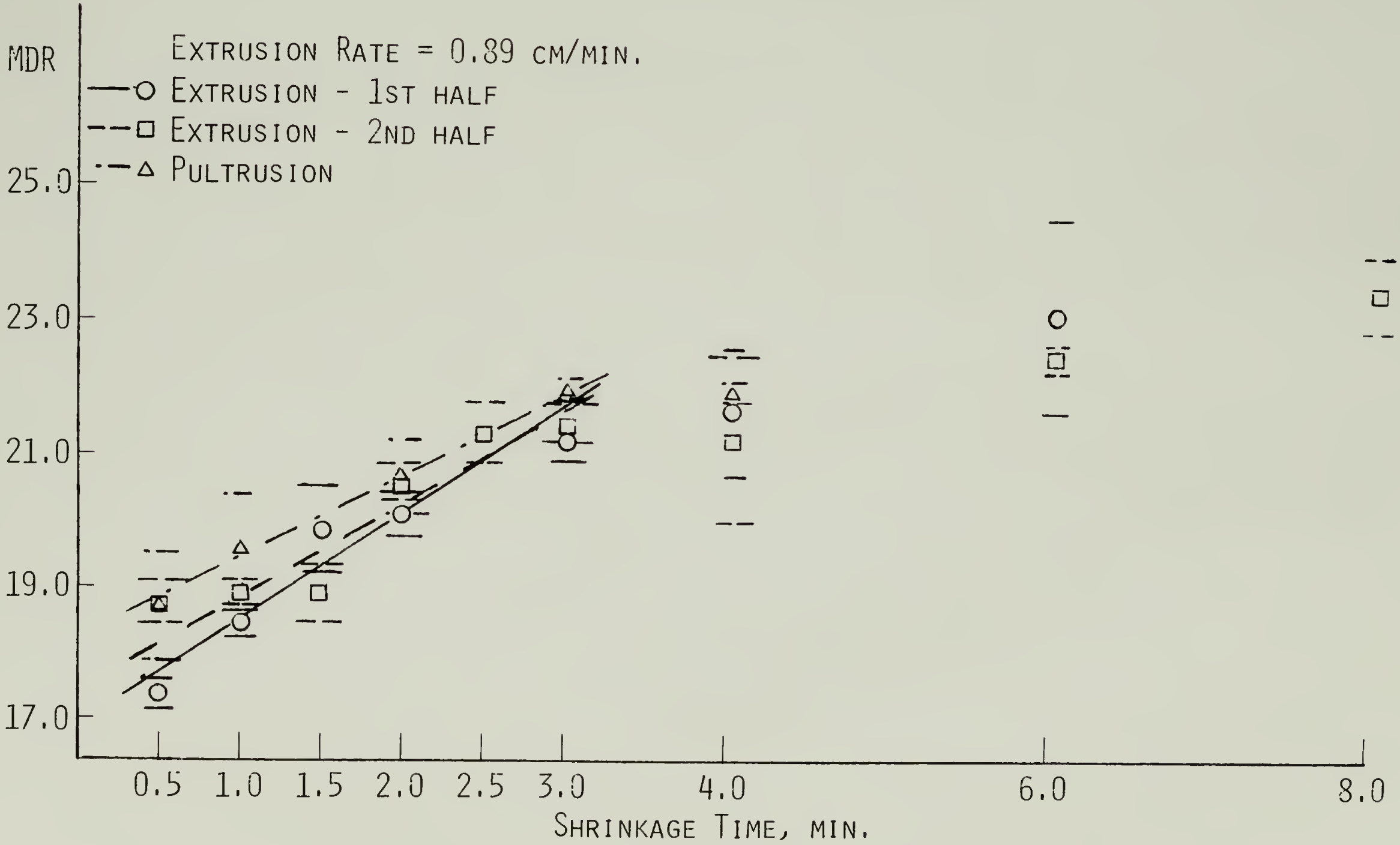

FIG. 10. SAMPLE SHAPE AS A FUNCTION OF SHRINKAGE TIME

SHRINKAGE TIME, MIN.	0	0.5	2.0	8.0

Lines drawn on the sample before shrinkage showed the fibrillar nature of the extrudate as they reproduced any irregularities on the ends of the shrink sample. The lines were symmetrically curved around the sample midpoint showing that melting occurred at the sample's edges before its interior. Shrinkage near the sample's midline was briefly inhibited by the rigid interior before it melted causing the curvature.

In conclusion, although this procedure, 0.40 $\pm$0.02 mm thick samples shrunk for two minutes, does not give an exact measure of MDR, it does give a close approximation. It can be satisfactorily used to compare differences in MDR between samples. Although reproducibility is not good at short shrinkage times, it is acceptable at the time chosen for further experiments. There also appears to be no major differences in MDR between extruded and pultruded samples indicating similar efficiency of deformation.

The results of shrinkage measurements are reported in terms of MDR in Fig. 11. MDR decreased slightly as extrusion rate increased for all three extrusion conditions. Although the error is large compared to the change in MDR with extrusion rate, similar trends for all three conditions indicate that the change is small but real.

The higher MDR found at lower extrusion rates is consistent with the conclusion of the modulus study that slower extrusion allows more efficient deformation. Shrinkage has been attributed to contraction of extended chain crystals[150] and stressed tie molecules.[72,151] Large extended chain crystals reducing their high surface free energy by transforming into smaller crystals also contributes to the recovery force.[89,152] As bond deformation accounts for more and chain slippage for less of the bulk deformation, the tie molecule concentration and

FIG. 11. MDR VS. EXTRUSION RATE

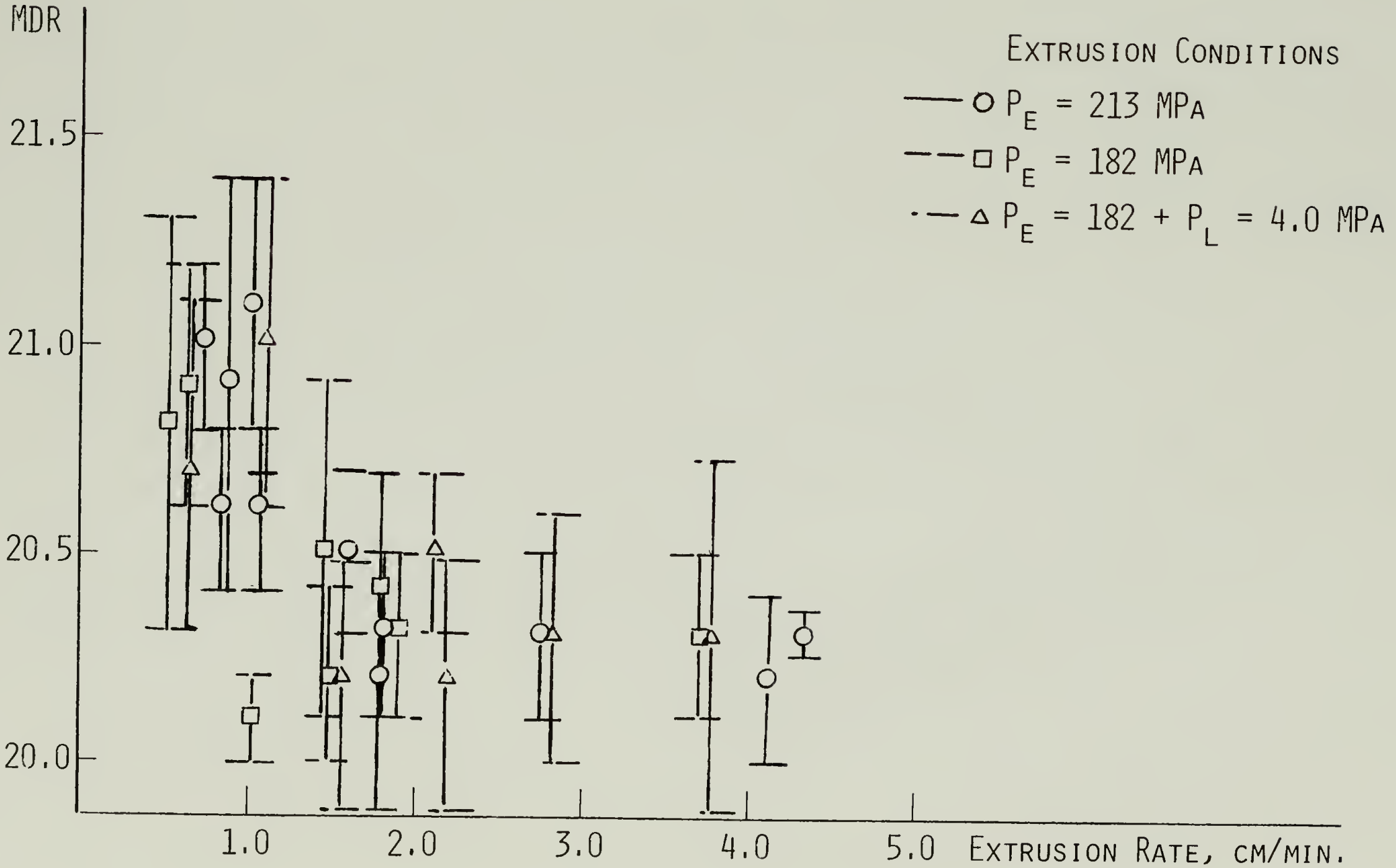

thus MDR at constant draw ratio increases.

Watts et al[63] reported that shrinkage and tensile modulus, both of which depend on tie molecule concentration, were linearly related in samples extruded at various temperatures to a constant draw ratio. The result correlates well with the similar increase, approximately 2%, in both MDR and modulus found at lower extrusion rates in this study.

Extrusion temperature determines the efficiency of deformation through competitive relaxation of deformed bonds. Polyethylene crystallized under the combined effects of orientation and pressure shows high orientation[153] while normally melt extruded samples show little orientation. This implies that the lower orientation of melt extrudates and higher temperature solid-state extrudates is due to relaxation of bonds that become deformed and oriented during extrusion. Extrusion rate determines efficiency by controlling the maximum orientation obtained without relaxation effects. The absence of dieswell indicates that MDR is lower than extrudate draw ratio exclusively due to viscous flow during the extrusion process itself. However, the correlation between the two studies implies that extrusion rate has a small but similar effect as temperature on overall efficiency and consequently extrudate properties.

There was no observable change in MDR with extrusion conditions. This result is unexpected because of the correlations previously found between MDR and tensile modulus and the mechanisms developed to explain the effects of extrusion conditions on the deformation process. These results are also surprising because MDR reproduced the small (2%) increase in modulus with decreasing extrusion rate but not the larger (10%) increase with increasing extrusion pressure or through pultrusion. The proposed dependence of both shrinkage and modulus on tie molecule

concentration predicted that they should vary directly with each other.

The cause of these results is unknown. There was no correlation between billet crystallization conditions and MDR. Assuming the data is correct, it indicates that factors other than tie molecule concentration determine modulus and have an effect only at low temperature. For example, Peterlin proposed that higher extrusion pressure enhances adhesion between fibrils.[34] Cohesive forces, such as Van der Waals forces, are stronger at lower temperatures. Modulus increases with decreasing test temperature as chain slip becomes more difficult. Tie molecule concentration remains constant. However, this effect is diminished by increasing the temperature and vanishes in the melt. Therefore shrinkage results from samples possessing varying degrees of cohesiveness would be equivalent. This example cannot be applied to this study because higher tie molecule concentration was proposed to be the cause of higher modulus observed at increased extrusion pressure. However, the mechanism may be correct.

Variation of Properties as a Function of Radial Position in the Extrudate

Variation in properties as a function of radial position was studied on a pultruded sample of draw ratio 29.1 with an extrusion rate of 0.89 cm/min. Table 17 shows the original DSC data and Table 18 shows the same data with the inconsistent values excluded. Shrinkage results, reported in terms of MDR, are listed in Table 20. Averages by section within each table were compared statistically at the .05 confidence level to determine if the averages were different. The results of these comparisons are shown in Tables 19 and 21. The sections are ranked in Table 22 from highest to lowest in each characterization.

Table 17

Thermal Properties as a Function of Position in the Extrudate - Original DSC Data

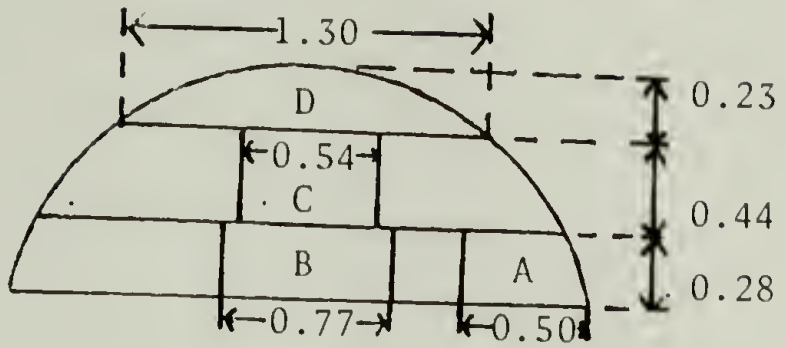

Extrusion Conditions: Draw Ratio = 29.1, Die Angle = 20°, Extrusion Temperature = 120°C, P_E = 182 MPa, Extrusion Rate = 0.89 cm/min.

Section	Tms, K	Tmp, K	Crystallinity, %	Peak Width, mm
A	398.56	410.88	77.6	12.32
"	400.75	412.25	75.8	11.30
"	397.75	410.75	76.9	13.00
Average ± Standard Deviation	399.02±1.55	411.29±.83	76.8±0.9	12.21±0.48
B	397.31	411.63	79.3	14.32
"	397.75	410.44	79.6	12.69
"	399.25	410.31	76.5	11.06
Average ± Standard Deviation	398.10±1.02	410.79±.73	78.5±1.7	13.02±1.68
C	399.00	410.25	75.2	12.50
"	399.13	409.94	75.6	10.81
"	398.94	409.88	75.3	10.94
Average ± Standard Deviation	399.02±.09	410.01±.19	75.4±.2	11.42±0.95
D	400.25	410.88	75.5	10.63
"	398.13	410.56	78.7	12.43
"	398.94	410.88	76.0	11.94
Average ± Standard Deviation	399.11±1.06	410.77±.18	76.7±1.7	11.67±0.93

Table 18

Thermal Properties as a Function of Position in the Extrudate - Best DSC Data

Section	Tms, K	Tmp, K	Crystallinity, %	Peak Width, mm
A	398.56	410.88	77.6	12.32
"	397.75	410.75	76.9	13.00
"				
Average ± Standard Deviation	398.16±0.57	410.82±0.09	77.3±0.5	12.66±0.48
B	397.31		79.3	
"	397.75	410.44	79.6	12.69
"		410.31		
Average ± Standard Deviation	397.53±0.31	410.38±0.09	79.5±0.2	12.69
C	399.00	410.25	75.2	
"	399.13	409.94	75.6	10.81
"	398.94	409.88	75.3	10.94
Average ± Standard Deviation	399.02±0.09	410.02±0.19	75.4±0.2	10.88±0.09
D		410.88	75.5	
"	398.13	410.56		12.43
"	398.94	410.88	76.0	11.94
Average ± Standard Deviation	399.54±0.57	410.77±.18	75.8±0.4	75.8±0.4

Table 19

Statistical Comparison of
Extrudate Position Based on Thermal Analysis

Original Data

At the .05 confidence level,		Tms	Tmp	Crystallinity
A is the same as	B	Yes	Yes	Yes
A	C	Yes	Yes	Yes
A	D	Yes	Yes	Yes
B	C	Yes	Yes	No, >
B	D	Yes	Yes	Yes
C	D	Yes	No, <	Yes

Best Data

At the .05 confidence level,		Tms	Tmp	Crystallinity
A is the same as	B	Yes	No, >	No, <
A	C	Yes	No, >	No, >
A	D	Yes	Yes	Yes
B	C	No, <	Yes	No, >
B	D	No, <	No, <	No, >
C	D	Yes	No, <	Yes

Table 20

Molecular Draw Ratio as a
Function of Position in the Extrudate

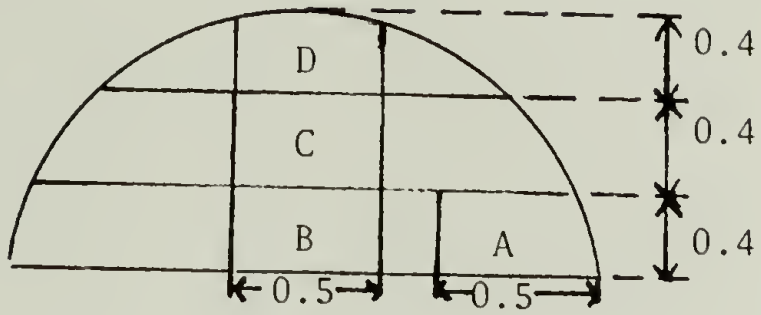

Dimensions in mm

Section	MDR ± Standard Deviation
A	20.9±0.2
B	19.9±0.4
C	19.3±0.7
D	21.0±0.1

Table 21

Statistical Comparison
of Extrudate Position Based on MDR

Sections Compared at the .05 Confidence Level	Statistically Different MDR
A-B	Yes
A-C	Yes
A-D	No
B-C	Yes
B-D	Yes
C-D	Yes

Table 22

Ranking of Extrudate Position
Based on MDR and Thermal Analysis

Ranking	Tms	Tmp	Peak Width	Crystallinity	MDR
Highest - 1	D	AD	AB	B	AD
2	C	AD	AB	A	AD
3	B	B	D	CD	B
Lowest - 4	A	C	C	CD	C

Seven of the eighteen "best data" DSC averages and five of the six MDR averages compared were different at the .05 confidence level indicating that morphology changes with position. However, logical trends in terms of sample position could not be found. For example, section D should have the lowest properties since it is next to the die wall where shear stresses are highest. Section B should have the highest properties since it benefits most from both greater elongational flow and the stress relief allowed by the split billet in its central position in the full extrudate. However, D has the highest Tmp, Tms, and MDR whereas B is third lowest in those properties.

MDR is expected to correlate with DSC values since more efficient deformation should increase MDR, melting point, and crystallinity. A correlation was found between MDR and Tmp only. However, the expected relationship between DSC values, higher melting point with higher crystallinity, was not found. This indicates the correlation between MDR and Tmp was coincidental. Therefore, although DSC and MDR values may be related, it cannot be detected in the small changes in their values in this study.

In conclusion, the results show that there may be real differences between the sections in the extrudate but the differences are small. Variation in morphology that may exist at lower draw ratios, as observed by Farrell and Keller,[57] may be lost at high draw ratios, >15, due to the greater deformation of all sections.

Summary

Extrudate properties were only slightly affected by variations in extrusion rate produced by differences in billet lubrication. Modulus and MDR increased slightly with decreasing extrusion rate but thermal properties were constant. It is proposed that the increase in modulus and MDR was due to the lower extrusion rate allowing more efficient deformation and consequently increasing tie molecule concentration. The constancy of thermal properties indicates that efficiency is improved only above draw ratio 15 where thermal properties are independent of deformation.

Only modulus was increased by higher extrusion pressure and pultrusion although modulus, MDR, and thermal properties have been previously shown to be related. Modulus is proposed to increase at higher extrusion pressure through increased undercooling. However, if this were valid, MDR and thermal properties should also have been affected. Thus, either the mechanism is incorrect or the level of undercooling that does occur has no significant effect on morphology.

In conclusion, although lower extrusion rates produced by less lubrication may allow slightly more orderly deformation, extrudate properties are nearly independent of extrusion rate in the range studied. Only modulus is affected by changes in deformation produced by variation in extrusion pressure and by pultrusion.

CHAPTER V

PULTRUSION

Introduction

Pultrusion, the combination of pushing and pulling pressures, has been shown to produce faster extrusion rates than simple solid-state extrusion, i.e., by a pushing pressure alone, at equivalent total pressures. The relative effectiveness of pushing to pulling pressure in causing deformation has been quantified by λ, the ratio of pushing to pulling pressures that produce equivalent extrusion rates.[84] Several mechanisms were proposed in Chapter II-C-8 to explain the effect of a pulling force on deformation during extrusion. They include more uniform deformation, an increase in elongational and decrease in shear flow, more efficient use of deformational force, and reduction of hydrostatic pressure. Based on these mechanisms it was predicted that increasing die angle and draw ratio and decreasing extrusion temperature should increase λ.

In this chapter the pultrusion process will be examined experimentally. Several methods to evaluate λ will be discussed and the effects of draw ratio, die angle, and extrusion temperature on λ will be presented. The influence of these factors on billet deformation profiles will also be reported. Inferences about deformation during pultrusion made from these results will be integrated with the mechanism developed thus far.

Procedure

Experiments were run using the same pultrusion apparatus, procedure, and polymer (high density polyethylene, Alathon 7050, DuPont, M_W = 59,000, M_N = 19,900) as in the extrusion rate-properties study. Billets were crystallized at 91 MPa and split longitudinally for extrusion. Extrusion rates were measured by following the motion of a marker placed on the extrudate with a cathetometer and pultrusion rates by means of a revolving potentiometer connected to a recorder, Fig. 3. Rates were recorded when they had become constant. In pultrusion, this was determined by linearity of the recorder trace. Conical dies with 20° entrance angles were used in the draw ratio and temperature experiments. The effect of draw ratio on λ was determined at draw ratios 33.3, 29.1, 23.4, and 14.5. All tests were made at 120°C. The effect of extrusion temperature was studied at 105, 120, and 130°C at a constant draw ratio of 23.4. The effect of die angle was measured at 20 and 30°, both at a draw ratio of 23.4 and a temperature of 120°C.

Methods for Evaluation of λ

Several methods can be used to evaluate λ. Shimada and coworkers[84] maintained a set pushing pressure, P_E, and measured pultrusion rates as a function of different pulling pressures, P_L. This procedure was repeated for a series of pushing pressures producing the family of curves shown in Fig. 12. The combinations of P_E and P_L that produced a constant extrusion rate were then plotted, see Fig. 13. The absolute value of the slope of each line of constant extrusion rate is λ and represents the relative levels of P_E and P_L required to produce that rate.

FIG. 12. EXTRUSION RATE AS A FUNCTION OF P_E AND P_L

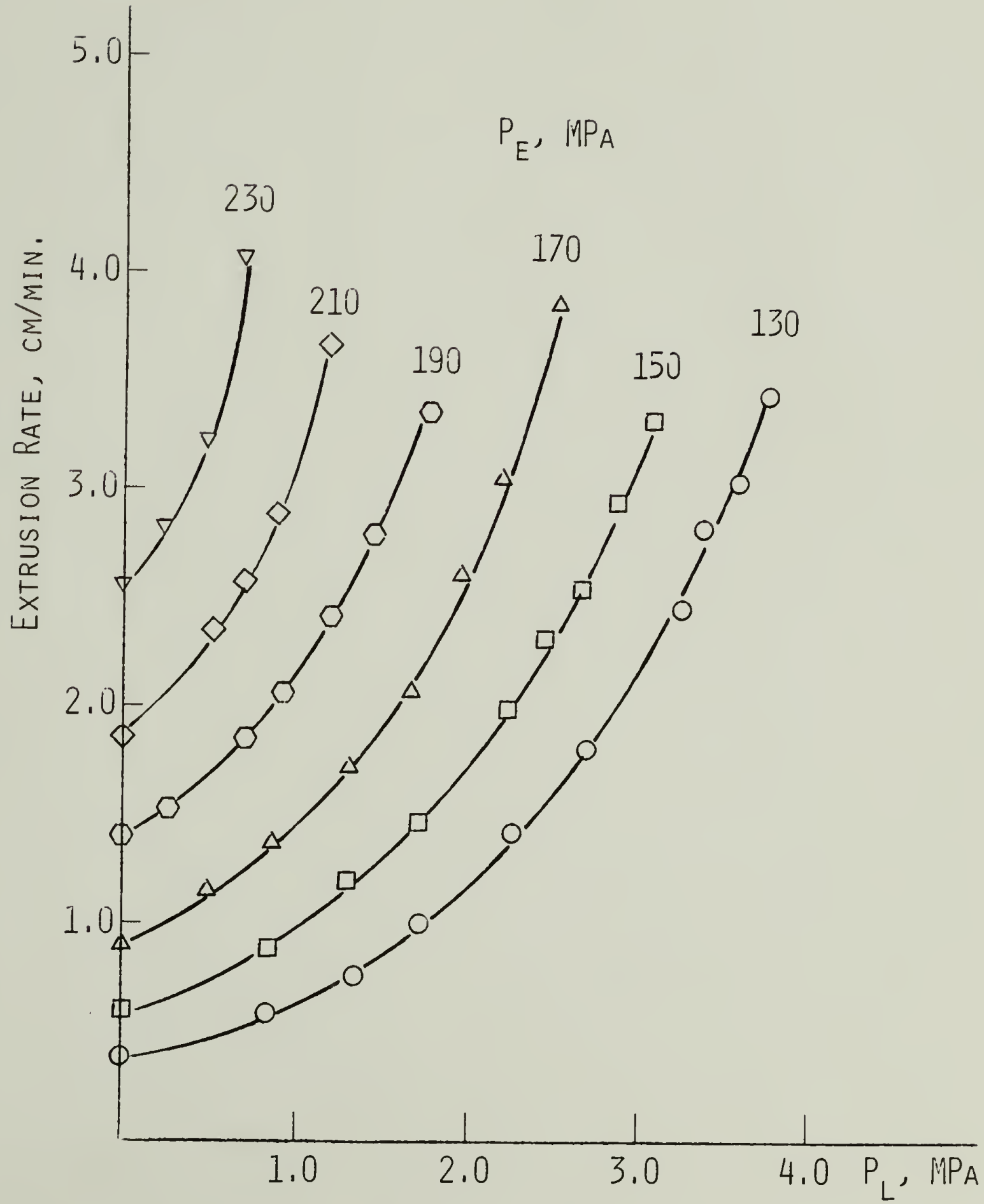

FIG. 13. CALCULATION OF λ USING SEVERAL BILLETS

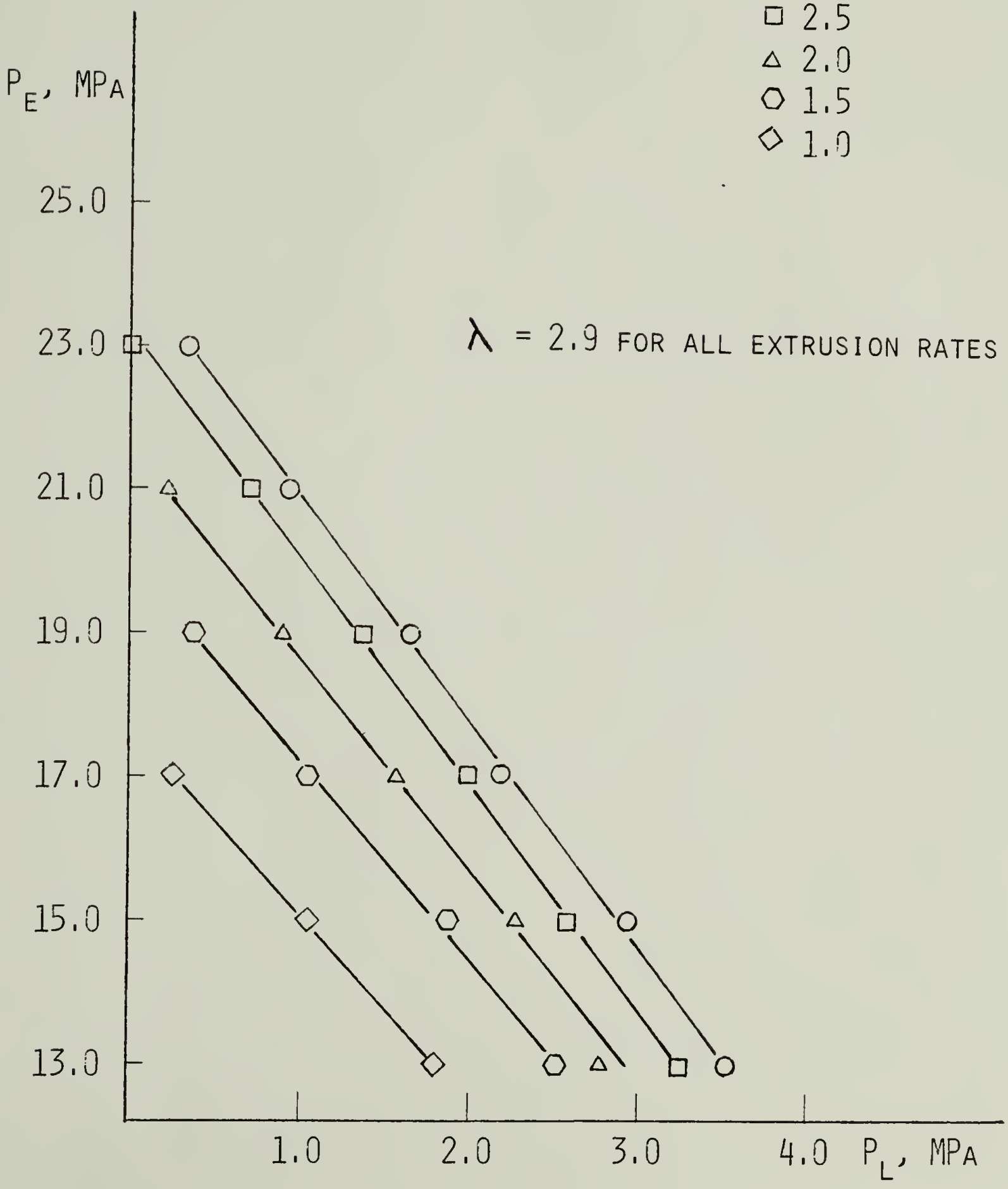

λ = 2.9 FOR ALL EXTRUSION RATES

Shimada's method for determining λ assumes that billets extruded under identical pressures will have very similar extrusion rates. However, this could not be assumed in this study due to uncontrolled billet lubrication acquired during handling of the billet. Lubrication is necessary to achieve high draw ratio extrudates. Fracture occurred at draw ratio 14.5 when both the billet and die were thoroughly washed with soap and water and rinsed with acetone. Therefore, several experiments were performed in an attempt to provide uniform lubrication for extrusion. These methods include spraying the die with a fluorocarbon lubricant, dipping the billet in a 4% solution by weight of sodium dodecyl sulfate in water, and rubbing the billet thoroughly by hand. However, none of these techniques yielded satisfactorily consistent extrusion rates. Relative levels of billet lubrication and thus the validity of λ can be determined by inspection of extrusion pressure - extrusion rate curves such as Fig. 12. This procedure will be explained in the Results section. However, because of the low probability of equal billet lubrication, Shimada's method was used only for the 33.3 draw ratio die.

To avoid using several billets to determine λ, combinations of P_E and P_L that produced similar extrusion rates in a single billet were recorded. The normal pultrusion procedure was followed. After an extrusion rate had been established at a P_E and P_L, P_L was increased and then P_E decreased until the original rate was reestablished. The factor λ was calculated through comparison of the new combination of P_E and P_L to the original. All billets were thoroughly rubbed by hand prior to extrusion in an attempt to provide uniform lubrication. Decreased lubrication impedes deformation and may, following the logic of the other predictions, increase λ. As a precaution against any dependence of λ

on extrusion rate, measurements in all experiments were made at an extrusion rate of 0.90 ± .05 cm/min.

This method was used to determine the effects of draw ratios 29.1, 23.4, and 14.5 and extrusion temperature on λ . It generally worked well, producing a constant λ or a gradual trend in λ with increasing P_L. However, sharp increases in rate with little change in pressure and small changes in rate with large changes in pressure were sometimes encountered. These results were not used to calculate λ and their cause is unknown.

A third method was devised to evaluate λ which was to employ Shimada's technique on a single billet. Extrusion rate was to be measured as a function of increasing P_E. P_E would then be reduced to its original level and the rate measured as a function of increasing P_L. λ would be determined by dividing the increase in P_E over the original P_E which produced any selected extrusion rate by the P_L which also produced that rate. This method was never used due to the failure of preliminary control experiments. Extrusion rate was measured at a low P_E. P_E was increased for a short period of time and then returned to its original level. However, the extrusion rate did not return to its original level. It was thought that the high pressure may have caused an alteration in the deformational flow profile and thereby changed the extrusion rate. Therefore, the conical section of the billet was cut off and the billet reextruded. Again, the original extrusion rate was not reproduced. The change in rate may be due to unequal lubrication along the billet. However, constant extrusion rates were usually observed. Since equal initial extrusion rates for extrusion and pultrusion could not be established, this technique could not be used to evaluate λ . The cause of the change

in extrusion rate is unknown.

Results and Discussion

Draw Ratio

Shimada's method, described above, was used for the 33.3 draw ratio die. The extrusion pressure - extrusion rate curves and P_E-P_L plot are shown in Fig. 14 and 15 respectively; λ, initially at 4.4 at low extrusion rates, increased with increasing rate and become constant at approximately 8.8. The value of λ represents the relative effectiveness of P_L to P_E in producing an extrusion rate. Thus, at low extrusion rates, a P_E 4.4 times as great as P_L is necessary to produce a similar rate.

The effect of draw ratio on λ was evaluated using the single billet method at draw ratios 29.1, 23.4, and 14.5. Results are shown in Tables 23, 24, and 25; λ was calculated from all combinations of P_E and P_L, as illustrated in Table 23, enabling detection of inconsistencies and trends in λ. At draw ratio 29.1, λ was constant at 3.3 for all combinations of P_E and P_L. Draw ratio 23.4 exhibited an initial λ of 4.6 which decreased with increasing P_L and reached a limiting value of 3.6. At draw ratio 14.5, λ began at 4.9 and decreased with increasing P_L without reaching a lower limit. The variation in λ with P_L prevents comparison of average λ values for the three draw ratios. However, through comparison of individual λ's at similar changes in P_E, a trend of decreasing λ with increasing draw ratio was observed.

Shimada, who also extruded Alathon 7050 at 120°C, found a λ of 2.9 $\pm$ .2 at draw ratio 30. This is similar to the λ of 3.3 found at draw 29.1 using the one billet method. This result, the possibility of unequal billet lubrication, and the decrease in λ found at higher draw

FIG. 14. EXTRUSION RATE VS. P_L AT THREE LEVELS OF P_E

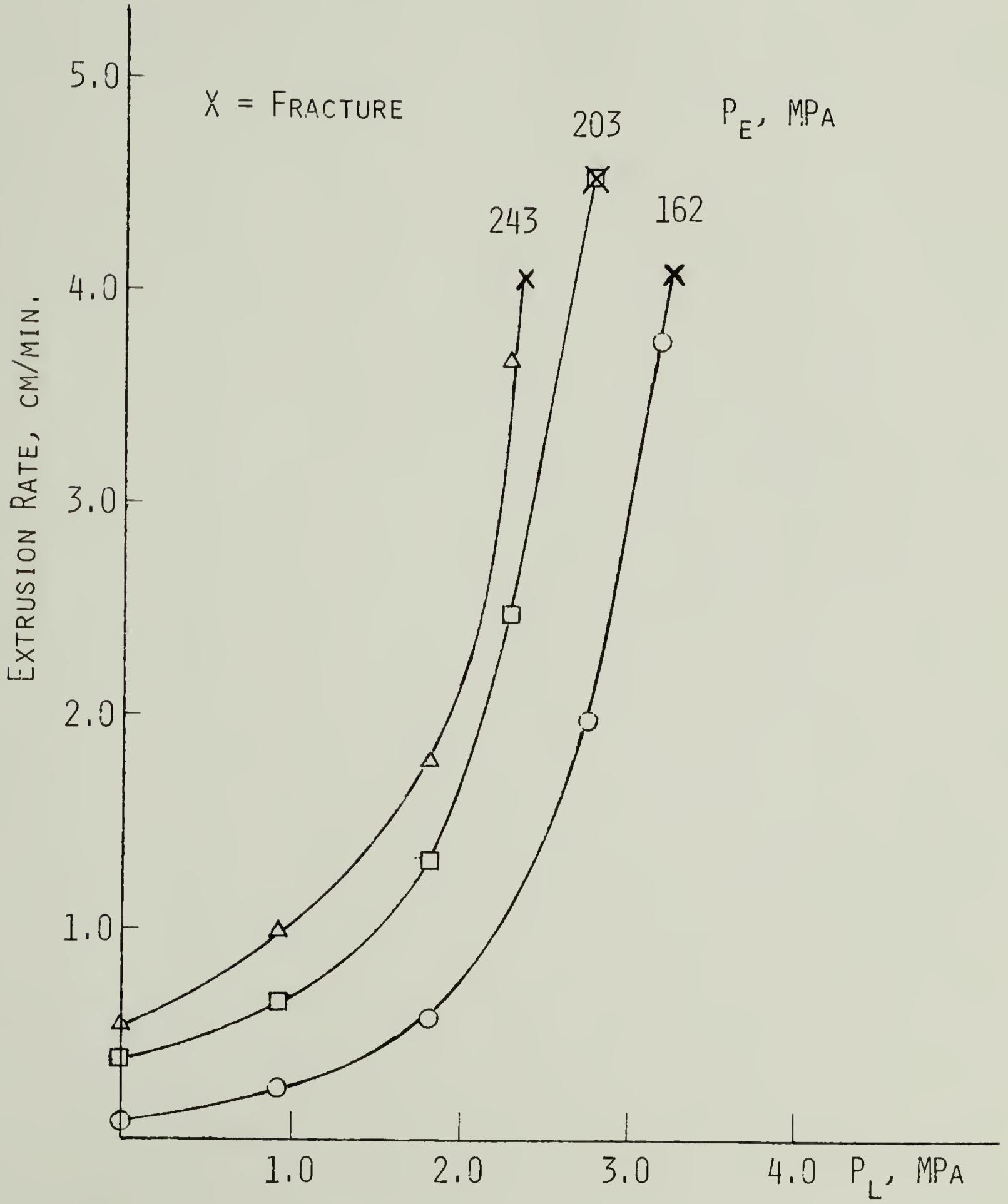

FIG. 15. P_E VS. P_L AT CONSTANT EXTRUSION RATE - CALCULATION OF λ

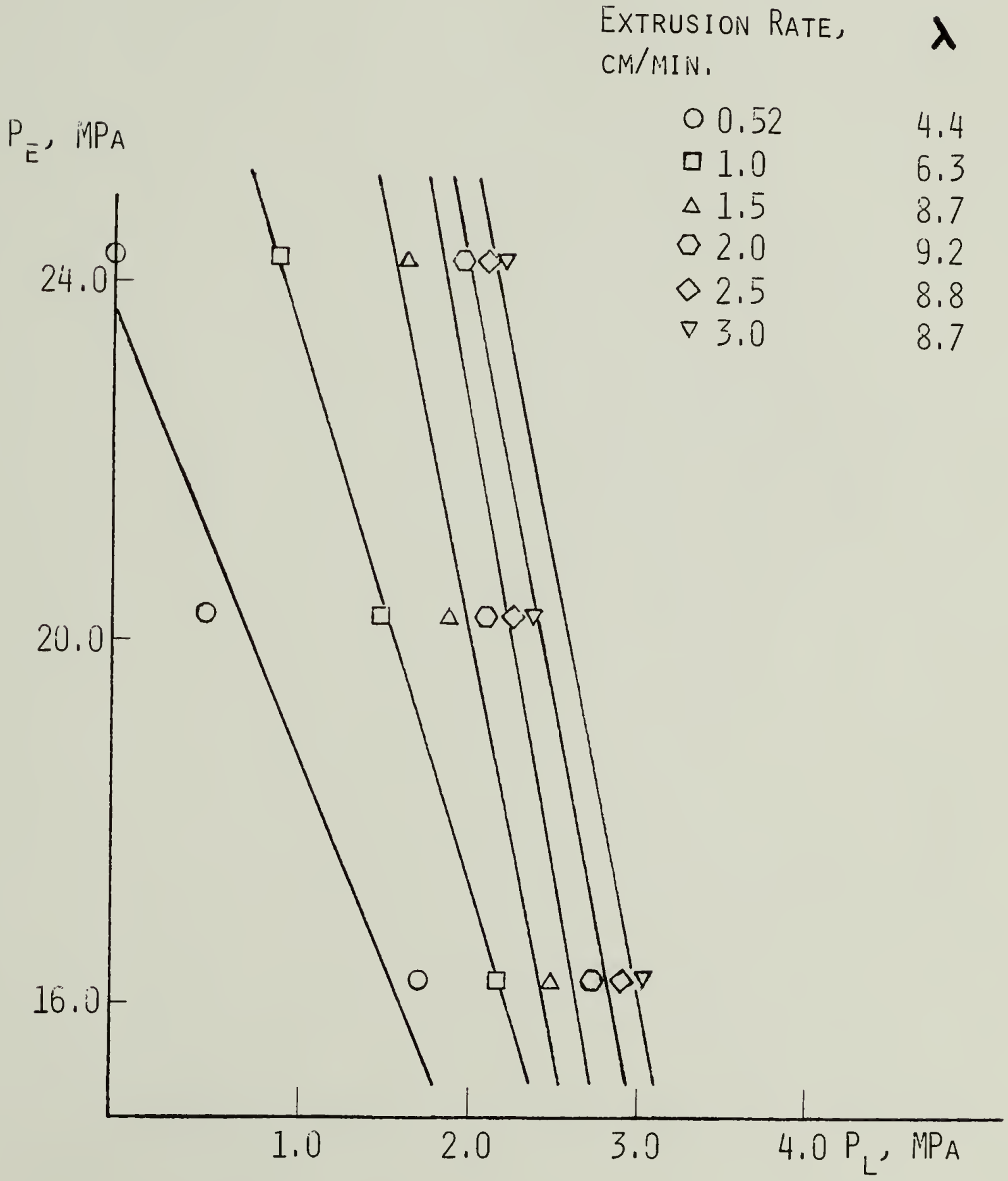

Table 23

Effect of Draw Ratio on λ - Draw Ratio = 29.1

Draw Ratio = 29.1, Die Angle = 20^{o}, Extrusion Temperature = $120^{o}C$,

$\lambda_{Average} = 3.3 \pm 0.1$

$$\lambda = \left(\frac{Atm._2 - Atm._1}{Kg_2 - Kg_1}\right) (2.528 \times 10^{-2})$$

λ_1 at $P_E = 1663$, $P_L = 1$ is calculated from values at

$P_E = 1788$, $P_L = 0$ and $P_E = 1663$, $P_L = 1$

λ_1 at $P_E = 1527$, $P_L = 2$ is calculated from values at

$P_E = 1788$, $P_L = 0$ and $P_E = 1527$, $P_L = 2$

λ_2 at $P_E = 1527$, $P_L = 2$, is calculated from values at

$P_E = 1663$, $P_L = 1$ and $P_E = 1527$, $P_L = 2$

P_E, atm.	P_L, kg	Extrusion Rate, cm/min.	λ_1	λ_2	λ_3	λ_4
1788	0	0.91				
1663	1	0.90	3.16			
1527	2	0.92	3.30	3.44		
1253	4	0.91	3.38	3.46	3.47	
1130	5	0.96	3.33	3.34	3.18	3.32

Fracture above 5 kg

Table 24

Effect of Draw Ratio on λ - Draw Ratio = 23.4

Draw Ratio = 23.4, Die Angle = 20^{o}, Extrusion Temperature = $120^{o}C$

$\lambda = (\frac{\Delta atm}{\Delta kg})(3.144 \times 10^{-2})$

P_E, atm.	P_L, kg	Extrusion Rate, cm/min.	λ_1	λ_2	λ_3	λ_4	λ_5
1461	0	0.86					
1423	1	0.87	1.18				
1166	2	0.83	4.58	7.97 Average			
929	4	0.84	4.13	~~5.11~~	3.68		
810	5	0.83	4.04	~~4.76~~	3.68	3.69	
694	6	0.86	3.97	~~4.53~~	3.66	3.65	3.60

NOTE: λ_1 = 1.18 was an erroneous reading as λ_2 = 7.97 shows. These two numbers can be averaged. However, all other λ_2 readings are based on P_E = 1423 atm. which is incorrect.

Table 25

Effect of Draw Ratio on λ - Draw Ratio = 14.5

Draw Ratio = 14.5, Die Angle = 20^{o}, Extrusion Temperature = $120^{o}C$

$$\lambda = \left(\frac{\Delta \text{ atm}}{\Delta \text{ kg}}\right)(5.078 \times 10^{-2})$$

P_E, atm.	P_L, kg	Extrusion Rate, cm/min.	λ_1	λ_2	λ_3	λ_4
1008	0	0.96				
912	1	0.96	4.87			
846	2	0.99	~~4.11~~	3.35		
642	4	0.93	4.64	~~4.57~~	5.18	
513	6	0.95	4.19	~~4.05~~	4.23	3.27

Average

ratios using the one billet method, question the λ of 8.8 found at draw ratio 33.3. However the pressure-rate curves in Fig. 14 are similar to Shimada's shown in Fig. 12. The lower extrusion rates in this experiment are at least partially due to the higher draw ratio and possibly to less lubrication. Extrusion rate increases less than linearly with increasing pressure, opposite to Shimada's results. However, this trend is normally observed at high draw ratios.

Data from the extrusion rate-properties study indicates that the billets were similarly lubricated. Fig. 16 shows the increase in extrusion rate produced by the addition of a P_L of 4.0 MPa to a P_E of 182 MPa as a function of the extrusion rate produced by the P_E of 182 MPa alone. The effect of P_L is greater for billets with initially higher extrusion rates. Therefore, unequal lubrication should produce non-parallel increases in extrusion rate with increasing P_L among the three

FIG. 16. INCREASE IN EXTRUSION RATE BY ADDING P_L = 4.0 MPA TO P_E = 182 MPA VS. EXTRUSION RATE AT P_E = 182 MPA

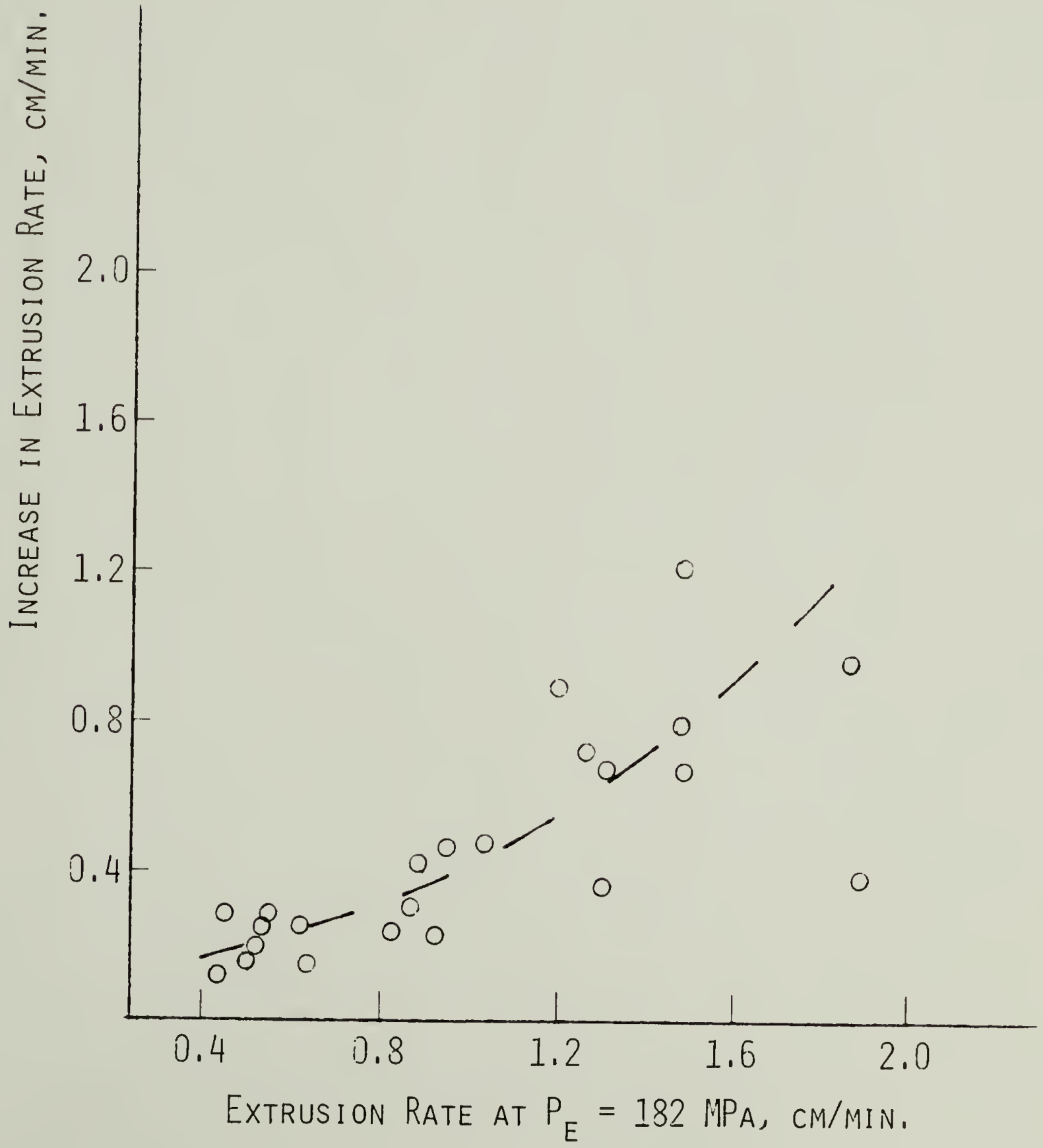

billets at draw ratio 33.3. The essentially parallel pressure-rate curves observed, similar to Shimada's, indicates that lubrication was fairly even.

The increase in λ with increasing extrusion rate observed in this experiment may be related to the small increase in extrusion rate generated by increasing P_E. Generally, extrusion rate increases more than linearly with both increasing P_E and P_L. A P_L has a greater effect on extrusion rate when combined with a high P_E than with a low P_E. P_L and P_E can be described as activation pressures for deformation. In an ideal case in which P_E has no undercooling effect, extrusion rates are equal when total activating pressures, P_A, defined as $P_E + \lambda P_L$ in Shidada's notation, are equal. An addition of a P_L to equal P_A's, although composed of different relative amounts of P_E and P_L, produces the same effect on extrusion rate. Therefore, λ is constant for all extrusion rates.

In this experiment, extrusion rate increases more than linearly with increasing P_L but less than linearly with increasing P_E. This indicates that increasing P_E is acting partially as a hydrostatic pressure and partially as a shear activating pressure. However, P_L still has a greater effect on extrusion rate than P_E indicating that it acts as and transforms P_E into an activating force. Although equal extrusion rates of 0.52 cm/min. were generated by three different combinations of P_E and P_L, their total activating forces were not equal. Thus, a P_L at this extrusion rate added to a P_A consisting of 162 MPa plus 1.74 MPa P_L does not have as much effect as the same P_L added to the same P_A consisting of 243 MPa P_E. This lowers the λ calculated at this extrusion rate. Greater P_L must be added to the 162 MPa P_E than to the 243 MPa P_E to maintain equal extrusion rates. This gradually reduces the difference

between total activating forces which become equal approximately at a rate of 1.5 cm/min. λ increases to 8.8 at this extrusion rate and remains constant at higher rates.

The much greater λ measured at draw ratio 33.3 compared to draw ratio 30 is consistent with the prediction made in Chapter II and observations of pultrusion experiments at higher draw ratios. The change in λ with extrusion rate indicates that at high draw ratios P_E acts partially as a hydrostatic pressure which can be at least partially relieved by P_L. Increasing the draw ratio increases the hydrostatic effect of P_E and thus increases the relative effectiveness of P_L. At draw ratio 48, extrusion rates are very slow and independent of P_E above approximately 250 MPa. However, the extrudate can still be easily pulled out of the die at these high pressures. Pultrusion at these conditions would give very high values of λ. Thus the λ at 8.8 calculated at draw ratio 33.3 is believed to be valid.

The trend of increasing λ with decreasing draw ratio observed in the 29.1, 23.4, and 14.5 draw ratio dies is opposite to that found at draw ratio 33.3 and to predicted results. This suggests that P_L may operate through a different mechanism at low draw ratios where hydrostatic pressure is not a factor. Several potential causes of these diverging results have been eliminated. The λ of 3.3 found at draw ratio 29.1 is similar to the value of 2.9 at draw ratio 30 reported by Shimada. This indicates the "one billet" method used in these experiments is a legitimate technique for evaluating λ. Uniformity of billet lubrication cannot be determined. However, the P_E required to produce an extrusion rate of ~0.9 cm/min. decreased with decreasing draw ratio as expected indicating there were no significant differences in lubrication.

These results indicate that drawing by P_L is a more efficient deformation mechanism than extrusion by P_E at low draw ratios. This implies that tensile drawing to a low draw ratio at a pulling pressure should occur at a faster rate than extrusion to the same draw ratio at an equivalent extrusion pressure. If this hypothesis is valid, it suggests that deformation occurs increasingly by drawing and decreasingly by extrusion pressure as draw ratio decreases. The die acts as a shaping force that determines the draw ratio but does not significantly affect the deformational flow pattern.

The decrease in λ as P_E decreases and P_L increases at draw ratios 23.4 and 14.5 is unexplained. At high draw ratios, these results may be explained as a reduction in undercooling with decreasing P_E which consequently reduces λ. However, P_E is not expected to act as a hydrostatic force at these low draw ratios and there is no change in λ at draw ratio 29.1 where the effects of undercooling should be most evident. This again indicates that P_L is effective through a different mechanism at low draw ratios.

Extrusion Temperature

The effect of extrusion temperature on λ was studied at 105, 120, and 130°C at draw ratio 23.4, again using the one billet method described above. Results are reported in Tables 26, 27, and 28. At 130°C, λ decreased from 3.6 to 3.1 with increasing P_L without reaching a limit. The 120°C sample, previously reported in the draw ratio study, showed an initial λ of 4.6 which decreased with increasing P_L and became constant at 3.6. At 105°C, λ also decreased with increasing P_L from 6.7 to 1.7 also without becoming constant. The variation in λ at each temperature

Table 26

Effect of Extrusion Temperature on λ - Temperature = $130^{o}C$

Draw Ratio = 23.4, Die Angle = 20^{o}, Extrusion Temperature = $130^{o}C$

$\lambda = (\frac{\Delta \text{ atm}}{\Delta \text{ kg}})(3.144 \times 10^{-2})$

P_E, atm.	P_L, kg	Extrusion Rate, cm/min.	λ_1	λ_2	λ_3	λ_4	λ_5
705	0	1.08					
647	0.5	1.08	3.60				
595	1	1.10	3.41	3.23			
489	2	1.09	3.35	3.27	3.29		
416	3	1.11	2.99	2.87	2.78	2.27	
348	3.5	1.07	3.17	3.09	3.07	2.92	4.22

Table 27

Effect of Extrusion Temperature on λ - Temperature = $120^{o}C$

Draw Ratio = 23.4, Die Angle = 20^{o}, Extrusion Temperature = $120^{o}C$

$\lambda = (\frac{\Delta \text{ atm}}{\Delta \text{ kg}})(3.144 \times 10^{-2})$

P_E, atm.	P_L, kg	Extrusion Rate, cm/min.	λ_1	λ_2	λ_3	λ_4	λ_5
1461	0	0.86					
1423	1	0.87	1.18				
1166	2	0.83	4.58	7.97 Average			
929	4	0.84	4.13	~~5.11~~	3.68		
810	5	0.83	4.04	~~4.76~~	3.68	3.69	
694	6	0.86	3.97	~~4.53~~	3.66	3.65	3.60

Table 28

Effect of Extrusion Temperature on λ - Temperature = 105°C

Draw Ratio = 23.4, Die Angle = 20°, Extrusion Temperature = 105°C

$\lambda = (\frac{\Delta atm}{\Delta kg})(3.144 \times 10^{-2})$

P_E, atm.	P_L, kg	Extrusion Rate, cm/min.	λ_1	λ_2	λ_3	λ_4	λ_5	λ_6	λ_7
2188	0	0.95							
2119	1	0.97	2.14						
1756	2	0.95	6.70	11.27					
1658	3	0.94	5.48	~~7.15~~	3.04				
1543	4	0.93	5.00	~~5.96~~	3.31	3.56			
1401	5	0.98	4.89	~~5.57~~	3.67	3.99	4.41		
1311	6	0.91	4.54	~~5.02~~	3.45	3.59	3.60	2.79	
1256	7	0.91	4.13	~~4.46~~	3.10	3.12	2.97	2.25	1.71

Average

thus necessitated λ's of each temperature to be compared at equal values of P_L. A trend of increasing λ with decreasing temperature was observed. This result fulfills the prediction made in Chapter II that λ should decrease as temperature increases due to a reduction in the difference in efficiency between pultrusion and extrusion. However, it does not identify which, if any, of the mechanisms on which the prediction was based is correct. The decrease in λ again observed with decreasing P_E cannot be explained. It is uncertain whether it is due to a change in the deformation mechanism or is a by-product of the one billet procedure. Beginning the extrusion at a low P_E and a high P_L and then maintaining the extrusion rate by increasing P_E and decreasing P_L, opposite to the

procedure used, may eliminate this result.

Die Angle

One experiment was run on the effect of die angle on λ. The results from a draw ratio 23.4 die with an entrance angle of 30^{o} used at $120^{o}C$ are shown in Table 29. No consistent trend of λ with P_L was found. However, the λ values are generally greater than those of the 23.4 draw ratio, 20^{o} entrance angle die also run at $120^{o}C$ at similar pressures, see Table 27.

It was predicted that λ should increase with increasing die angle. Higher angles increase shear deformation resulting in a large decrease in extrusion rate. The partial elimination of shear deformation by the addition of the tensile pulling force thus appears to have a greater effect on extrusion rate at higher angles.

Table 29

Effect of Die Angle on λ - Angle = 30^{o}

Draw Ratio = 23.4, Die Angle = 30^{o}, Extrusion Temperature = $120^{o}C$

$\lambda = (\frac{\Delta atm}{\Delta kg})(3.144 \times 10^{-2})$

P_E, atm.	P_L, kg	Extrusion Rate, cm/min.	λ_1	λ_2	λ_3	λ_4
1494	0	0.93				
1379	1	0.92	3.57			
1229	2	0.94	4.11	4.66		
991	4	0.91	3.90	4.01	3.69	
787	5	0.91	4.32	4.59	4.57	6.33

Deformation Profiles

Introduction

The effect of extrusion conditions on the deformation process can be examined directly through deformation profiles. These patterns can be obtained by imprinting horizontal lines on the interior surfaces of the billet halves prior to extrusion. Differences between profiles may be related to variations in extrudate properties and can be used to verify mathematical models for the extrusion process. Previous work by Kanamoto et al[92] focused on the effects of extrusion temperature and rate, die draw ratio and entrance angle, molecular weight, and lubrication on the flow pattern. In this study, the effects of draw ratio, entrance angle, and lubrication again are examined along with that of pultrusion. Billets of Alathon 7050 were prepared for extrusion by the procedure previously discussed. The horizontal lines were drawn by hand using a permanent felt tip marking pen.

Effect of Draw Ratio

The effect of draw ratio was studied at draw ratios 14.5 and 29.1. An entrance angle of 20^{o} and an extrusion temperature of $120^{o}C$ were used in both cases and the results are shown in Fig. 17 and 18. Profiles at both draw ratios exhibited an initial slight upward bow which reversed direction at approximately draw ratio 1.6. This draw ratio was calculated from the billet width at the point of reversal. The bow transformed into a parabola characteristic of shear flow with increasing draw ratio. The greatly increased shear deformation approaching the die wall is due to the combined effects of billet-die friction, die geometry,

FIG. 17. EFFECT OF PULTRUSION ON DEFORMATION - DRAW RATIO = 14.5

DRAW RATIO = 14.5
DIE ANGLE = 20°
EXTRUSION TEMPERATURE = 120°C

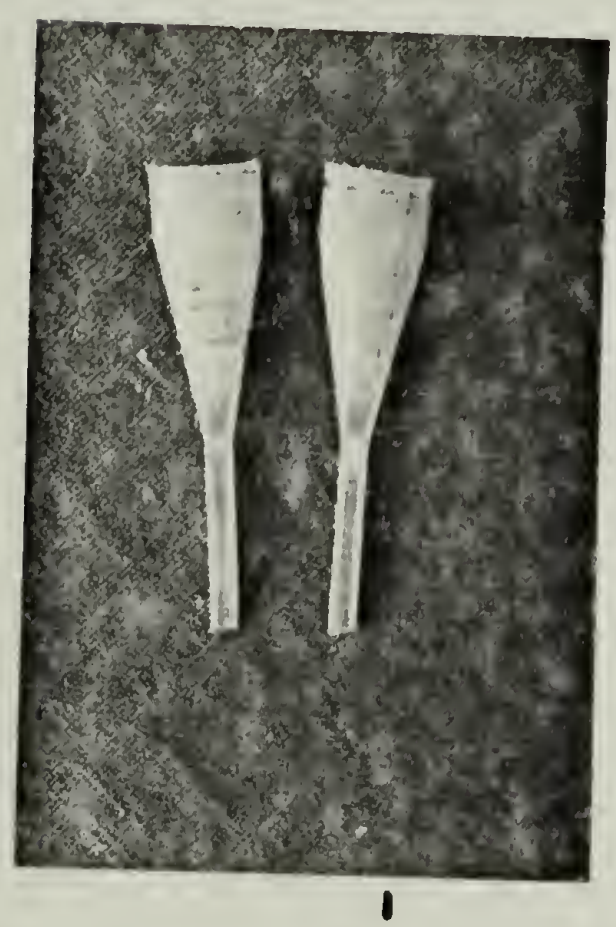

EXTRUSION
P_E = 116 MPA
EXTRUSION RATE =
0.96 CM/MIN.

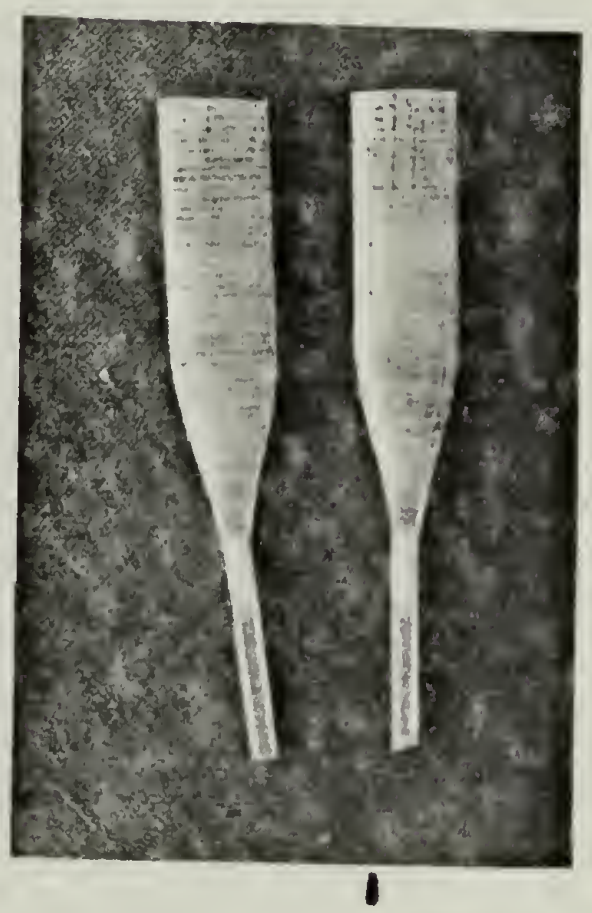

PULTRUSION
$P_E = 5.3 + P_L$ = 14.0 MPA
EXTRUSION RATE =
0.95 CM/MIN.

FIG. 18. EFFECT OF PULTRUSION ON DEFORMATION - DRAW RATIO = 29.1

DRAW RATIO = 29.1, DIE ANGLE = 20°, EXTRUSION TEMPERATURE = 120°C

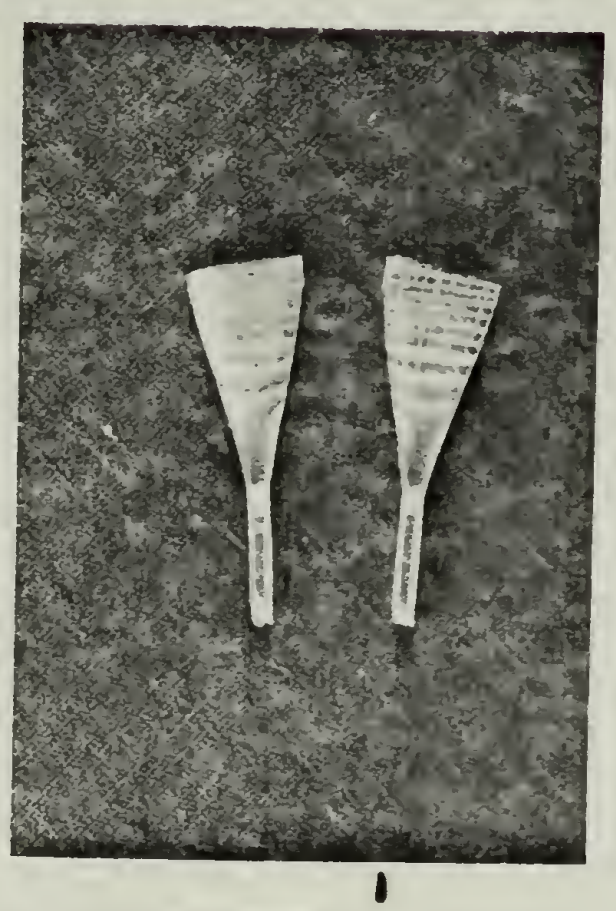

EXTRUSION
P_E = 182 MPA
EXTRUSION RATE =
0.63 CM/MIN.

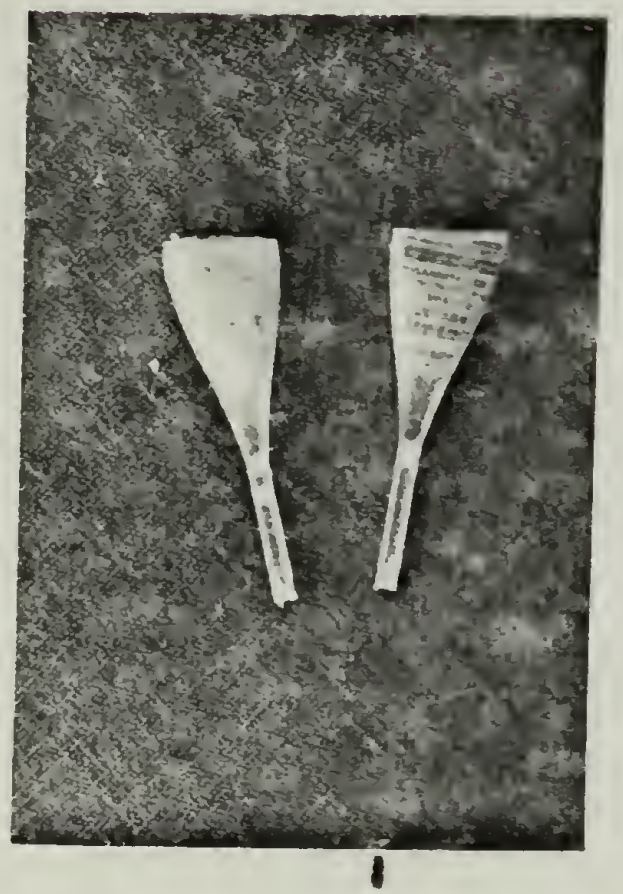

PULTRUSION
$P_E = 182 + P_L$ = 4.0 MPA
EXTRUSION RATE =
1.02 CM/MIN.

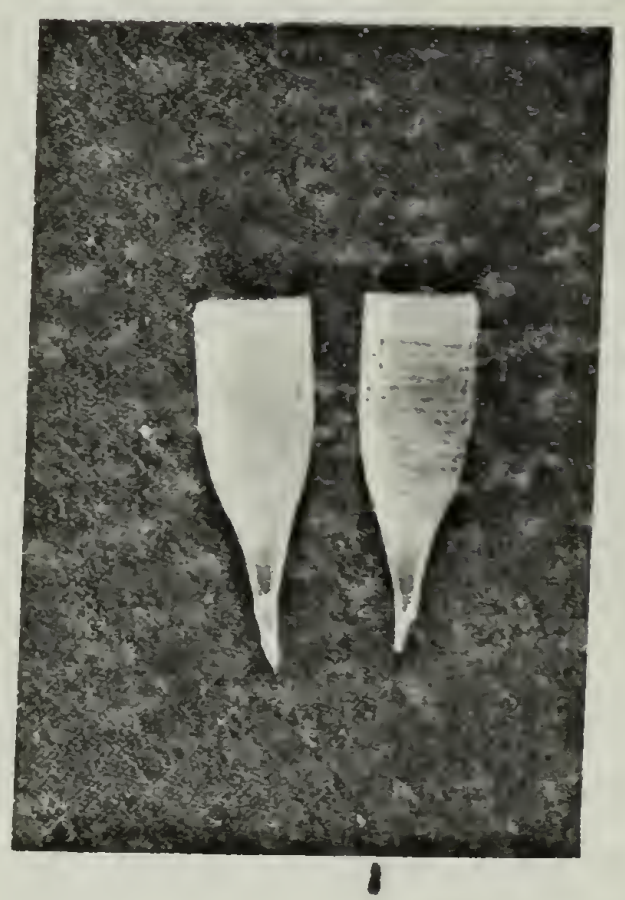

PULTRUSION
$P_E = 182 + P_L$ = 16.0 MPA
EXTRUSION RATE >
5 CM/MIN.

and possibly to the high shear forces at the corner between the die cone and capillary. Both slip line[125] and upper bound[71] analyses predicted the parabolic shape at high draw ratios but not the slight upward bow at low draw ratios. This suggests that the stress field in the die is more complex than that assumed in these analyses. It also indicates that billet-die friction is low at the die entrance allowing the circumference of the billet to deform before the center.

There were no visible significant differences between the deformation patterns of the two draw ratios. The pattern at draw ratio 29.1 appears to be a continuation of that at 14.5. The higher extrusion pressure required to extrude at 29.1 also does not seem to affect the die stress field. However, subtle changes in deformation, possibly caused by undercooling, may still occur undetected by this method. Kanamoto[92] found that a 30^{o}C difference in extrusion temperature, known to produce a large change in physical properties, caused only a small change in deformation profiles.

Effect of Pultrusion

The effect of pulling pressure on deformation was studied by comparing the deformation profiles of extruded and pultruded samples at draw ratios 29.1 and 14.5. Experimental conditions and results are also shown in Fig. 17 and 18. The same billet was used for both extrusion and pultrusion at each draw ratio to eliminate differences in lubrication between billets and its consequent effect on flow patterns. The addition of 14 MPa P_L to 116 MPa P_E caused a large increase in extrusion rate. Therefore, to eliminate any effect of extrusion rate on the flow pattern, P_E was reduced until the original extrusion rate

was reestablished.

Draw ratio 14.5, see Fig. 17, will be discussed first. At equivalent points at extrudate draw ratios less than 1.6, the pressure extrudate had more upward curvature than its pultruded counterpart. The flow lines became straight at approximately draw ratio 1.6 and then equally parabolic as draw ratio further increased in both samples. The pultruded billet had slightly rounded corners, suggestive of the neck observed in drawn samples, at the die entrance and the intersection of of the cone and capillary. An extruded billet will also freely neck in the die when it is highly lubricated. However, since the same billet was used for both extrusion and pultrusion, the "necked" shape is due solely to the pulling pressure. Pultrusion can be viewed as the combination of extrusion and conventional drawing. Therefore, it is not surprising that the influence of drawing on billet shape, the neck, is observed.

Results at draw ratio 29.1 are shown in Fig. 18. No change in flow pattern was observed between extrusion and pultrusion with 4.0 MPa P_L. However, with 16 MPa P_L, a reduction in upward curvature at low extrudate draw ratio and rounded corners were evident as at die draw ratio 14.5. There was no observable change in deformational flow at high extrudate draw ratios through pultrusion between die draw ratios 29.1 and 14.5

These results do not present an obvious reason for the ability of a P_L to produce a faster extrusion rate than an equivalent P_E or for the difference in λ's determined at draw ratios 29.1 and 14.5. The slight change in flow pattern at low draw ratio between extruded and

pultruded samples is not suspected of being a significant factor in determining extrusion rate. Although the rounded corners are suggestive of necking, there are no other indications of increased elongational flow, which may increase extrusion rate, during pultrusion. The similarity in flow patterns also shows that billet-die friction is not reduced by pulling pressure. The hydrostatic component of P_E should be insignificant at these draw ratios where extrusion occurs with relative ease. Therefore, P_L does not act to reduce its flow inhibiting effect. As explained in Chapter II-C-8, P_L may increase extrusion rate by placing maximum pressure at the tip of the die cone where draw ratio and flow stress are highest. This mechanism also is not expected to alter the flow profile. The pressure drop in the die should increase as draw ratio increases. Therefore, the relative effectiveness of P_L should increase with draw ratio. Although this mechanism explains the increase in from draw ratio 29.1 to 33.3, it does not explain the decrease from 14.5 to 29.1. This again indicates that P_L does not operate through the same mechanism at all draw ratios. A slight change in mechanism, undetectable by deformation profiles, may be responsible for the small decrease in λ from draw ratio 14.5 to 29.1.

Effect of Lubrication

The effect of lubrication on deformation was determined at three qualitative levels: none, light, and heavy. To eliminate any lubrication acquired by handling, both the billet and die were washed with soap and water and rinsed with acetone. Light and heavy layers of lubrication were obtained by briefly and thoroughly rubbing the billet by hand respectively. The same billet was used for all three extrusions which were done at draw ratio 29.1 with an entrance angle of 20^{o} and at

an extrusion temperature of 120°C. The extrusion rates and extrudates' appearance, shown in Fig. 19, reflect the differences in lubrication. The extrusion rate increased from 0.66 to 1.40 to 5.00 cm/min. with increasing lubrication. Without lubrication the extrudate fractured. Both the lightly and heavily lubricated billets produced unfractured extrudates but the interfacial surfaces of the heavily lubricated extrudate were much smoother than those of the lightly lubricated.

There also was a significant difference in deformation profiles with level of lubrication. The upward bow previously observed at low draw ratios was absent in the unlubricated billet. Shear deformation was strikingly evident creating a V pattern as compared to the usual U pattern. Fracture did not occur until the juncture of the cone and capillary was reached. Although shear deformation may increase at this point, it appears that fracture is due to the sharp redirection of flow and not to excessive shear stresses. No pattern could be seen in the fractured extrudate.

The lightly and heavily lubricated billets exhibited similar profiles with initial upward bows converting to downward parabolas. However, the transformation occurred at a slightly higher draw ratio, 2.3 compared to 1.8, for the heavily lubricated billet. At draw ratio 3.2 the decrease in shear flow with increased lubrication is readily seen. These patterns indicate that elongational flow is greatly increased by lubrication through a decrease in billet-die friction. Although the extrusion rate-properties study indicated that the type of flow had little effect on extrudate properties, it may have an effect on λ. P_L may produce higher extrusion rates than P_E through a reduction of billet-die friction.

FIG. 19. EFFECT OF LUBRICATION ON DEFORMATION

DRAW RATIO = 29.1, DIE ANGLE = 20°, EXTRUSION TEMPERATURE = 120°C, P_E = 240 MPA

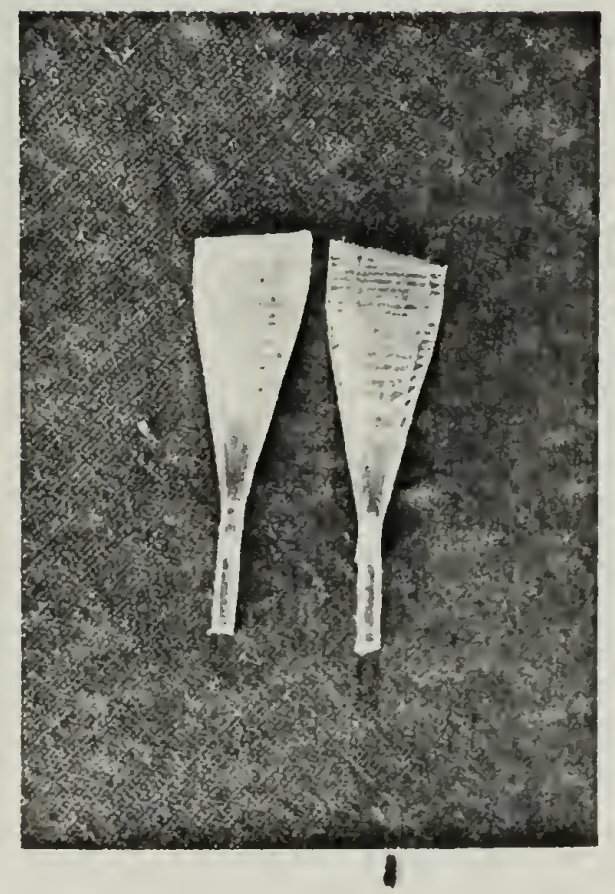

UNLUBRICATED
EXTRUSION RATE =
0.66 CM/MIN.

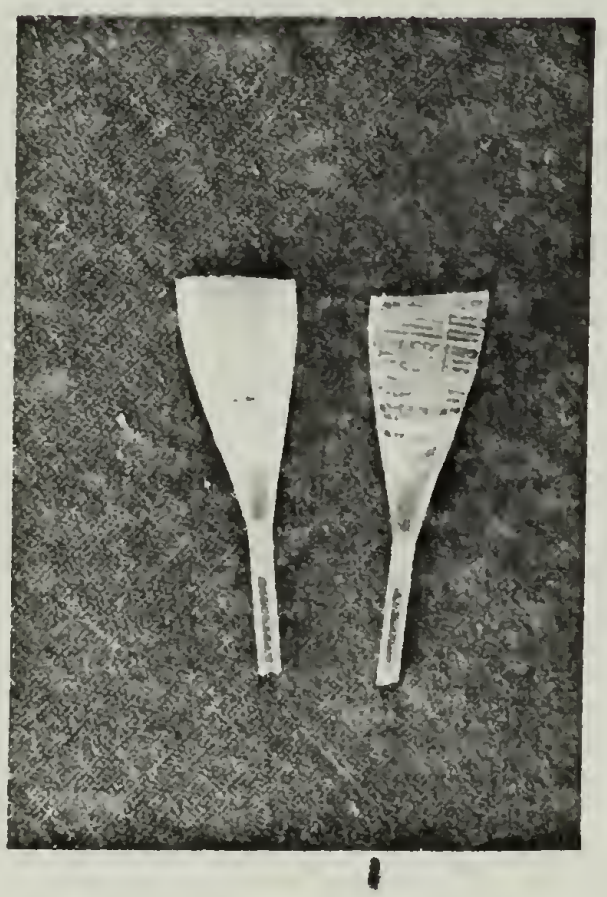

LIGHTLY LUBRICATED
EXTRUSION RATE =
1.40 CM/MIN.

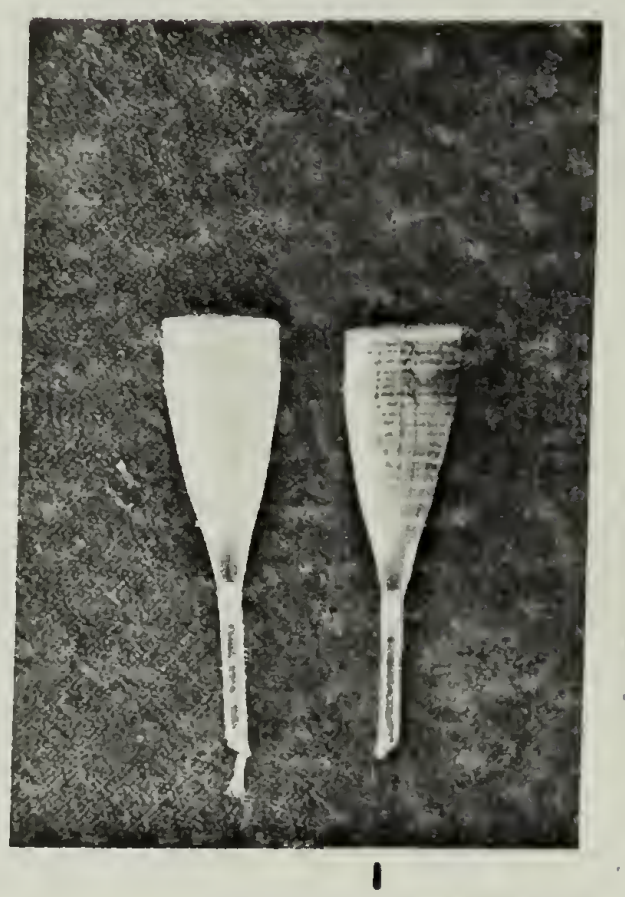

HEAVILY LUBRICATED
EXTRUSION RATE =
5.00 CM/MIN.

P_L will have less effect if friction is initially at a low level and will be reduced. Shimada[84] reached the same conclusion through a mathematical model of the pultrusion process.

Effect of Die Angle

Deformation profiles were obtained at entrance angles of 20 and 30° both at draw ratio 29.1, see Fig. 18 and 20. Opposite to the expected result, shear flow decreased with increasing angle. However, the 30° billet had to be heavily lubricated to obtain an unfractured extrudate which, as demonstrated in the lubrication study, greatly reduces shear flow. Thus, a true comparison of the flow patterns at the two angles cannot be made. However, this data again shows that the flow pattern determines the success of an extrusion and that, within limits, lubrication has a greater effect on deformation than die geometry.

Summary

The effect of extrusion conditions on λ and deformation profiles has been studied with a single high density polyethylene. Increasing temperature and decreasing die entrance angle decreased λ. λ was found to increase with draw ratio above draw ratio 29.1 and to increase with decreasing draw ratio below 29.1. Although the exact mechanism was not identified, these results validate the prediction made in Chapter II that P_L should become increasingly more effective relative to P_E as extrusion becomes more difficult. The increase in λ from draw ratio 29.1 to 14.5 indicates that P_L operates through a different mechanism in this range. This may be due to the absence of any hydrostatic effect from P_E.

FIG. 20. EFFECT OF DIE ANGLE ON DEFORMATION
DIE ANGLE = 30°

DRAW RATIO = 29.1
DIE ANGLE = 30°
EXTRUSION TEMPERATURE = 120°C
P_E = 273 MPA
EXTRUSION RATE = 0.75 CM/MIN.
COMPARE WITH FIG. 18 - EXTRUSION

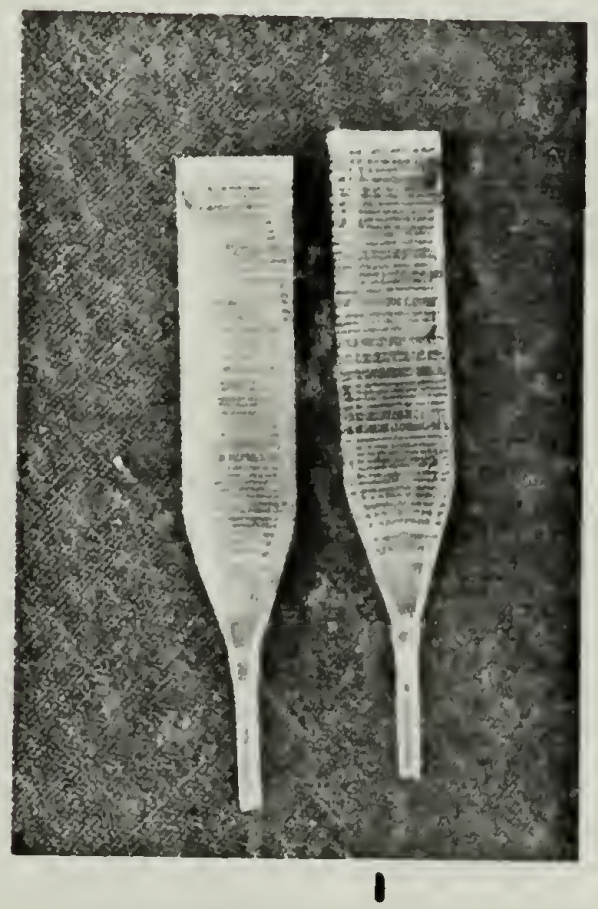

Deformation profiles gave little indication of the effect of P_L on deformation. A decrease in upward curvature at low draw ratio and a slight suggestion of necking are the only features that distinguished pultruded from extruded samples. The patterns also showed that deformation at high draw ratio is an extension of deformation at low draw ratio. Lubrication exhibited the most significant effect on deformation and can be directly related to the ability to obtain an unfractured extrudate under a variety of extrusion conditions.

In conclusion, the relative effectiveness of pulling pressure to pushing pressure in producing an extrusion rate increases as extrusion conditions become more severe. Lubrication, within limits, was observed to have the greatest effect on deformation.

CHAPTER VI

METHODS TO INCREASE DRAW RATIO AND TENSILE MODULUS

Introduction

Although most properties for drawn high density polyethylene reach a limit at approximately a draw ratio of 15, modulus continues to increase with increasing draw ratio, at a constant temperature, and is ultimately limited by fracture during extrusion at high draw ratios.[51] To obtain higher moduli, the causes of fracture must be identified and methods to avoid or forestall them must be devised. In this chapter, several suspected causes of fracture derived from observation of the extrusion process and examination of fractured extrudates are presented. Results of several experiments utilizing techniques designed to delay fracture and thereby achieve higher draw ratios are also presented.

Causes of Extrudate Fracture

Fracture is probably caused by a combination of several factors which culminate in localized areas of high stress. This includes, but is not limited to, the application of forces exceeding the bond strength of interfibrillar tie molecules connecting the ends of microfibrils as proposed in Peterlin's model of deformation.[37] His model explained fracture during tensile deformation. However, the observation of fracture planes oriented at oblique angles to the extrudate's long axis indicates that fracture occurs primarily by shear and/or compression during extrusion. Deformation profiles (Chapter V) also show the

existence of shear deformation and associated increased shear flow with decreased extrusion rate and fracture at low draw ratios. Shear deformation was increased by reducing billet lubrication. To conclusively show the effect of lubrication on extrusion rate and fracture, the following experiments were conducted.

A draw ratio 29.1, die angle 20^{o} die and billet were washed with an aqueous soap solution and then with acetone. Handling of the billet was subsequently limited to surfaces which would not be in contact with the die. Extrusion at 120^{o}C produced a cracked extrudate at a rate of 0.63 cm/min. A billet which had previously given an unfractured extrudate was similarly washed and extruded. It also produced a fractured extrudate. This billet was then rubbed by hand to lubricate it and re-extruded. It gave an unfractured extrudate at a rate of approximately 5.5 cm/min. Extrusion of the billet after rewashing it and the die again produced a fractured extrudate at a rate of 0.8 cm/min. Fracture also occurred at draw ratio 14.5 when no lubrication was applied. These experiments show that lubrication obtained from handling can produce a wide range of extrusion rates, including the range investigated in the extrusion rate-properties study. Lubrication by handling also allows higher draw ratios to be obtained.

The shape of the billet removed from the die after extrusion suggests a mechanism by which lubrication may act to enhance extrusion. Unlubricated billets which produced fractured extrudates closely followed the die geometry and had sharp corners at the entrance and exit of the conical portion of the die. Lubricated billets that produced unfractured extrudates were necked (wine glass shaped), pulling away from the die wall as the die narrowed. They also showed less shear and more

elongational deformation. Billets extruded at low draw ratios giving unfractured extrudates do not neck. These observations indicate that necking is associated with high draw ratios and lubrication is needed for necking to occur.

Lubrication may allow necking to occur by two avenues. First, necking is the natural deformation mechanism of polyethylene during tensile deformation. Extrusion is, in result, a tensile deformation process although it acts predominantly through compression. However, adhesive forces between an unlubricated billet and the die wall may prevent the billet from necking. Lubrication interferes with these forces and allows the billet to pull away from the die wall.

Second, necking may only be able to occur when there is a sufficient level of elongational flow in the deformation pattern. Cogswell and Moore[154] showed mathematically and experimentally that polyisobutylene will neck when deformed by elongation and by biaxial extension, but not by shear. If their reasoning can be applied to the extrusion of polyethylene, lubrication may induce necking by increasing elongational flow.

Although necking allows higher draw ratios to be obtained, the mechanism of its effect is unknown. It may produce morphologies capable of withstanding higher stresses. It may also retard the development of high stress concentrations. Relative to a conical shape, necking increases the strain rate at low draw ratios where deformation occurs easily and decreases the strain rate at high draw ratios where deformation becomes increasingly more difficult.

Necking may also facilitate extrusion by smoothing the sharp corner between the exit of the cone and the capillary in the die. This changes

the distribution of redundant work, the work needed to change the direction of flow, from a concentration at the juncture of the cone and capillary to a continuous arc. A more uniform flow is produced which reduces the formation of stress concentrations. Two observations support this theory. A billet extruded in a die of draw ratio 23.7 fractured at the intersection of the cone and capillary. The billet extruded through a die of draw ratio 30 was unfractured at draw ratio 23.7, a position located in the die cone, but again fractured at the intersection. Similarly at die draw ratio 48.0, the billet successfully extruded past draw ratio 30, but fractured at the same location in the die. Secondly, a length of extrudate can be shaped into an arc without affecting its appearance. However, creating the same total deflection by putting a sharp corner in the extrudate causes crazing at the corner. Crazes are precursors for gross fracture. These observations indicate that the billet is capable of deformation to high draw ratios if it is not sharply bent during extrusion.

Additional evidence supporting this theory is obtained from several authors who have shown that kink bands are formed when drawn or extruded samples are compressed,[155] sheared,[156] or redrawn[157] at angles oblique to the original draw direction. Forcing the already highly extended chains around a sharp corner combines bending, compression, and shear. This may cause the formation of kink bands and lead to fracture.

In summary, possible causes of fracture have been derived from observations of the extrusion process and examination of fractured extrudates. They are high deformation stresses (probably shear stresses when lubrication is not applied), the increasing strain rate with

increasing draw ratio produced by the conical shape of the die, and the sharp change in direction at the corner of the cone and capillary.

Results and Discussion

Several techniques were developed to delay the formation of stress concentrations that cause fracture. It was expected that an individual or a combination of techniques would enable higher draw ratios and thereby moduli to be obtained. In all experiments, the billet of Alathon 7050 was lubricated, enabling it to neck. Dies were lubricated with a fluorocarbon spray. Billets were split longitudinally down the middle prior to extrusion. Some billets were pultruded in an attempt to enhance neck formation. In these experiments, cone-tipped billets were used and the pultrusion force was attached to the emerging extrudate before the full die draw ratio had been achieved. This allowed the flow pattern produced by the pultrusion process to be fully established before high draw ratio was approached. However, while lubrication and splitting of the billet definitely aid extrusion, it is uncertain whether pultrusion also has a beneficial effect.

Coextrusion

The first technique tried in an attempt to obtain higher draw ratios and higher tensile moduli for extrudates was to coextrude an extrudate core with a billet sheath, see Fig. 21, similar in geometry to the technique of Kanamoto et al.[158] Coextrusion had previously been successfully used in both concentric billet[158,159] and film-split billet geometries.[160,161] In the adaptation used here, a billet was extruded to a low draw ratio. A hole the diameter of the extrudate was drilled in

FIG. 21. CONCENTRIC BILLET COEXTRUSION GEOMETRY

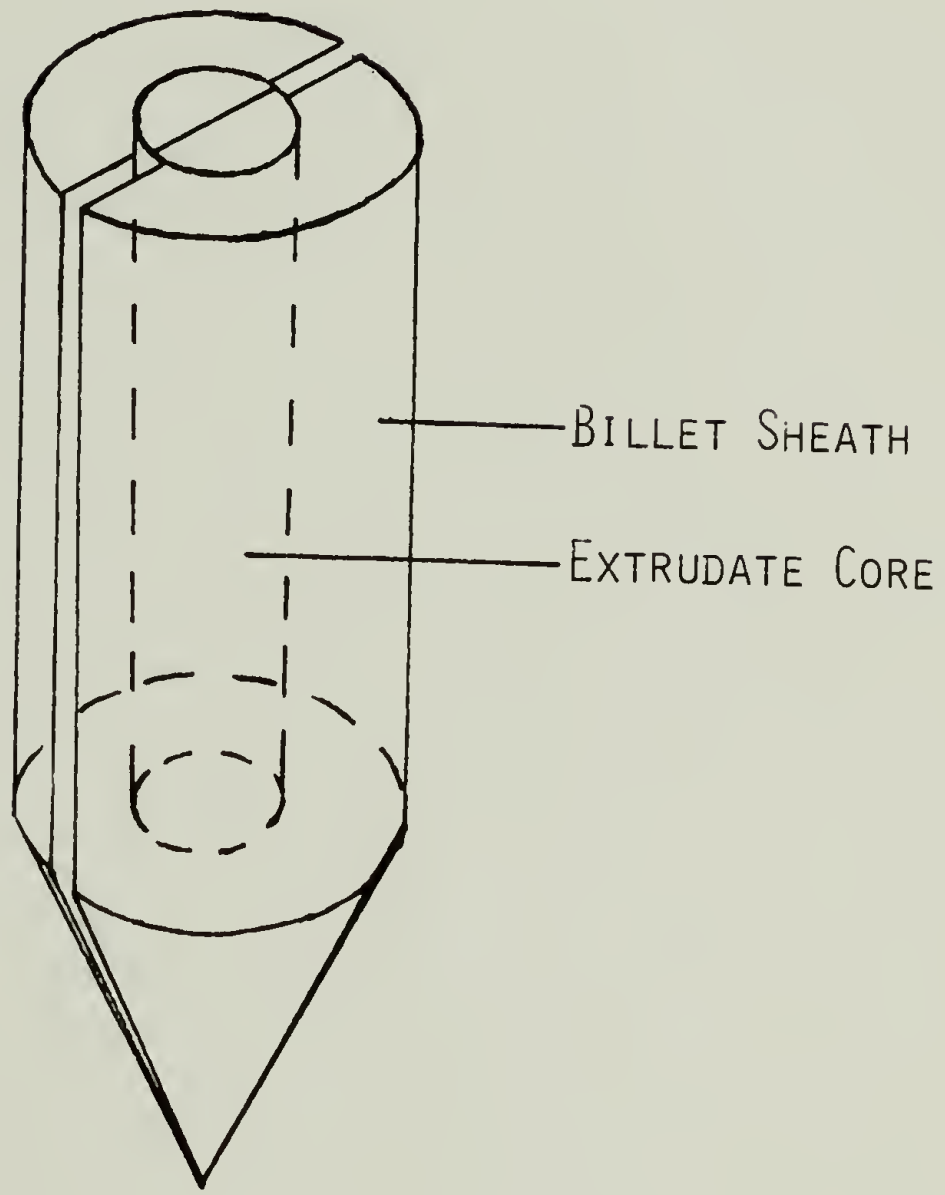

a new billet. This billet was then split and both interior and exterior surfaces were lubricated by rubbing by hand. The extrudate-core and billet-sheath were fit together with split surfaces aligned and co-extruded at 120°C. The die draw ratio for the coextrusion was chosen such that it multiplied by the core-extrudate draw ratio, equaled approximately 50. Combinations of 2.2-23.1, 5.5-9.2, 9.2-5.5, and 14.5-3.4 core-die draw ratios, respectively, were tried. Die angle was 20°.

It was expected that high draw ratios could be obtained by co-extrusion for two reasons. First, the total billet, consisting of core and sheath, is split into four sections. This may further aid extrusion since higher extrusion rates and draw ratios can be obtained from a billet split once than from a solid billet. Second, the sheath removes the core from the high shear stresses at the die wall allowing it to undergo greater elongational deformation. Increased elongational deformation, produced by lubrication, has been associated with higher extrusion rates and draw ratios in this thesis.

The 2.2 draw ratio extrudate fractured and became welded to the sheath when coextruded through the 23.1 draw ratio die. The sheath extruded around the 14.5 draw ratio extrudate, breaking and separating it into separate pieces. The best combination was the 5.5 draw ratio extrudate coextruded through the 9.2 draw ratio die, producing a rough but unfractured extrudate. The resulting draw ratio of the core, determined from measurement of its diameter, was 46.7, below the expected draw ratio of 50.6 determined from multiplication of core and die draw ratios. This indicates that the die draw ratio of 9.2 was slightly below that necessary to generate a pressure in the die sufficient to fully

deform the extrudate. This is a less extreme example of the 14.5 core - 3.4 die coextrusion in which the core was not deformed at all and the sheath extruded around it. Tensile modulus of the 46.7 draw ratio extrudate, determined under the same conditions used in the extrusion rate-modulus study, was 30.0 GPa. This is only slightly higher than the ~27 GPa moduli obtained from draw ratio 29.1 extrudates in that study. This indicates that molecular relaxation occurred, possibly due to the low pressure in the die being unable to maintain sufficient force on the extrudate to prevent relaxation. A high extrusion rate of 4.7 cm/min. was obtained at a P_E of only 30 MPa. This may be due to the splitting of the billet into four parts. The high extrusion rate suggests that coextrudates may be obtained at lower temperatures or at higher draw ratios, conditions which are likely to increase modulus. Higher moduli might also be obtained from optimization of the combination of core-extrudate and die draw ratios.

The film-split billet coextrusion geometry was also tried. A polyethylene film 0.70 mm thick and 5.0 mm wide was placed between the halves of a split billet and coextruded through a 44.8 draw ratio, 20^{o} die angle die at $120^{o}C$. It was expected that this geometry would allow higher draw ratios to be obtained because, as in concentric coextrusion, the total billet is split into four pieces and the film is removed from high shear stresses at the die wall. Additionally, coextrusion of a thin film would produce a very thin extrudate. Pennings and Meihuizen[162] showed that thin, high modulus polyethylene fibers, crystallized from stirred polymer solutions, could be wound on a spool, whereas 0.14 cm diameter extrudates fracture when bent. Apparently, the thinness of the fibers allows bending stresses to be absorbed without fracture. Thus it

was suspected that a thin extrudate may also absorb high stresses during deformation without fracture. However, the thin extrudate fractured and imbedded in the split billet sheath during coextrusion.

Billet Splitting

A second technique attempted to obtain higher draw ratios was to extrude billets split into four sections. As in coextrusion, it was expected that extrusion would be aided more by splitting the billet into four sections than into two. Prior to extrusion, each section of the billet was lubricated by immersing it in a 4% solution of sodium dodecyl sulfate in water. Billets were extruded at 120^{o}C through a draw ratio 48.0 die with a die angle of 20^{o}. Extrusion of a billet split into four quarters by two perpendicular, longitudinal cuts through the center of the billet produced a fractured extrudate. Extrusion of a billet split into four sections of equal width by three parallel, longitudinal cuts was partially successful. One section was completely unfractured and the other three had solid regions interspersed with fractured regions. Although an exact extrusion rate was not measured, qualitatively it was greater than that expected from the extrusion pressure of 267 MPa used. Analyses of the extrudate by WAXS, SAXS, DSC, and tensile testing have not been completed. However, the partial success of the extrusion indicates that splitting the billet into four sections reduces stress concentrations and enables higher draw ratios to be obtained. It is expected that additional work employing this technique with improved die geometries and lubrication from rubbing by hand will be successful.

Die Geometry

The consistent initiation of extrudate fracture at the intersection

of the die cone and capillary and the ability of necked billets to achieve higher draw ratios than unnecked billets suggest that higher draw ratios may be obtained through elimination of sharp corners in the die. Removal of sharp corners would benefit extrusion in two ways. First, it would reduce the concentration of redundant work exerted at the corner to change the direction of flow and spread it over a larger area. Second, it would also reduce the exponential increase in draw ratio that occurs in a conical die as the die narrows. This may be particularly beneficial because further deformation becomes increasingly more difficult as draw ratio increases. To test these ideas, the corner at the junction of the cone and capillary was rounded by cutting into a 46.7 draw ratio, 20^{o} die angle die both above and below the corner. All corners created by the cutting were smoothed by grinding. The surface was then polished, lubricated with a fluorocarbon spray, and buffed. A once-split billet was lubricated by rubbing by hand and extruded at a P_E of 311 MPa. The high P_E was used to produce an extrusion rate above 0.35 cm/min. Previous work had shown that fracture occurs when Alathon 7050 is extruded at a rate below this level.[84] A short piece of partially fractured extrudate was produced and analyzed by wide angle X-ray (WAXS), small angle X-ray (SAXS), and thermal mechanical analysis (TMA) to determine the efficiency of deformation.

The SAXS contour intensity patterns of the 46.7 draw ratio extrudate and a 12.0 draw ratio extrudate, also produced at $120^{o}C$ are shown in Fig. 22. They were obtained using the Oak Ridge National Laboratory 10 m Small Angle X-ray System at the National Center for Small Angle Scattering Research, Oak Ridge, Tennessee. Previous SAXS work had shown that crystalline long period decreases[51] and crystalline

FIG. 22. SMALL ANGLE X-RAY SCATTERING CONTOUR INTENSITY PATTERNS OF DRAW RATIO 46.7 AND 12.0 EXTRUDATES

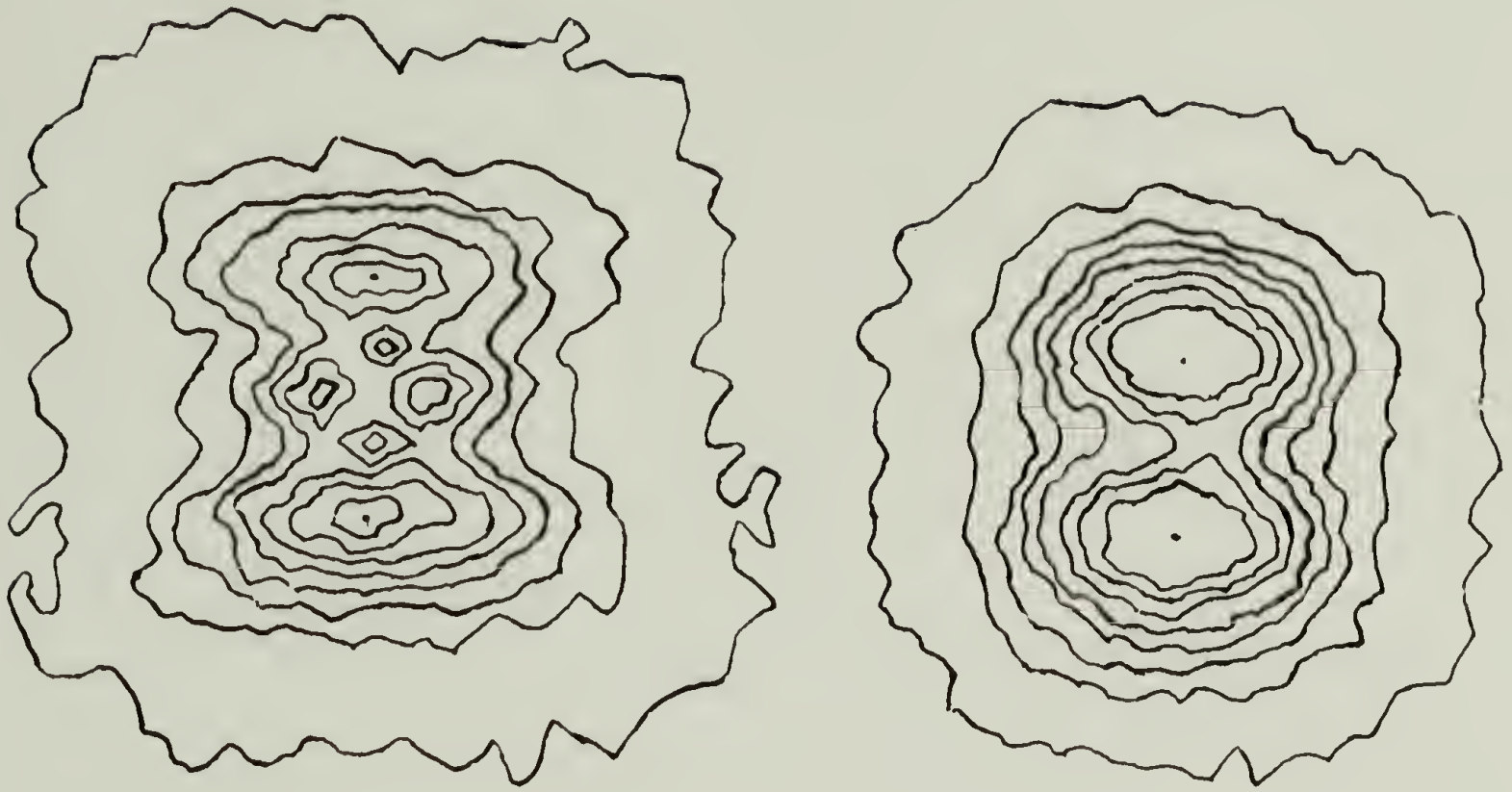

DRAW RATIO 46.7 DRAW RATIO 12.0

and amorphous phases become less distinct[51,58] with increasing draw ratio. Crystalline long period is inversely proportional to the distance between the centers of the two vertically spaced, concentric domains in a SAXS pattern. As deformation continues, fibrils elongate and narrow through intermicrofibrillar slip. Fibril width is inversely proportional to the width of the SAXS pattern. Scattering intensity decreases with increasing draw ratio as the crystalline and amorphous phases become less distinct. Inspection of Fig. 22 shows that the crystalline long period, fibril width, and scattering intensity of the draw ratio 46.7 extrudate is less than that of the draw ratio 12.0 extrudate. This indicates that the 46.7 extrudate is more highly deformed than the 12.0. Comparison with a 36.0 draw ratio extrudate showed the 36.0 and 46.7 extrudates to be approximately equal in fibril width and crystalline long period. This may be due to relaxation allowed by the low level of fracture.

A WAXS pattern was obtained using an Elliot rotating anode generator and copper K_{α} radiation. It showed points slightly sharper than those of a 36.0 draw ratio extrudate. Qualitatively, this is indicative of higher crystal coherence and perfection. There was an equivalent level of crystalline orientation in the extrudates. However, this was expected since orientation reaches a limit above draw ratio 15.[51] Several points were tilted, possibly due to slightly misaligned crystals in fractured areas of the extrudate.

Thermal mechanical analyses of drawn and solid-state extruded polyethylenes indicate a negative thermal expansion coefficient in the draw direction (i.e. $\alpha_{\parallel}$ - parallel to the c-axis) and a positive coefficient perpendicular to the draw direction ($\alpha_{\perp}$). Mead et al[60]

reported that $\alpha_{\parallel}$ of extrudates produced at 120°C became more negative with increasing draw ratio and reached a limit at $\sim -0.6 \times 10^{-5}\ ^{o}C^{-1}$ above approximately draw ratio 20. They also showed that $\alpha_{\parallel}$ became more negative with decreasing extrusion temperature at a constant draw ratio, indicating increased efficiency of deformation. $\alpha_{\parallel}$ and $\alpha_{\perp}$ of the draw ratio 46.7 extrudate and of a draw ratio 29.1 extrudate, also produced at 120°C, were measured on a TMS-1 coupled with a DSC-1B, both by Perkin-Elmer. Measurements were taken from 123 to 330 K at a scanning rate of 10 K/min under helium. A load of 3.5g was used. Results are shown in Fig. 23.

As expected, $\alpha_{\parallel}$ was negative and $\alpha_{\perp}$ was positive for both extrudates. $\alpha_{\parallel}$ of the 29.1 draw ratio extrudate was slightly more negative and $\alpha_{\perp}$ more positive than the corresponding values of the 46.7 extrudate. This, again, may be due to either a lower efficiency of deformation or relaxation due to fracture in the 46.7 extrudate. At 25°C $\alpha_{\parallel}$ was -11.2 and $-12.3 \times 10^{-6}\ ^{o}C^{-1}$ for the 46.7 and the 29.1 extrudates respectively. This is more negative than $\alpha_{\parallel}$'s reported by Mead[60] and Porter[53,163] and coworkers and indicative of high deformation.

In conclusion, SAXS, WAXS, and TMA analyses of the 46.7 draw ratio extrudate show it to be deformed to approximately the same level as a 36.0 extrudate. The loss of efficiency is probably due to relaxation allowed by the low level of fracture in the extrudate. However, the near success of this experiment suggests that elimination of sharp corners in the die does benefit extrusion.

Other die geometries may also improve the deformation process. Draw ratio increases exponentially as the cone narrows in a conical die. This increases the strain rate as deformation is becoming increasingly

FIG. 23. COMPARISON OF DRAW RATIO 46.7 AND 29.1 EXTRUDATES BY THERMAL MECHANICAL ANALYSIS

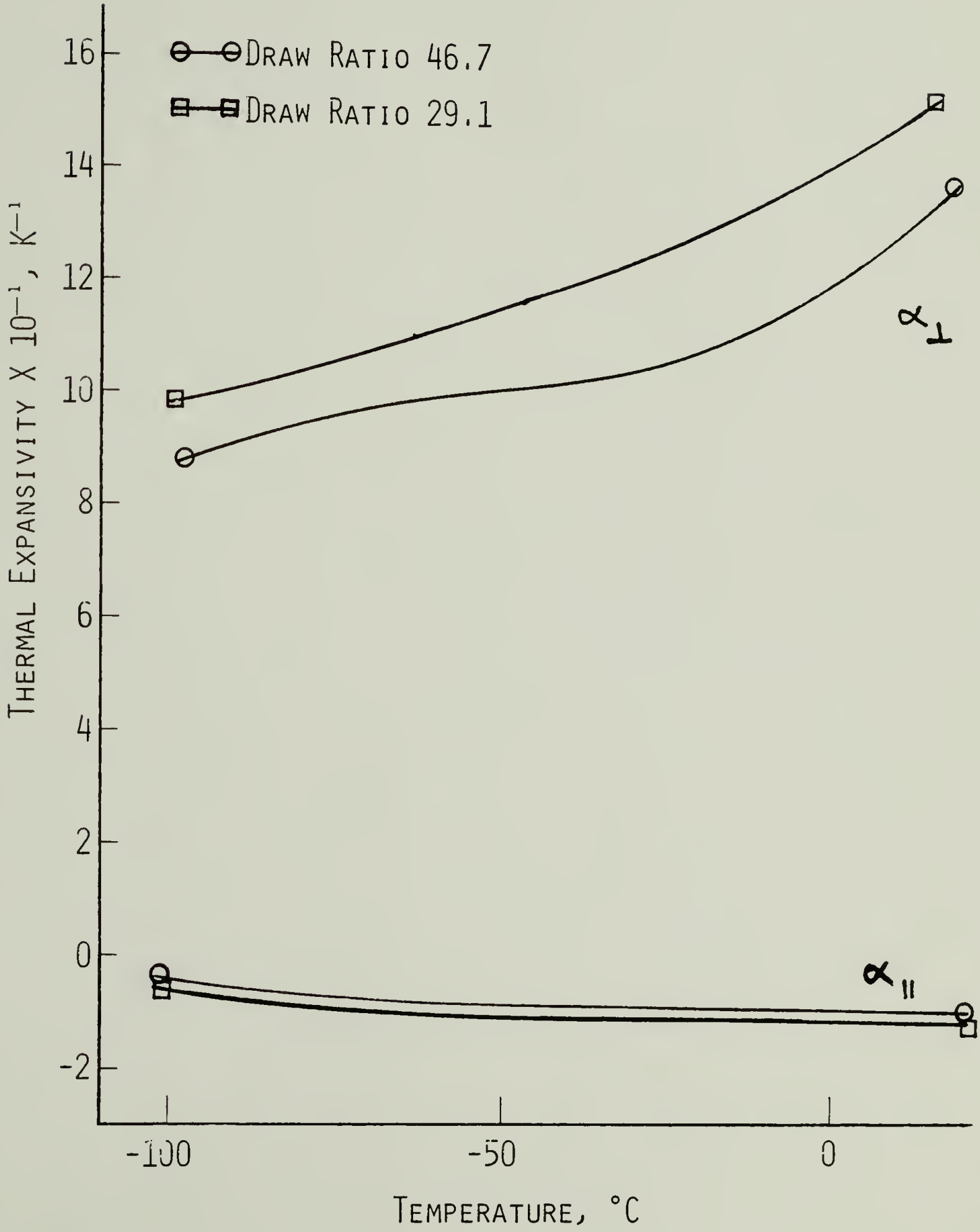

more difficult. A constant strain rate would be obtained from a trumpet bell-shaped (parabolic) geometry. This shape would also provide a smooth transition into the capillary of the die. However, the nearly perpendicular intersection of the capillary of the rheometer with the bell of the die may cause fracture even though it is in a position of low draw ratio. To prevent this, a 20^{o} cone could replace the bell above the point where the slope of the bell is equal to that of the cone. The die described above was built with some modifications. The continuously changing shape of the bell could not be built. It was approximated by a series of angles with the corners at the intersections of angles smoothed. The exit of the capillary was flared. This has been found to prevent fracture in wire drawing dies. The die was made of oil-hardened drill rod steel which can be more highly polished and has a lower coefficient of friction than brass. The die geometry and equations used to build the die are shown in Table 30. Experiments to date with this die have not been successful.

Higher draw ratios without fracture have been obtained from billets that neck during extrusion. This may be due to the partial elimination of sharp corners, a slower increase in strain rate with increasing draw ratio, or necking being a more natural deformation geometry than following the conical die geometry. To encourage this type of flow, a die could be built in the shape of a neck. Dimensions of a necked billet were taken using a Cordex machine by Bendix. Dimensions are listed in Table 31. These dimensions would have to be modified to build a die with a smoother transition into the die capillary.

Table 30

Specifications for Combined 20^{o} Cone-Trumpet Bell Geometry Die

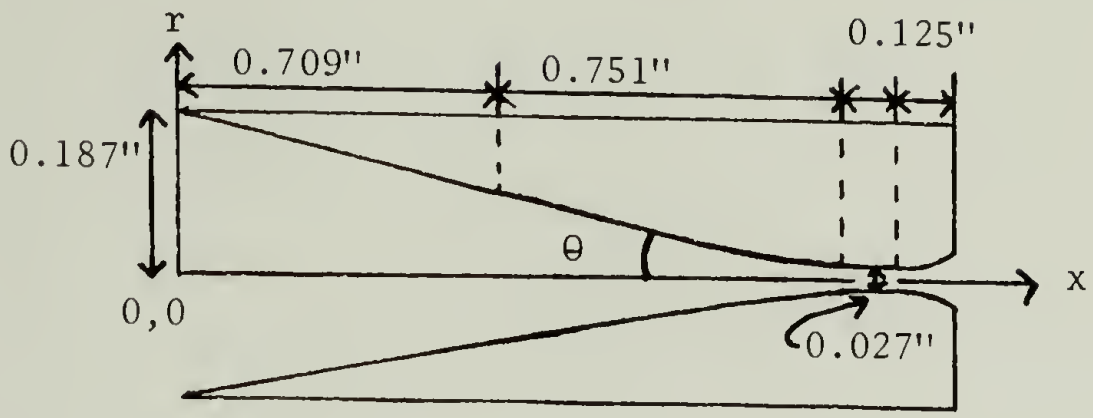

Initial Specifications

From x = 0" to x = 0.709" : r = -0.176 x +0.187

From x = 0.709" to x = 1.460" : $r = \frac{0.187}{(\frac{x}{0.0193} - 27.632)^{\frac{1}{2}}}$

From x = 1.460" to x = 1.586 : r = 0.027"

Modified Specifications

From x =	to x =	θ =	r =	to r =
0.000"	0.713",	10^{o},	0.187"	0.061"
0.713	0.765	8	0.061	0.054
0.765	0.807	6	0.054	0.050
0.807	0.920	4	0.050	0.042
0.920	1.225	2	0.042	0.031
1.225	1.460	1	0.031	0.027
1.460	1.585	0 - Capillary - r = 0.027"		
1.585	1.710	flare		

Table 31

Coordinates of a Necked Billet

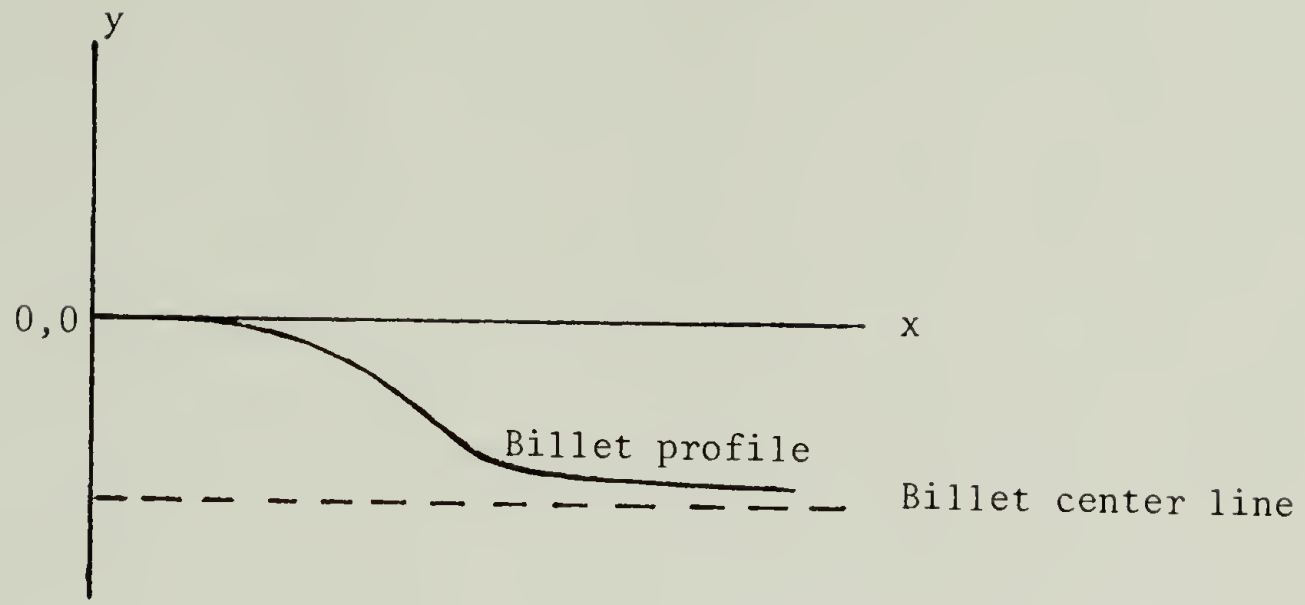

x, in. x 10^{-2}	y, in. x 10^{-4}	x, in. x 10^{-2}	y, in. x 10^{-4}
0	0	15	187
.25	3	16	205
1	12	17	224
2	16	18	243
3	28	19	263
4	39	20	283
5	46	21	305
6	58	22	327
7	69	23	349
8	84	24	372
9	97	25	395
10	110	26	419
11	125	27	444
12	140	28	468
13	155	29	494
14	171	30	521

Table 31, continued

x, in. x 10^{-2}	y, in. x 10^{-4}	x, in. x 10^{-2}	y, in. x 10^{-4}
31	548	55	1262
32	580	56	1284
33	612	57	1306
34	645	58	1328
35	678	59	1351
36	714	60	1373
37	749	61	1396
38	785	62	1419
39	821	63	1441
40	856	64	1461
41	891	65	1477
42	925	66	1486
43	957	67	1494
44	988	68	1500
45	1016	69	1504
46	1044	70	1508
47	1069	71	1512
48	1096	72	1517
49	1121	73	1520
50	1145	74	1522
51	1169	75	1524
52	1193	76	1525
53	1217	77	1526
54	1240		

Summary

Several techniques have been identified which appear to aid extrusion. Splitting the billet into four sections of equal width by three parallel cuts seems to reduce stress concentrations. Billet lubrication increases elongational flow and facilitates necking. To date, rubbing by hand has been found to be the most effective type of billet lubrication. A fluorocarbon spray lubricant buffed into the die's interior surface may also aid extrusion. Elimination of sharp corners in the die spreads redundant work, used to change the direction of flow, over a larger area. Removing the billet from high shear forces at the die wall by concentric coextrusion may also be beneficial. Pultrusion may allow more effective use of deformational forces and promote necking. Optimization of each technique or a combination of techniques may allow higher draw ratios without flaw and thus higher tensile moduli extrudates to be obtained.

CHAPTER VII

SUMMARY

Conclusions

Several generalizations about the extrusion process can be made from the extrusion rate and extrusion conditions - properties, pultrusion, and methods to obtain higher draw ratios studies. Variations in extrusion rate, produced by differences in lubrication, had little effect on extrudate properties. However, a slower extrusion rate appears to allow slightly more efficient deformation. Pultrusion and a small increase in extrusion pushing pressure only affects modulus, increasing it approximately 10%. These results indicate that extrusion rate and conditions have little effect on extrudate morphology in the ranges studied. The effectiveness of a pulling pressure relative to that of a pushing pressure in producing an extrusion rate increases as extrusion conditions become more severe. Lubrication and splitting of the billet are essential to obtain high draw ratios.

Future Work

Extrusion Conditions-Extrudate Properties

There was only a small difference among conditions in the extrusion conditions-extrudate properties study. Differences could be increased to determine if properties are truly independent of conditions or if the ranges used in this study were too small to have an effect on properties. Extrusion at 150 and 250 MPa pushing pressure and

pultrusion at 150 MPa pushing pressure plus 16 MPa pulling pressure (4 kg at draw ratio 29.1) should be sufficient to produce differences in properties.

Pultrusion

The effect of die angle on λ could be more clearly defined by a range of angles below 20^{o} where unfractured extrudates could be obtained without heavy lubrication. Increased molecular weight is known to make extrusion more difficult and was predicted in Chapter II-C-8 to increase λ. A range of molecular weights could be used to determine the validity of this prediction. Billet and/or die preparation techniques that will give reproducible extrusion rates at constant extrusion conditions are needed so that direct comparison of λ's at different conditions can be made.

Methods to Increase Draw Ratio and Tensile Modulus

Further work could be done to optimize or combine technqiues developed thus far. Other lubricants, such as those used in wire drawing, could be used. A 5.0 draw ratio extrudate coextruded through a 10.0 draw ratio die may be the optimum combination for coextrusion, generating sufficient pressure to fully deform the core-extrudate. The neck-shaped or a shorter cone-trumpet bell combination die also could be tried.

REFERENCES

1. L. Holliday and J. W. White, Pure Appl. Chem., 26, 545 (1971).
2. W. Wu and W. B. Block, Polym. Eng. Sci., 19, 1163 (1979).
3. M. A. Wilding and I. M. Ward, Polymer, 19, 969 (1978).
4. G. Capaccio and I. M. Ward, Polym. Eng. Sci., 15, 219 (1975).
5. J. M. Andrews and I. M. Ward, J. Mater. Sci., 5, 411 (1970).
6. G. Capaccio and I. M. Ward, Polymer, 15, 233 (1974).
7. G. Capaccio and I. M. Ward, Polymer, 16, 239 (1975).
8. P. D. Coates and I. M. Ward, Polymer, 20, 1553 (1979).
9. A. G. Gibson and I. M. Ward, J. Mater. Sci., 15, 979 (1980).
10. J. H. Southern and R. S. Porter, J. Macromol. Sci., 3, 541 (1970).
11. J. H. Southern and R. S. Porter, J. Appl. Polym. Sci., 14, 2305 (1970).
12. J. D. Hoffman, Polymer, 20, 1071 (1979).
13. A. Coombes and A. Keller, J. Polym. Sci., 17, 1637 (1979).
14. A. Zwinjnenberg and A. J. Pennings, J. Polym. Sci., Polym. Letters, 14, 339 (1976).
15. D. M. Bigg, Polym. Eng. Sci., 16, 725 (1976).
16. K. Imada, T. Yamamoto, K. Shigematsu and M. Takayanagi, J. Mater. Sci., 6, 537 (1971).
17. D. Pradecki and W. O. Statton, J. Polym. Sci., Polym. Letters, 10, 87 (1972).
18. W. T. Mead and R. S. Porter, J. Polym. Sci. C, 63, 289 (1978).
19. W. T. Mead and R. S. Porter, Int. J. Polym. Mater., 7, 29 (1979).
20. S. Kojima and R. S. Porter, J. Appl. Polym. Sci., Appl. Polym. Symp., 33, 129 (1978).

21. F. W. Billmeyer, Jr., "Textbook of Polymer Science," 2nd edn., Ch. 13, Wiley - Interscience, New York (1971).

22. B. Wunderlich and T. Arakawa, J. Polym. Sci. A, 2, 3697 (1964).

23. A. Peterlin, "Ultra-High Modulus Polymers," I. M. Ward and A. Ciferri, eds., Ch. 10, Applied Science Pub., Essex, England (1979).

24. A. Peterlin, "Man-Made Fibers, Science and Technology," H. F. Mark, S. M. Atlas and E. Cernia, eds., pp. 283-340, Wiley - Interscience, New York (1967).

25. P. B. Bowden and R. J. Young, J. Mater. Sci., 9, 2034 (1974).

26. R. S. Stein, J. Polym. Sci. C, 15, 185 (1966).

27. A. Peterlin, J. Polym. Sci. C, 18, 123 (1967).

28. D. P. Pope and A. Keller, J. Polym. Sci. - Polym. Phys., 13, 533, (1975).

29. R. J. Cembrola and R. S. Stein, J. Polym. Sci., 18, 1065 (1980).

30. U. W. Gedde, "On the Necking and Fracture Behavior of Polyethylene," Ph.D. Thesis, Institionen for polymerteknologi, Stockholm, Sweden (1980).

31. N. G. McCrum, B. E. Read and G. Williams, "Anelastic and Dielectric Effects in Polymeric Solids," Ch. 10, Wiley, New York (1967).

32. R. J. Gaylord, Polym. Eng. Sci., 19, 955 (1979).

33. S. G. Burney and G. W. Groves, J. Mater. Sci., 13, 639 (1978).

34. A. Peterlin, Polym. Eng. Sci., 17, 188 (1977).

35. A. G. Gibson and I. M. Ward, J. Mater. Sci., 14, 1838 (1979).

36. R. J. McCullough, J. Polym. Sci. - Polym. Phys., 15, 1805 (1977).

37. A. Peterlin, J. Macromol Sci., B7, 705 (1973).

38. C. G'sell and J. J. Jones, J. Mater. Sci., 14, 583 (1979).

39. P. I. Vincent, Polymer, 1, 7 (1960).

40. E. H. Andrews, Proc. Roy. Soc., A 277, 562 (1964).

41. G. Capaccio, A. G. Gibson and I. M. Ward, "Ultra-High Modulus Polymers," I. M. Ward and A. Ciferri, eds., Ch. 1, Applied Science Pub., Essex, England (1974).

42. D. G. Fatheringham and B. W. Cherry, J. Mater. Sci., 13, 951 (1978).

43. I. Marshall and A. B. Thompson, Proc. Roy. Soc., A 221, 541 (1954).

44. Y. S. Lazurkin, J. Polym. Sci., 30, 595 (1958).

45. R. E. Robertson, J. Chem. Phys., 44, 3050 (1966).

46. M. H. Litt and P. Koch, J. Polym. Sci., Polym. Letters, 5, 251 (1967).

47. C. E. Pearson and R. N. Perkins, "The Extrusion of Metals," Chapman and Hall Ltd., London (1960).

48. W. G. Perkins, "Solid-State Extrusion of High Density Polyethylene and Nylons 11 and 12; The Process and Physical Properties of Extrudates," Ph.D. Thesis, University of Massachusetts (1978).

49. N. J. Capiati and R. S. Porter, J. Polym. Sci., Polym. Phys., 13, 1177 (1975).

50. A. Peterlin, Polym. Eng. Sci., 14, 627 (1974).

51. A. E. Zachariades, W. T. Mead and R. S. Porter, "Ultra-High Modulus Polymers," I. M. Ward and A. Ciferri, eds., Ch. 2, Applied Science Pub., Essex, England (1979).

52. A. Peterlin, Polym. Eng. Sci., 18, 488 (1978).

53. R. S. Porter, N. E. Weeks, N. J. Capiati and R. J. Krzewki, J. Thermal Anal., 8, 547 (1975).

54. W. Glenz and A. Peterlin, J. Polym. Sci., Polym. Phys., 9, 1191 (1971).

55. S. Kojima, C. R. Desper and R. S. Porter, J. Polym. Sci., Polym. Phys., 16, 1721 (1978).

56. K. Nakayama and H. Kanetsuna, J. Mater. Sci., 10, 1105 (1975).

57. C. J. Farrell and A. Keller, J. Mater. Sci., 12, 966 (1977).

58. A. Peterlin and R. Corneliussen, J. Polym. Sci., Polym. Phys., 6, 1273 (1968).

59. A. Peterlin and G. Meinel, J. Polym. Sci., Polym. Letters, 3, 783 (1965).

60. W. T. Mead, C. R. Desper and R. S. Porter, J. Polym. Sci., Polym. Phys., 17, 859 (1979).

61. R. H. Baughman and E. A. Turi, J. Polym. Sci., Polym. Phys., 11, 2453 (1973).

62. J. R. Falender and D. Hansen, J. Appl. Phys., 43, 1611 (1972).

63. M. P. C. Watts, A. E. Zachariades and R. S. Porter, J. Mater. Sci., 15, 426 (1980).

64. S. Kojima and R. S. Porter, J. Polym. Sci., Polym. Phys., 16, 1729 (1978).

65. A. Peterlin, Polym. Eng. Sci., 19, 118 (1979).

66. D. C. Prevorsek, Y. D. Kwan and R. K. Sharma, J. Mater. Sci., 12, 2310 (1977).

67. T. L. Smith, Polym. Eng. Sci., 17, 129 (1977).

68. D. G. Peiffer, Polym. Eng. Sci., 20, 167 (1980).

69. W. N. Taylor and E. S. Clark, Polym. Eng. Sci., 18, 518 (1978).

70. D. L. M. Cansfield, G. Capaccio and I. M. Ward, Polym. Eng. Sci., 16, 721 (1976).

71. S. Muruyama, K. Imada and M. Takayanagi, Inter. J. Polym. Mater., 2, 125 (1973).

72. K. D. Pae and S. K. Bhateja, J. Macromol. Sci. - Revs. Macromol. Chem., C13, 1 (1975).

73. J. A. Sauer, K. D. Pae and S. K. Bhateja, J. Macromol. Sci. - Phys. B9, 391 (1974).

74. H. L1. D. Pugh, E. F. Chandler, L. Holliday and J. Mann, Polym. Eng. Sci., 11, 463 (1971).

75. L. A. Davis and C. A. Pampillo, J. Appl. Phys., 42, 4659 (1971).

76. W. A. Spitzig and O. Richmond, Polym. Eng. Sci., 19, 1129 (1979).

77. J. S. Harris, I. M. Ward and J. S. C. Perry, J. Mater. Sci., 6, 110 (1971).

78. H. N. Yoon, K. D. Pae and J. A. Sauer, Polym. Eng. Sci., 16, 564 (1976).

79. E. Jones Parry and D. Tabor, Polymer, 14, 617 (1973).

80. B. Wunderlich, J. Polym. Sci. - A, 2, 3697 (1964).

81. A. Silano, S. K. Bhateja and K. D. Pae, Inter. J. Polym. Mater., 3, 117 (1974).

82. D. R. Mears, K. D. Pae and J. A. Sauer, J. Appl. Phys., 40, 4229 (1969).

83. J. S. Trent, A. Y. Maet, M. J. Miles and E. Baer, Polym. Eng. Sci., 18, 1235 (1978).

84. T. Shimada, A. Zachariades, M. P. C. Watts and R. S. Porter, J. Appl. Polym. Sci., 26, 1309 (1981).

85. S. Gladstone, K. J. Laidler and H. Eyring, "The Theory of Rate Processes," 1st edn., McGraw-Hill, New York (1941), p. 480.

86. L. L. Blyer and A. C. Hart, Polym. Eng. Sci., 10, 193 (1970).

87. P. D. Coates, A. G. Gibson and I. M. Ward, J. Mater. Sci., 15, 359 (1980).

88. N. J. Capiati and R. S. Porter, J. Polym. Sci., Polym. Phys., 13, 1177 (1975).

89. W. T. Mead and R. S. Porter, J. Appl. Phys., 47, 4278 (1976).

90. A. Buckley and H. A. Long, Polym. Eng. Sci., 9, 115 (1969).

91. G. Capaccio and I. M. Ward, Polymer, 15, 233 (1974).

92. T. Kanamoto, A. E. Zachariades and R. S. Porter, Polymer J., 11, 307 (1979).

93. T. Williams, J. Mater. Sci., 8, 59 (1973).

94. L. A. Davis, Polym. Eng. Sci., 14, 641 (1974).

95. R. Gupta and P. G. McCormick, J. Mater. Sci., 15, 619 (1980).

96. K. Nakayama and H. Kanetsuna, Kobunshi Ronbunshu, 31, 321 (1974).

97. M. T. Shaw, J. Appl. Polym. Sci., 19, 2811 (1975).

98. A. E. Everage and R. L. Ballman, J. Appl. Polym. Sci., 18, 933 (1974).

99. T. Kanamoto, E. S. Sherman and R. S. Porter, Polymer J., 11, 497 (1979).

100. G. Capaccio, T. A. Crompton and I. M. Ward., Amer. Chem. Soc. Polym. Preprints, 18, #2, 343 (1977).

101. D. M. Tarin and E. L. Thomas, Polym. Eng. Sci., 19, 1017 (1979).

102. V. A. Marikhin and L. P. Myasnikova, J. Polym. Sci., Polym. Symp., 58, 97 (1977).

103. A. G. Gibson, I. M. Ward, B. N. Cole and B. Parsons, J. Mater. Sci., 9, 1193 (1974).

104. L. Jarecki and D. J. Meier, Polymer, 20, 1078 (1979).

105. D. E. Bosley, J. Polym. Sci., C, 20, 77 (1967).

106. G. Capaccio and I. M. Ward, J. Polym. Sci., Polym. Phys., 14, 1641 (1976).

107. G. Capaccio and I. M. Ward, Polymer, 16, 239 (1975).

108. G. Capaccio, T. A. Crompton and I. M. Ward, J. Polym. Sci., Polym. Phys., 18, 301 (1980).

109. G. Capaccio, T. A. Crampton and I. M. Ward, Polymer, 17, 644 (1976).

110. G. Capaccio, I. M. Ward and M. A. Wilding, J. Polym. Sci., Polym. Phys., 16, 2083 (1978).

111. G. Meinel and A. Peterlin, J. Polym. Sci., A-2, 9, 67 (1971).

112. D. M. Bigg, E. G. Smith, M. M. Epstein and R. J. Fiorentino, Polym. Eng. Sci., 18, 908 (1978).

113. P. J. Phillips and J. Patel, Polym. Eng. Sci., 18, 943 (1978).

114. D. C. Bassett and D. R. Carder, Phil. Mag., 28, 535 (1973).

115. H. H. Hoehn, R. C. Ferguson and R. R. Herbert, Polym. Eng. Sci., 18, 547 (1978).

116. J. M. Lupton and J. W. Regester, J. Appl. Polym. Sci., 18, 2407 (1974).

117. W. G. Perkins, N. J. Capiati and R. S. Porter, Polym. Eng. Sci., 16, 200 (1976).

118. P. S. Hope, A. G. Gibson and I. M. Ward, J. Polym. Sci., Polym. Phys., 18, 1243 (1980).

119. A. G. Gibson and I. M. Ward, J. Polym. Sci., Polym. Phys., 16, 2015 (1978).

120. A. E. Zachariades, T. Kanamoto and R. S. Porter, J. Polym. Sci., Polym. Phys., 18, 575 (1980).

121. W. Johnson and H. Kudo, "The Mechanics of Metal Extrusion," Manchester Univ. Press, Manchester, England (1962).

122. N. H. Cook, "Manufacturing Analysis," Addison-Wesley Publishing Co., Inc., Reading, Mass. (1966).

123. H. Ll. D. Pugh, "Mechanical Behavior of Materials Under Pressure," H. Ll. D. Pugh, ed., Ch. 9, Elsevier Publishing Co., London (1970).

124. S. Maruyama, K. Imada and M. Takayanagi, Inter. J. Polym. Mater., 2, 105 (1973).

125. K. Imada and M. Takayanagi, Inter. J. Polym. Mater., 2, 89 (1973).

126. K. Nakamura, K. Imada and M. Takayanagi, Inter. J. Polym. Mater., 2, 71 (1973).

127. A. G. Kolbeck and D. R. Uhlmann, J. Polym. Sci., Polym. Phys., 15, 27 (1977).

128. G. R. Snelling and J. F. Lontz, J. Appl. Pm. Sci., 3, 257 (1960).

129. K. Nakayama and H. Kanetsuna, Kobunshi Kagaku, 30, 713 (1973).

130. P. S. Hope and B. Parson, Polym. Eng. Sci., 20, 389 (1980).

131. A. G. Gibson and I. M. Ward, J. Mater. Sci., 15, 979 (1980).

132. P. D. Coates and I. M. Ward, Polymer, 20, 1553 (1979).

133. A. G. Gibson and I. M. Ward, J. Mater. Sci., 14, 1838 (1979).

134. G. Capaccio, I. M. Ward and T. J. Chapman, Polymer, 16, 469 (1975).

135. N. Kasai and M. Kakuda, J. Polym. Sci., A, 2, 1955 (1964).

136. B. Wunderlich and Cormier, J. Polym. Sci., A-2, 5, 987 (1967).

137. E. L. V. Lewis, J. Mater. Sci., 14, 2343 (1979).

138. R. G. Arridge and M. J. Folkes, Polymer, 17, 495 (1976).

139. R. G. Arridge, P. J. Barham, C. J. Farrell and A. Keller, J. Mater. Sci., 11, 788 (1976).

140. B. Wunderlich and T. Arakawa, J. Polym. Sci., A, 2, 3697 (1964).

141. M. Wai, personal communication.

142. E. W. Fischer and H. Puderback, Kolloid-Z., 235, 1260 (1969).

143. G. Capaccio, I. M. Ward, M. A. Wilding and G. W. Longman, J. Macromol. Sci. - Phys., B15, 381 (1978).

144. D. C. Bassett and D. R. Carder, Polymer, 14, 387 (1973).

145. W. Glenz, A. Peterlin and W. Wilke, J. Polym. Sci., A-2, 9, 1243 (1971).

146. J. B. Smith, A. J. Manuel and I. M. Ward, Polymer, 16, 57 (1975).

147. S. Kojima, C. R. Desper and R. S. Porter, J. Polym. Sci., Polym. Phys., 16, 1721 (1978).

148. W. Adams, personal communication.

149. M. A. Wilding and I. M. Ward, Polymer, 19, 969 (1978).

150. R. S. Porter, N. E. Weeks, N. J. Capiati and R. J. Krzewki, J. Thermal Anal., 8, 547 (1975).

151. J. R. Falender and D. Hansen, J. Appl. Phys., 43, 1611 (1972).

152. J. M. Peterson, J. Polym. Sci., Polym. Letters, 7, 231 (1969).

153. C. R. Desper, J. H. Southern, D. R. Ulrich and R. S. Porter, J. Appl. Phys., 41, 4284 (1970).

154. F. N. Cogswell and D. R. Moore, Polym. Eng. Sci., 14, 573 (1974).

155. K. Shigematsu, K. Imada and M. Takayanagi, J. Polym. Sci., Polym. Phys., 13, 533 (1975).

156. R. E. Robertson, J. Polym. Sci., A-2, 9, 453 (1971).

157. R. A. Duckett, B. C. Goswami and I. M. Ward, J. Polym. Sci., Polym. Phys., 14, 1257 (1976).

158. T. Kanamoto, A. E. Zachariades and R. S. Porter, J. Polym. Sci., Polym. Phys., 17, 2171 (1979).

159. J. M. Lupton and J. W. Regester, J. Appl. Polym. Sci., 18, 2451 (1974).

160. A. E. Zachariades, E. S. Sherman and R. S. Porter, J. Appl. Polym. Sci., 24, 2137 (1979).

161. T. Shimada, A. E. Zachariades, W. T. Mead and R. S. Porter, J. Cryst. Growth, 48, 334 (1980).

162. A. J. Pennings and K. E. Meihuizen, "Ultra-High Modulus Polymers," I. M. Ward and A. Ciferri, eds., Ch. 2, Applied Science Pub., Essex, England (1974).

163. N. J. Capiati and R. S. Porter, J. Polym. Sci., Polym. Phys., 15, 1427 (1977).